

UNIVERSIDADE DE LISBOA
FACULDADE DE MEDICINA VETERINÁRIA



PORTABLE “LAB-ON-CHIP” PLATFORM FOR BOVINE MASTITIS DIAGNOSIS
IN RAW MILK

CARLA MARGARIDA PINHEIRO CARDOSO DUARTE

Orientador(es): Professor Doutor José Ricardo Dias Bexiga

Professor Doutor Paulo Jorge Peixeiro de Freitas

Tese especialmente elaborada para a obtenção do grau de Doutor em Ciências Veterinárias, na
Especialidade de Ciências Biológicas e Biomédicas

2016



PORTABLE “LAB-ON-CHIP” PLATFORM FOR BOVINE MASTITIS DIAGNOSIS
IN RAW MILK

CARLA MARGARIDA PINHEIRO CARDOSO DUARTE

Orientador(es): Professor Doutor José Ricardo Dias Bexiga

Professor Doutor Paulo Jorge Peixeiro de Freitas

Tese especialmente elaborada para a obtenção do grau de Doutor em Ciências Veterinárias, na
Especialidade de Ciências Biológicas e Biomédicas

Júri:

Presidente: Professor Doutor Rui Manuel de Vasconcelos e Horta Caldeira

Vogais:

- Professor Doutor Miguel de França Teixeira dos Prazeres
- Professora Doutora Cidália Irene Azevedo Pina Vaz
- Professor Doutor Virgílio da Silva Almeida
- Professor Doutor Luís André de Oliveira Pinho
- Professor Doutor José Ricardo Dias Bexiga

À minha Professora Cristina Vilela

ACKNOWLEDGEMENTS

This study is the result of a multidisciplinary work and would not be accomplished without the help of many people. Foremost, I wish to express my sincerest thanks to all of them.

To Prof. Cristina Vilela for her welcome, stunning reasoning, positivity and encouragement. With her I learned in a pleasant way, so much about immunology. My heart still keeps her good mood, geniality and smiling blue eyes...

To Prof. Ricardo for his friendship, supervision and attendance whenever I asked him to. Thank you for his guidance which helped me to grow as a researcher.

To Prof. Paulo for his welcome, outstanding knowledge, interesting discussions and persistence. His scientific work is an example for me.

To my sister Susana for her welcome, support, positivity and encouragement. All I know about sensors fabrication and quality control, I learned it from her.

To Prof. Ana Duarte for her friendship and availability to discuss immunological results.

To Susana Martins for her help and useful explanations of BCA method.

To Carla Carneiro, Margarida Simões and Sofia Henriques for their friendship and availability for helping me, even at late hours. Thank you for all good laugh moments.

To Carolina Fernandes and Filipe Cardoso who initiated me to the nanotechnology world.

A special thanks to Tiago Costa for his availability to help and teach me about electronics.

To Rita Soares, Andrei Jitariu, Oleksandr Korsun and Hua Lv for shared work, availability and good discussions.

To Costica Hlenschi, Sorin Corodeanu, Oana Dragos, João Costa and Fernando Franco for their availability and assistance.

To INESC-MN clean room engineers: Fernando Silva, Virgínia Soares and José Bernardo for their help and availability.

To Marcos Martins for his availability to analyze magnetic results.

To my parents for their support during PhD years. Without them it should be more difficult to conciliate time between being a mother, a house manager and a student.

To my sister Rafaela for her incentive and for being a good listener.

To my husband for his encouragement and for being an example of persistence.

To Miguel, Vasco and Beatriz for their happiness, support and understanding about mother's less availability.

FINANCIAL SUPPORT

The present work was partially funded by Instituto de Engenharia de Sistemas e Computadores – Microsistemas e Nanotecnologias (INESC MN) and IN – Institute of Nanoscience and Nanotechnology, both FCT projects (EXCL/CTM-NAN/0441/2012) and (Pest-OE/CTM/LA0024/2011); by CIISA-46 (UID/CVT/00276/2013) and by Magnomics, SA.



Título da Tese: Plataforma portátil “lab-on-chip” para diagnosticar mastite bovina em leite cru.

RESUMO

A mastite bovina representa um custo económico relevante para os produtores de leite principalmente devido ao decréscimo da produção leiteira, abate prematuro e custos associados ao tratamento veterinário. Consequentemente, a identificação atempada dos agentes etiológicos é crítica para a implementação de medidas de controlo adequadas, redução do risco de infecções crónicas e aplicação de uma terapia microbiana específica. O objectivo deste estudo foi desenvolver e validar um método de detecção magnética capaz de identificar *Streptococcus agalactiae*, *Streptococcus uberis*, *Staphylococcus aureus* e *Staphylococcus epidermidis* em amostras de leite cru.

As amostras de leite mastítico utilizadas foram recolhidas de 81 animais com mastite subclínica, de 12 explorações leiteiras nacionais. As amostras de leite de 91 quartos de úbere foram selecionadas tendo em conta os resultados bacteriológicos. Todas as amostras foram analisadas por PCR e pelo citómetro magnetoresistivo “lab-on-chip”, tendo sido necessário neste caso, adicionar uma solução com partículas magnéticas funcionalizadas com anticorpos específicos. Este reconhecimento imunológico detectou presença bacteriana acima das 100 ufc/ml, dependendo do anticorpo e da bactéria-alvo. Comparando com os resultados da análise por PCR, este método de detecção magnética apresentou sensibilidades de 73% e 41%, valores de especificidade de 25% e 57%, e valores VPP de 35% e 54% para identificar espécies de *Streptococcus* com os anticorpos anti-*S. agalactiae* e anti-GB *Streptococcus*, respectivamente. No que diz respeito às espécies de *Staphylococcus*, os valores de sensibilidade encontrados foram de 57.1% e 79.3%, de 75% e 50% para a especificidade, e de 40% e 95.8% para VPP com os anticorpos anti-*S. aureus* e anti-*Staphylococcus* spp., respectivamente. Os dois estudos apontam para uma potencial utilização do tipo “cow-side”, tornando a plataforma integrada potencialmente utilizável para uma rápida monitorização de infecção bacteriológica, após melhorias futuras. O método desenvolvido apresenta algumas restrições e limitações relativamente à quantificação bacteriana.

Palavras-chave: sensores magnetoresistivos, patogénicos de mastite bovina, leite, reconhecimento imunogénico, micro fluídico.

Title of the Thesis: Portable “lab-on-chip” platform for bovine mastitis diagnosis in raw milk

ABSTRACT

Bovine mastitis is an economic burden for farmers mostly because of decreased milk yield, premature culling and cost of veterinary treatments. The identification of mastitis pathogens is of major importance in order for adequate control measures to be taken, to reduce the risk of appearance of chronic infections, and to target antimicrobial therapy. The aim of this study was to develop and validate a sensitive method for magnetic detection of *Streptococcus agalactiae*, *Streptococcus uberis*, *Staphylococcus aureus* and *Staphylococcus epidermidis* in raw milk samples.

Mastitic milk samples were collected aseptically from 81 cows with subclinical mastitis, from 12 Portuguese dairy farms. Ninety one quarter milk samples were selected based on bacteriological results. All samples were submitted to PCR analysis. In parallel, these milk samples were mixed with a solution combining specific antibodies and magnetic nanoparticles, to be analyzed using a lab-on-a-chip magnetoresistive cytometer, with microfluidics sample handling. This immunological recognition was able to detect bacterial presence above 100 cfu/ml, depending on antibody and targeted bacteria. Comparison with PCR results showed sensitivities of 73% and 41%, specificity values of 25% and 57%, and PPV values of 35% and 54% for magnetic identification of streptococci species with an anti-*S. agalactiae* antibody and an anti-GB *Streptococcus* antibody, respectively. Regarding staphylococci species, the sensitivity values found were of 57.1% and 79.3%, specificities of 75% and 50%, and PPV values of 40% and 95.8% for magnetic identification with an anti-*S. aureus* antibody and an anti-*Staphylococcus* spp. antibody, respectively. Both bacterial genus studies translated a fair expectation for a “cow-side” use application, making this integrated platform of potential use after further improvements for fast bacteriological infection screening.

Some constraints are described as well as the method’s limitations in bacterial quantification.

Keywords: magnetoresistive sensors, bovine mastitis pathogens, milk, immunogenic recognition, microfluidic.

PREFÁCIO

Nesta dissertação serão apresentados os resultados do trabalho de investigação desenvolvido entre 2011 e 2015, no Laboratório de Microbiologia do Centro de Investigação Interdisciplinar em Sanidade Animal, da Faculdade de Medicina Veterinária e no INESC-MN em Lisboa, sob orientação do Professor Doutor Ricardo Bexiga e co-orientação do Professor Doutor Paulo Freitas.

Este trabalho teve como principais objectivos, seleccionar anticorpos específicos para a identificação de três agentes contagiosos (*Staphylococcus aureus*, *Streptococcus agalactiae* e *Streptococcus uberis*) e um ambiental (*Staphylococcus epidermidis*); fabricar um contador magnético capaz de identificar e contar bactérias em leite cru; validar o novo método de detecção magnética com amostras de leite mastítico; e por último, comparar os resultados obtidos pelo novo método com os resultados do método genotípico de referência PCR.

A presente tese encontra-se dividida em sete capítulos. No primeiro capítulo é feita uma introdução sobre os métodos de diagnóstico existentes actualmente para a detecção de mastite bovina. No segundo, a metodologia e os resultados obtidos para a selecção de anticorpos específicos e nos capítulos três a seis são expostos os objectivos do trabalho experimental descritos nesta tese, conduzindo à exposição dos resultados alcançados. Por fim, no sétimo e último capítulo é apresentada uma discussão integrada de todos os resultados obtidos, apresentando-se as conclusões finais do presente trabalho e perspectivas futuras. Como previsto no Regulamento de Doutoramentos da Universidade de Lisboa, parte integral dos resultados apresentados encontra-se publicada, ou já submetida em revistas internacionais correspondendo aos seguintes capítulos:

I Technological advances in Bovine Mastitis Diagnosis – an overview.

C.M. Duarte, P.P. Freitas, R. Bexiga (2015). Journal of Veterinary Diagnostic Investigation 27(6), 665 –672.

III Lab-on-chip cytometry based on magnetoresistive sensors for bacteria detection in milk.

A.C. Fernandes, C.M. Duarte, F.A. Cardoso, R. Bexiga, S. Cardoso, P.P. Freitas (2014). Sensors, 14, 15496-15524.

IV Magnetic counter for Group B Streptococci detection in milk.

C.M. Duarte, A.C. Fernandes, F.A. Cardoso, R. Bexiga, S. Cardoso, P.P. Freitas (2015). *IEEE Transactions on Magnetics*, 51(1).

V Semi-quantitative method for Streptococci magnetic detection in raw milk.

C.M. Duarte, T. Costa, C. Carneiro, R. Soares, A. Jitariu, S. Cardoso, M.S. Piedade, R. Bexiga, P.P. Freitas (2016). *Biosensors*, 6(2), 19.

VI Semi-quantitative method for Staphylococci magnetic detection in raw milk.

C.M. Duarte, C. Carneiro, S. Cardoso, P.P. Freitas, R. Bexiga (2016). Submitted to *Journal of Dairy Research*.

INDEX

ACKNOWLEDGEMENTS	i
FINANCIAL SUPPORT	ii
RESUMO	iii
ABSTRACT	v
PREFÁCIO	vii
INDEX	ix
FIGURE INDEX	xiii
TABLE INDEX	xvii
ABREVIATIONS	xix
CHAPTER I	1
Technological advances in Bovine Mastitis Diagnosis – an overview.	1
Abstract	3
1. Introduction	4
1.1. Identification of pathogens causing intramammary infection	4
1.1.1. Phenotypic methods	4
1.1.2. Genotypic methods.....	6
1.1.3. Immunoassays	9
1.2. Mastitis detection	10
1.2.1. Cell counting	10
1.3. Ion variation: milk conductivity	13
1.4. Biomarker evaluation	13
2. Discussion	15
3. Future trends.....	16
4. Conclusion.....	17
CHAPTER II.....	19
Specific antibodies selection.	19
1. Introduction	21
2. Material and Methods.....	23
2.1. Staphylococci protein extraction	23
2.2. Streptococci protein extraction.....	24
2.3. Protein quantification	25
2.4. Selected antibodies.....	25
2.5. Immunoblotting.....	26
2.6. Direct ELISA	27
3. Results and Discussion.....	28
3.1. Immunoblotting.....	28
3.2. Direct ELISA	33
4. Conclusions	34

CHAPTER III.....	35
Lab-on-chip cytometry based on magnetoresistive sensors for bacteria detection in milk.....	35
Abstract	37
1. Introduction	38
2. Sensor Design and Detection Scheme.....	41
3. Experimental Methods	44
3.1. Beads Functionalization	46
3.2. Bacterial Cells Magnetic Labeling	47
3.3. Milk Samples Preparation	47
3.4. Sensor Fabrication.....	48
3.4.1. MR sensor fabrication	48
3.4.2. Microfluidic channels fabrication	49
3.4.3. Bonding and encapsulation	50
3.5. Samples Measurement.....	51
4. Results and Discussion.....	52
4.1. Sensors characterization and magnet calibration	52
4.2. Sensors magnetic behavior, signal amplitude and shape.....	54
4.3. Detection of Streptococcus agalactiae cells	63
5. Conclusions/Outlook.....	70
CHAPTER IV	71
Magnetic counter for Group B Streptococci detection in milk.....	71
Abstract	73
1. Introduction	74
2. Material and methods	75
2.1. Sensor fabrication.....	75
2.2. Microfluidic channel fabrication	77
2.3. Readout electronics	77
2.4. Particles' functionalization.....	77
2.5. Bacterial cells magnetic labeling.....	78
2.6. Milk samples preparation	79
2.7. Sample measurement.....	79
3. Results and discussion.....	80
A. Typical signals.....	80
B. Quantification results	81
4. Conclusions	83
CHAPTER V.....	85
Semi-quantitative method for Streptococci magnetic detection in milk.....	85
Abstract	87
1. Introduction	88
2. Material and methods	89

2.1. Method principles.....	89
2.2. Biosensor fabrication.....	90
2.3. Microfluidic channel fabrication.....	92
2.4. Readout electronics	92
2.5. Magnetic detection method calibration	93
2.6. Bacterial cells	93
2.7. Sterile milk samples	94
2.8. Mastitic milk samples.....	94
2.9. PCR reference method analysis.....	95
2.10. Biosensor analysis	95
2.11. Data Analysis	97
3. Results	98
3.1. Evaluation of biosensor’s bacterial quantification	98
3.2. Validation of magnetic detection	100
4. Discussion	103
5. Conclusions	105
CHAPTER VI	107
Semi-quantitative method for Staphylococci magnetic detection in milk	107
Abstract	109
1. Introduction	110
2. Material and methods.....	111
2.1. Milk samples	111
2.2. Bacterial cells	112
2.3. Biosensor detection	114
2.4. Data Analysis	116
3. Results.....	117
3.1. Evaluation of biosensor’s quantification.....	117
3.2. Validation of magnetic detection	117
4. Discussion	120
CHAPTER VII	125
General Discussion, Conclusions and Future Directions.	125
DISCUSSION	127
1. Doctoral study overview	127
2. Strengths, Weaknesses, Opportunities and Threats.....	132
CONCLUSIONS	138
FUTURE DIRECTIONS.....	139
REFERENCES.....	140

FIGURE INDEX

- Figure 1.** Immunogenic proteins from *Staphylococcus aureus* identified by rabbit anti-*S. aureus* ScpA (ab 92983) are evidenced as dark brown blots. Molecular weights (kDa) of evaluated proteins are indicated on the left of immunoblot images. **29**
- Figure 2.** Immunogenic proteins from *Staphylococcus aureus* and *Staphylococcus epidermidis* identified by mouse anti-*Staphylococcus* spp. (MCA 5793) are evidenced as dark brown blots. Molecular weights (kDa) of evaluated proteins are indicated on the left of immunoblot images. **30**
- Figure 3.** Immunogenic proteins from *Streptococcus agalactiae* and *Streptococcus uberis* identified by rabbit anti-*Streptococcus* Group B (8435-2000) are evidenced as dark brown blots. Molecular weights (kDa) of evaluated proteins are indicated on the left of immunoblot images. **31**
- Figure 4.** Immunogenic proteins from *Streptococcus agalactiae* identified by mouse anti-*Streptococcus agalactiae* (MA1-10871) are evidenced as dark brown blots. Molecular weights (kDa) of evaluated proteins are indicated on the left of immunoblot images. **32**
- Figure 5.** Schematics of magnetic detection device for identification and quantification of cells. **41**
- Figure 6.** Resistance vs. magnetic field transfer curve of a linear spin-valve at a given sense current. **42**
- Figure 7.** Schematics of MR sensor detection of magnetically labeled targets flowing above the sensor, from the left (position 1) to the right (position 5). **43**
- Figure 8.** Schematics of immuno-magnetic functionalization of cells (a) Incubation of functionalized beads with *Streptococcus agalactiae* cells and (b) biological affinities between beads protein A, polyclonal IgG antibodies and bacterial cell wall epitopes. **46**
- Figure 9.** (a) Device CAD mask and sensor dimensions; (b) Microscope photo of one set of seven microfabricated SVs. **49**
- Figure 10.** Schematics of the contact microlithography steps: (a) UV exposure setup; (b) Sample holder with hard-mask assembled over SU-8 substrate; (c) SU-8 negative resist exposure process. **50**
- Figure 11.** Wire-bonding silicon-protected assembled device. **50**
- Figure 12.** Acquisition Setup. (a) Electrical circuit of the acquisition setup; (b) Biasing box; (c) Acquisition setup assembly. **51**
- Figure 13.** Transfer curve for a selected sensor with an area of $100 \times 3 \mu\text{m}^2$. Inset shows the multilayer structure used for these sensors. **52**
- Figure 14.** (a) Schematics of the geometry used for the nanoparticle magnetization using an external permanent magnet underneath the sensor and the magnetic field components (transverse, perpendicular and longitudinal) with respect to the free and

pinned layer magnetization orientations; (b) Impact on the sensor response of each magnetic field component (set by magnet position) transfer curves.	54
Figure 15. Out-of-plane magnetic field application for magnetic label sensing measurement schematics.	55
Figure 16. Schematics of sensor and channel geometry considered for output signal simulation in Wolfram Mathematica 7.0.	56
Figure 17. Axis and angles considered for Wolfram Mathematica 7.0 simulations.	57
Figure 18. Schematics of cell orientations along x, y and z axis considered for cells in flow (x axis direction) in Wolfram Mathematica 7.0 simulations.	57
Figure 19. Signal simulation for <i>Streptococcus agalactiae</i> . (a) Pair of cells oriented according with each axis; (b) Signal variation with height from the sensor according with x axis.	58
Figure 20. Signal simulation for two <i>Streptococcus agalactiae</i> along x axis. (a) Schematics of cell pair's orientation considered for simulation; (b) Cells at a given distance along x axis; (c) Signal variation with height from the sensor for cells at 10 μm distance from each other along x axis.	59
Figure 21. Signal simulation for two <i>Streptococcus agalactiae</i> along z axis. (a) Cells at a given distance along z axis; (b) Signal variation with height from the sensor for cells at 2 μm distance from each other along z axis.	60
Figure 22. Signal simulation for two <i>Streptococcus agalactiae</i> along y axis. (a) Cells at a given distance along y axis; (b) Signal variation with height from the sensor for cells at 10 μm distance from each other along y axis.	60
Figure 23. (a) Schematics of cell flow over two types of SVs; (b) Signal amplitude for two types of SVs obtained from simulations for two pairs of cells oriented along y axis and separated by 2 and 10 μm	61
Figure 24. Schematics of axis and configuration considered for simulation in Mathematica 7.0 on the signal influence by both perpendicular and parallel components of fringe field.	62
Figure 25. Signal simulation for detection of a <i>Streptococcus agalactiae</i> cell using a $100 \times 3 \mu\text{m}^2$ sensor (a) oriented along x axis considering different magnetic moment angles relative to the x axis; (b) Selection of simulated angles.	63
Figure 26. Acquired signal for raw milk samples (a) as collected; (b) spiked with functionalized nanoparticles and (c) spiked with magnetically labeled <i>Streptococcus agalactiae</i> cells at 50 $\mu\text{l}/\text{min}$	64
Figure 27. Schematics of inertial focusing in square microchannels. (a) Two lift forces in action, wall-induced F_w and shear-induced F_s lift forces; U is the migration velocity of cell; (b) In square channels randomly distributed particles or cells focus into four equilibrium positions at the wall centers.	65

Figure 28. Acquisition signal for raw milk samples with magnetically labeled <i>Streptococcus agalactiae</i> cells at 50 $\mu\text{l}/\text{min}$	67
Figure 29. Direct comparison of experimental and simulated peaks. The simulation considered two <i>Streptococcus agalactiae</i> cells flowing at 50 $\mu\text{l}/\text{min}$, with a rotation of the magnetization by an angle of $-\pi/10$ with respect to the vertical.....	67
Figure 30. Acquisition signal of (a) PBS; (b) defatted and (c) raw milk samples spiked with magnetically labeled <i>Streptococcus agalactiae</i> cells at 50 $\mu\text{l}/\text{min}$	69
Figure 31. a) Device CAD mask showing microfluidic channels, sensors and sensor contact leads. Each channel crosses several sensors, b) Microscope photo of one microchannel aligned over 7 microfabricated SVs.	75
Figure 32. Selected transfer curve for a SV sensor with $100 \times 3\mu\text{m}^2$	76
Figure 33. Schematics of immuno-magnetic functionalization of cells a) Incubation of functionalized beads with bacteria cells and b) biological affinities between beads protein A, polyclonal IgG antibodies and bacterial cell wall epitopes.....	78
Figure 34. Dynamic detection and differences between sensor signals on the passage of: a) PBS, PBS with beads (10x) and <i>Streptococcus agalactiae</i> cells (100 CFU/ μl) and a cleaning solution; b) defatted milk, defatted milk with beads (10x) and <i>Streptococcus agalactiae</i> cells (100 CFU/ μl) and a cleaning solution.....	81
Figure 35. Differences between a) peak numbers in defatted milk and PBS samples with 100 CFU/ μl of <i>Streptococcus agalactiae</i> and different concentrations of functionalized beads. Peak details in b) defatted milk with lower (10x) and c) higher concentration (100x) of functionalized beads and in PBS samples with d) lower (10x) and e) higher (100x) concentration of functionalized beads.....	82
Figure 36. Schematics of immuno-magnetic detection of cells. (A) Incubation of functionalized NPs with bacteria cells and (B) biological affinities between different functionalized NPs with bacterial cell wall immunogenic proteins. (C) Predictable protein A binding site to each antibody.....	90
Figure 37. (A) Final device with the magnetoresistive chip bonded to the polydimethylsiloxane (PDMS) microchannels. The sensor's wirebonding are protected with silicone. (B) Spinvalve (SV) sensor distribution along the microchannels. (C) Microscope photo of the fabricated SVs with the PDMS micro channel over them (20X amplification).....	91
Figure 38. (A) Acquisition setup assembly and (B) multi-channel PCB connected to external electronics.....	93
Figure 39. Biosensor analysis procedure steps.....	96
Figure 40. Sensor output for (A) negative control with the higher amplitude of 23 μV , (B) mastitic milk (without <i>S. agalactiae</i> according to the PCR) with NPs functionalized with mAb anti- <i>S. agalactiae</i> which presents an amplitude peak of 15 μV (9076AD sample code). The higher amplitude peaks found for each pair of bacteria-antibody were, (C) 193.6 μV in raw milk with anti-GB Streptococci and 1 CFU/ μl of <i>S. agalactiae</i> , (D) 917.5 μV in raw milk with anti-GB Streptococci and	

10 CFU/ μ l of <i>S. uberis</i> and (E) 923.7 μ V in raw milk with anti- <i>S. agalactiae</i> and 0.3 CFU/ μ l of <i>S. agalactiae</i>	97
Figure 41. Calibration trials results for milk samples with seven bacterial concentrations (<i>S. agalactiae</i> or <i>S. uberis</i>) and functionalized NPs with pAb anti-GB Streptococci (Ab8435) and mAb anti- <i>Streptococcus agalactiae</i> (Ab MA1). Peak number average for each bacteria-antibody pair are counted.	99
Figure 42. <i>Streptococcus agalactiae</i> cells microscopic image where a spherical cluster and an elongated cluster are evidenced (A). Experimental data fitting of the highest amplitude peaks obtained in PBS samples with different <i>S. agalactiae</i> concentrations (0.5 CFU/ μ l: 162 μ V (B) and 10 CFU/ μ l: 146 μ V (C)) during calibration curve settlement.....	100
Figure 43. Schematics of immuno-magnetic detection of cells. a) Incubation of functionalized beads with bacterial cells; (b) biological affinities between different functionalized nanoparticles with bacterial cell wall immunogenic proteins; (c) predictable protein A binding site to each antibody.	113
Figure 44. Sensor output for (A) negative control with the higher amplitude of 23 μ V, (B) mastitic milk (9077 T sample code without <i>S. aureus</i> accordingly with PCR) with NP's functionalized with pAb anti- <i>S. aureus</i> (Ab 92983) which presents an amplitude peak of 10.7 μ V. The higher amplitude peaks found for each pair of bacteria-antibody were, (C) 1703.4 μ V in raw milk with pAb anti- <i>S. aureus</i> and 10 CFU/ μ l of <i>S. aureus</i> , (D) 964.4 μ V in raw milk with mAb anti- <i>Staphylococcus</i> spp. (MCA 5793) and 10 CFU/ μ l of <i>S. aureus</i> and (E) 1030.5 μ V in raw milk with mAb anti- <i>Staphylococcus</i> spp. and 10 CFU/ μ l of <i>S. epidermidis</i>	115
Figure 45. Calibration trials results for milk samples with seven bacterial concentrations (<i>S. aureus</i> or <i>S. epidermidis</i>) and functionalized NP's with pAb anti- <i>S. aureus</i> (Ab 92983) or mAb anti- <i>Staphylococcus</i> spp. (Ab MCA 5793). Peak number average for each bacteria-antibody pair are counted.	117
Figure 46. Number of mastitic samples analyzed per antibody. The interception numbers corresponds to the common samples analyzed by respective antibodies.	134
Figure 47. Sampling design proposal.	135
Figure 48. Microfluidic microchannel's CAD masks. A) linear microchannels used for conclusive results. B) microchannels with pillars inside, tested for raw milk sieving.	136

TABLE INDEX

Table 1 - Results of SVs transport characteristics [28 sensors measured].	53
Table 2 - Identification of isolates in mastitic milk samples with both magnetic detection (mAb anti- <i>Streptococcus agalactiae</i> ; pAb anti-GB Streptococci) and with conventional microbiology, compared to PCR analysis as the reference method.	101
Table 3 - Sensitivity, specificity and positive predictive value of the magnetic detection and the conventional microbiology, using PCR analysis as the reference method.	102
Table 4 - Identification of isolates in mastitic milk samples with both magnetic detection (pAb anti- <i>Staphylococcus aureus</i> ; mAb anti- <i>Staphylococcus</i> spp.) and with conventional microbiology, compared to PCR analysis as the reference method.	118
Table 5 - Sensitivity, specificity and positive predictive value of the magnetic detection and the conventional microbiology, using PCR analysis as the reference method.	119

ABREVIATIONS

Ab	antibody
ADC	analogue to digital converter
AFLP	amplified fragment length polymorphism
Ag	antigen
ATCC strain	American type culture collection
bead	magnetic nanoparticle
CECT strain	Spanish type culture collection
CFU	colony forming units
CMT	California mastitis test
CNS	coagulase-negative staphylococci
COS	Columbia sheep blood agar
DC	direct current
DCC	differential cell count
DNA	desoxiribonucleic acid
DWL	direct write laser
ELISA	enzyme linked immunosorbent assay
Fc fraction	fragment crystallizable region
FM	ferromagnetic
Hp	haptoglobin
HRP	horseradish peroxidase
IBD	ion beam deposition
Ig	immunoglobulin
IMI	intramammary infection
kDa	kilo Dalton
LDH	lactate dehydrogenase
MLVA	multiple locus variable-number tandem repeat analysis
MR	magnetoresistive
NAGase	N-acetyl-d-glucosaminidase
NP	nanoparticle
Oe	Oersted, a CGS unit of magnetic field H strength. SI base unit: A.m ⁻¹

PBS	phosphate buffer saline
PCB	printed circuit board
PCR	polymerase chain reaction
PDMS	polydimethylsiloxane
PFGE	pulsed-field gel electrophoresis
PMMA	poly(methylmethacrylate)
PPV	positive predictive value
PVD	physical vapor deposition
PVDF	polyvinylidene fluoride
RFLP	restriction fragment length polymorphism
rRNA	ribossomic ribonucleic acid
RT	room temperature
RT-PCR	reverse transcriptase polymerase chain reaction
SAA	serum amyloid A
SCC	somatic cell count
SDS-PAGE	sodium dodecyl sulfate-polyacrylamide gel electrophoresis
Staph	<i>Staphylococcus</i>
Strep	<i>Streptococcus</i>
SV	spin valve
Tesla (T)	SI unit for magnetic induction B.
tDNA	transfer desoxiribonucleic acid
TSB	tripticasein soy broth
UVO	ultraviolet/ozone
VPP	valor positivo predictivo
WB	Western blot
WMT	Wisconsin mastitis test

CHAPTER I

Technological advances in Bovine Mastitis Diagnosis – an overview.

*C.M. Duarte, P.P. Freitas, R. Bexiga (2015). *Journal of Veterinary Diagnostic Investigation* 27(6), 665 –672.

* The author drafted the manuscript.

Abstract

Bovine mastitis is an economic burden for dairy farmers and preventive control measures are crucial for the sustainability of any dairy business. The identification of etiological agents is necessary in controlling the disease, reducing risk of chronic infections and targeting antimicrobial therapy. The suitability of a detection method for routine diagnosis depends on several factors, including specificity, sensitivity, cost, time in producing results, and suitability for large-scale sampling of milk. This article focuses on current methodologies for identification of mastitis pathogens and for detection of inflammation, as well as the advantages and disadvantages of different methods. Emerging technologies, such as transcriptome and proteome analyses and nano- and microfabrication of portable devices, offer promising, sensitive methods for advanced detection of mastitis pathogens and biomarkers of inflammation. The demand for alternative, fast, and reliable diagnostic procedures is rising as farms become bigger. Several examples of technological and scientific advances are summarized which have given rise to more sensitive, reliable and faster diagnostic results.

Key words: bovine mastitis, diagnostic methods, technological advances

1. Introduction

Bovine mastitis is an economic burden for farmers because of decreased milk yield, premature culling, cost of veterinary treatments, and other factors. Mastitis leads to changes in milk composition, which is dependent on the inflammatory response (Korhonen & Kaartinen, 1995). The most frequent standard in measuring inflammation is cytological investigation, including milk somatic cell count (SCC). The evaluation of milk quality for premium value or penalties applied to milk prices is generally assessed by SCC. Intramammary infections (IMI) are detected more frequently through milk culturing; however, pathogen isolation is not necessarily associated with inflammation. The identification of mastitis pathogens is of major importance in order for adequate control measures to be taken, risk of appearance of chronic infections reduced, and antimicrobial therapy targeted. This work aims to discuss the advantages and disadvantages of methods used in the diagnosis of bovine mastitis and technological advances that have the potential to offer a “cow-side” use.

1.1. Identification of pathogens causing intramammary infection

1.1.1. Phenotypic methods

Bacterial culture has for some time served as the gold standard for the examination of phenotypic characteristics. Appropriate use of culture-enhancement methods can significantly increase sensitivity in the detection of mastitis-associated organisms in milk, and targeted use of selective media may offer significant improvements in sensitivity in composite cow samples and bulk tank milk culture (Britten, 2012).

Phenotypic identification is based on an evaluation of morphology, growth characteristics, ability to metabolize substrates, antimicrobial resistance, and other features that result from DNA expression (Zadoks & Watts, 2009). Commercial manufacturers of diagnostic tests have developed a number of identification methods based on phenotypic traits, including test systems^{a-d} 1 and

¹ a. API microbial identification kits, BioMérieux Inc., Durham, NC.

b. Vitek microbial identification kits, BioMérieux Inc., Durham, NC.

c. Staph-Zym identification kit for staphylococci, Rosco Diagnostica A/S, Taastrup, Denmark.

other combinations of biochemical tests (Zadoks & Watts, 2009). Some advantages of phenotypic methods are that such methods rely on biochemical characteristics that are common and associated with bacterial species, are usually easy to perform, have good market availability, and have a relatively low cost. An inherent weakness in phenotypic methods is that there is variability in expression of characteristics by isolates belonging to the same species (Gonzalo, Linage, Carriedo, de la Fuente & Primitivo, 2006), and their interpretation may be subjective (Bourry & Poutrel, 1996). The reproducibility of these tests is limited by the variability in expression and interpretation of phenotypic characteristics. In addition to reproducibility, the typeability (proportion of isolates that are assigned a type by a typing system) (Riffon et al., 2001) is imperfect either at the species or at the strain level. Microbiological culture methods are also considered to be laborious and time consuming (Gillespie & Oliver, 2005).

On-farm culture systems are increasingly used, as they offer economic benefits to farmers by reducing therapy costs and the amount of discarded milk (Lago, Godden, Bey, Ruegg & Leslie, 2011). Studies on the diagnostic validity of on-farm culture systems showed acceptable performance, although the specificity recorded was relatively low (McCarron, Keefe, McKenna, Dohoo & Poole, 2009). Previous researchers (Lago et al., 2011; McCarron et al., 2009) compared 2 on-farm culture systems^{e,f 1} for clinical mastitis pathogen identification. One system^e consisted of a culture plate with 2 different media, one allowing the growth of both Gram-positive and Gram negative bacteria, and one selective for the growth of Gram negative bacteria. The other on-farm culture system^f included 2 media, one allowing the development of aerobic bacteria and another allowing the growth of coliform bacteria. Both methods were able to successfully categorize isolates of clinical cases of mastitis based on their ability to differentiate between Gram-positive and Gram-negative organisms, with sensitivities of 97.9%^e and 93.8%^f and specificities of 68.6%^e and 70.1%^f respectively, but neither had the ability to determine if a sample was contaminated.

d. BBLCrystal identification systems, BD, Franklin Lakes, NJ.

e. Minnesota Easy Culture system II bi-plate, University of Minnesota Laboratory for Udder Health, St. Paul, MN.

f. 3M Petrifilm plate methods, 3M Microbiology, St. Paul, MN.

Mass spectroscopy using the matrix-assisted laser desorption ionization–time of flight (MALDI-TOF MS) can also be performed to determine bacterial species (Barreiro et al., 2010; Raemy et al., 2013) and bacterial strains (Böhme, 2012) within a few minutes (Mellmann et al., 2009). It is a reliable, easy to use, and cost-effective technique that has the potential to replace and/or complement conventional phenotypic identification, reaching sensitivity and specificity values of 100% (Bizzini & Greub, 2010).

Nevertheless, the ability of MALDI-TOF MS in identification is limited to specific spectra databases of the existing bacterial protein profiles (Bizzini & Greub, 2010), and this technology is still too costly to be widespread in diagnostic laboratories.

1.1.2. Genotypic methods

Genotypic methods use DNA as the basis for identification and are used for species identification and strain typing (Zadoks & Watts, 2009). The genomic sequences of a number of mastitis-causing pathogens are now available and have been used to develop nucleic acid–based testing methods, such as polymerase chain reaction (PCR), which has become one of the most popular methods for direct detection of nucleic acids from infectious agents (Malou & Raoult, 2011). The high sensitivity of PCR, which is capable of detecting a single molecule of DNA, may be seen as an advantage for microbiological diagnostic purposes. Up to 30% of clinical mastitis samples yield no growth in bacterial culture (Taponen, Salmikivi, Simojoki, Koskinen & Pyörälä, 2009), but PCR analysis is sensitive enough to detect growth-inhibited and nonviable bacteria. This leads to a possible decrease in the rate of false-negative results. In addition, short throughput times and the potential for objective and user-independent identification (van Belkum et al., 2007) are other arguments in support of PCR assays. Identification of nonviable bacteria has the potential to enable integration of IMI diagnostics with SCC determination in dairy herd improvement programs through the use of bronopol-preserved samples (Koskinen et al., 2009). A previous study (Taponen et al., 2009) showed, through a PCR assay, that microbiologically negative samples often contained several common mastitis pathogens, some of which displayed high bacterial counts. Use of PCR-based tests may also be of interest

for IMI diagnosis when culturing only detects minor pathogens (Bexiga et al., 2011). Traditional PCR has advanced from detection at the reaction end-point, to detection while the reaction is occurring. This improvement was necessary because endpoint collection of PCR products is not quantitative. In contrast, real-time PCR is quantitative. Disadvantages of traditional PCR are the use of agarose gels in the detection of DNA amplification, in which resolution is very poor (~10-fold), while real-time PCR can detect as little as a 2-fold resolution variation (Willey, Sherwood & Woolverton, 2008). Another improvement in traditional PCR has been the multiplex PCR, which can simultaneously detect different genes making it potentially faster and cheaper, as all species can be amplified in a single reaction (Bustin, 2004). However, multi-target analysis by PCR has 2 main constraints. First, multiplex PCR is limited in the number of targets that can be consistently amplified simultaneously because of uncontrollable primer–primer interactions. Second, identifying solution phase multiplex PCR amplicons typically requires a secondary method for the separation of size or sequence verification prior to analysis and data interpretation (Edwards & Gibbs, 1994), which may increase direct costs. A previous study (Koskinen et al., 2009) asserts that the development of a PCR test capable of complementing or replacing conventional methods in IMI diagnosis presents a challenge because of the large number of pathogens responsible for IMI, many of which are closely related genetically. Furthermore, milk contains PCR-inhibiting substances, and an assay designed for use in mastitic milk must include dedicated DNA extraction protocols and reagents to obtain results.

Molecular diagnostic methods, in general, may also help identify particularly virulent strains of an organism or distinguish between clonal and non-clonal infection outbreaks. In a clonal outbreak, the predominance of a single strain could indicate contagious transmission of the organism or exposure of multiple cows to a particular environmental point source (Mueller & Wolfenbarger, 1999). Other molecular typing methods used for bovine mastitis pathogen identification include amplified fragment length polymorphism (AFLP) analysis at a species level (Taponen, Koort, Björkroth, Saloniemi & Pyörälä, 2007); restriction fragment length polymorphism (RFLP) analysis at a strain level (Saei, Ahmadi, Mardani & Batavani, 2010); multiple locus variable-number tandem repeat analysis (MLVA) at a strain level (Pinho, Thompson, Rosenbusch & Carnevalheira,

2012); ribotyping at a species level (Carretto et al., 2005); transfer DNA intergenic spacer length polymorphism analysis at a species (Heir, Sundheim & Holck, 1999) and strain level (Stepanović et al., 2005); pulsed field gel electrophoresis (PFGE) typing at a strain level (Douglas, Fenwick, Pfeiffer, Williamson & Holmes, 2000); and DNA sequencing of housekeeping genes at a species (Heikens, Fler, Paauw, Florijn & Fluit, 2005) and strain level (Heir et al., 1999). From these 8 methods, only 3 (AFLP (Taponen et al., 2007), RFLP (Saei et al., 2010), and PFGE (Douglas et al., 2000) have been performed directly from milk samples but all required prior isolate recovery by microbiological culture. There appears to be higher reproducibility, resolution, and sensitivity to AFLP, but both this technique and RFLP have a similar response time and cost efficiency (Munoz, Welcome, Schukken & Zadoks, 2007). According to a previous study (Carretto et al., 2005), automated ribotyping is a reproducible method, easy to perform, and operator-independent. However, when performed manually, it is time-consuming and technically demanding, requiring highly skilled personnel. The more recent typing methods provide a higher degree of reproducibility, such as MLVA (Pinho et al., 2012), triggered by the independent development of a large range of protocols by many different laboratories leading to several different typing schemes for each organism. This led to inter laboratory comparisons and is one of the main limiting factors in currently available genotyping techniques (Pinho et al., 2012). Nevertheless, MLVA has a strong discriminatory capacity, high robustness, portability, objectivity, and throughput (Hyytiä-Trees, Cooper, Ribot, & Gerner-Smidt, 2007; van Belkum et al., 2007) but low versatility, as most protocols are species or serotype specific. In comparison, PFGE, the current gold standard method for molecular subtyping, has a strong discriminatory capacity and versatility, but is less robust and portable, and has lower objectivity and throughput (Hyytiä-Trees et al., 2007). Other technological advances of genotypic methods for the identification of bovine mastitis pathogens include microarray technology, which is capable of detecting 7 common species of mastitis-causing pathogens within 6 hours, with an observed sensitivity of 94.1% and specificity of 100% (Lee et al., 2008). The platform used was based on PCR technology where pathogen-specific targets of DNA were amplified and transferred to react and hybridize with specific probes that were pre-spotted on the biochip. At the end of the process, colorimetric

techniques were used to identify pathogen patterns present in the sample. The detection limit of this method was 10^3 – 10^5 CFU/ml. A previous study (Cremonesi et al., 2009) also described a DNA chip, based on the use of a ligation detection reaction coupled to a universal array, developed to detect and analyze pathogens directly from milk samples. These bacterial groups were identified based on the 16S rRNA gene. Results demonstrated high specificity with sensitivity as low as 6 fmol per volume unit.

Another study (Supré et al., 2009) identified coagulase-negative staphylococci isolates with an updated tDNA-PCR, which resulted in 91.0% typeability and 99.2% accuracy. The study also showed that the updated tDNA-PCR associated with capillary electrophoresis was almost as accurate as gene sequencing but faster (increased automation) and cheaper (only \$3 per isolate).

1.1.3. Immunoassays

Immunological methods are often used because of their speed, simplicity, relatively low cost, and the availability of commercial kits (Gosling, 1990). The detection limits of enzyme linked immunosorbent assays (ELISAs) have been shown to range between 8×10^{-4} and 8×10^{-3} μ g of antibody/ml (Madigan, Martinko, Bender, Buckley & Stahl, 2010). Despite these features, ELISAs are not able to detect some antigens that are present at low concentrations (Malou & Raoult, 2011).

ELISAs exist for *Staphylococcus aureus* detection in cases of bovine mastitis (Bourry & Poutrel, 1996), but the antibody titer does not correlate well with the amount of infecting bacteria (Riffon et al., 2001). Other ELISAs have been developed to screen milk for natural contamination with *S. aureus* and *Listeria* sp. organisms (Riffon et al., 2001). A previous study (Yazdankhah, Helleman, Rønningen & Olsen, 1998) developed a magnetic bead-based ELISA employing monoclonal antibodies for the detection of staphylococci in milk. This method detected between 10^4 and 10^5 organisms/ml and took 3 hr. An earlier study (Matsushita et al., 1990) investigated a milk antibody test^g ² that detected *S. aureus* antibodies in milk samples. The ELISA results were scored both visually

^g ProStaph test, Proscience Corp., Sterling, VA.

^h Masta-Staph test, Mast Group Ltd., Bootle, Merseyside, UK.

and by means of an optical density plate reader and compared against positive controls. This test had several potential points of contention with microbiological tests: a cow in the early stages of infection could be culture positive but antibody negative, and a cow could be antibody positive but culture negative because of the intermittent shedding pattern of cows with chronic *S. aureus* mastitis, or because milk from a single infected quarter was not included (or was diluted) in composite milk samples. If cows were ≤ 30 days in milk or producing ≤ 13.6 kg of milk per day, the test was also not considered to be accurate. The sensitivity of this antibody test^{g 2} has been reported to range between 69% and 90%, while specificity values were 61–97% (Hicks, Eberhart & Sischo, 1994). Despite this test being available for several years, its use seems to be limited.

Another study (Zschöck, Nessler & Sudarwanto, 2005) for *S. aureus* identification in milk samples based on immune agglutination compares 6 commercially available slide agglutination tests, which are currently used in human medicine. The highest sensitivity (86.7%) and specificity (90.1%) was obtained for a test consisting of latex particles coated with human fibrinogen and immunoglobulin G.^{h 2}

1.2. Mastitis detection

1.2.1. Cell counting

Somatic cell count has been used as the gold standard for decades to diagnose subclinical mastitis and is an important parameter for the dairy industry as it affects the price of milk paid to the farmer. The mononuclear leukocytes, monocytes, and lymphocytes, along with the neutrophils, are often the only cells taken into account (Pilla, Schwarz, König & Piccinini, 2012). SCCs do not always correlate with infection of the udder, and they may be affected by other factors (e.g., lactation number, stage of lactation, milk production level, stress, season, and breed) (Schepers, Lam, Schukken, Wilmink, & Hanekamp, 1997). Suggested cutoff values for SCC in mastitis diagnosis differ between publications because different conventions are used in different countries as well as various types of milk samples (Holdaway, Holmes & Steffert, 1996). The most frequently used cutoff value to define subclinical mastitis is a SCC $\geq 200,000$ cells/ml (Pyörälä, 2003; Schepers, et al., 1997). Cell counts below this threshold in composite milk

samples indicate that a mammary gland is likely to be free of IMI (Dohoo & Leslie, 1991), but this threshold is based on the assumption that the culture test is perfect, which does not take into account the chances of false-negative results in a SCC \leq 200,000 cells/ml. Therefore, a study determining the accuracy of both SCC and culture to detect IMI (Vissio, Dieser, Agnelli, Odierno & Larriestra, 2014) proposes a lower threshold of 150,000 cells/ml, which can account for misclassification of the culture. The authors of that study suggest this is a more accurate SCC cutoff, providing information about the prevalence of subclinical mastitis corresponding to test sensitivity and specificity maximization. Even so, on an individual quarter basis, a SCC cutoff point of 100,000 cells/ml may be more appropriate (Pilla et al., 2012) if using differential cell counting as an alternative method in defining the presence of mastitis.

Somatic cell count can be measured by means of direct or indirect methods. Direct methods use either portable automatic cell counters, which are practical for field use, or automatic counters in a laboratory setting.^{i 3} There are a number of portable cell counters available. Some counters use an esterase-catalyzed enzymatic reaction^{j 3} and others^{k 3} count somatic cells optically by staining cell nuclei with a DNA-specific fluorescent reagent (propidium iodine). The advantages of these portable cell counters include cost-effectiveness, speed of use, and user friendliness, but they are generally considered to have poor sensitivity at low SCC (Viguier, Arora, Gilmartin, Welbeck & O’Kennedy, 2009). The laboratory cell counter^{i 3} operates on the principle of optical fluorescence as in the portable assay^{k 3} mentioned previously, but in this case the fluorescent reagent employed is ethidium bromide. The fluorescent signal generated is used to estimate the SCC in milk (Viguier et al., 2009). When comparing both methods,^{i,k} the automatic method has a higher repeatability (Gonzalo et al., 2006). The advantage with an automatic cell counter is that it is objective and accurate. Disadvantages are that it is time consuming because samples need to be sent to a laboratory, and the initial investment is high as the equipment is very expensive.

³ i. Fossomatic cell counter, FOSS, Hillerød, Denmark.

j. Portacheck somatic cell counter, Portacheck Inc., Moorestown, NJ.

k. Cell counter, DeLaval International AB, Tumba, Sweden.

Another direct detection method is differential cell count (DCC), which shows changes in relative cell proportions and can be used to differentiate healthy glands from inflamed glands. DCCs are performed on quarter milk samples by cytometry (Pilla et al., 2013) and have been proposed as a valid tool for the identification of inflammatory processes in cases with low SCC (Rivas, Quimby, Blue & Coksaygan, 2001). Recent studies (Pilla et al., 2012) have shown that DCC can reveal inflammatory mastitis processes with a sensitivity and specificity of 97.3% and 92.3%, respectively, even in milk with an SCC of 1,000 cells/ml (Pilla et al., 2013).

The California Mastitis Test (CMT) is a common indirect method for measurement of SCC. The test is performed by adding a detergent to a milk sample with a high cell count, which promotes cell lysis, nucleic acid release, and formation of a “gel-like” matrix. When the cell count is above a certain threshold, the sample viscosity interpretation is subjective, and might result in false positives or negatives (Viguier et al., 2009). A sensitivity of 66.7% and specificity of 54.8% using the CMT to detect IMI has been reported in fresh cows (Sargeant, Leslie, Shirley, Pulkrabek & Lim, 2001). The main advantages of CMT are that it is quick, cheap, simple, and is used as a “cow-side” test.

The Wisconsin Mastitis Test (WMT) is a laboratory test generally conducted on bulk tank milk samples. The scores can be used to predict the average number of somatic cells. This indirect method uses the same reagent as the CMT; however, the reaction is not estimated but measured by gel height in a tube, providing a more precise result than CMT. The results are generally reported in millimeters. The WMT is usually used as a screening test on producer’s milk because of its simplicity and objectivity, and also provides a convenient method of monitoring udder health on a herd basis.

In 2010, an indirect method to assess SCC and fat content in milk samples was published (Garcia-Cordero, Barrett, O’Kennedy & Ricco, 2010). The low-cost portable microfluidic sedimentation cytometer has a 15-min response time and shows a lower detection limit of 5×10^4 cells/ml.

1.3. Ion variation: milk conductivity

An effect of mastitis is changes in ion concentrations caused by increased vascular permeability (Kitchen, 1981) leading to modifications in electrical conductivity of milk. Electrical conductivity can be measured by rising conductance in milk caused by an increase in levels of sodium, potassium, calcium, magnesium, and chloride. To date, measurement of electrical conductivity is the most widespread automated detection method for mastitis in milking robots. In such systems, mastitis detection is generally performed through a combination of human inspection of animals, by electrodes in the milking system to detect changes in milk electrical conductivity, and by data analysis in herd management software to detect changes in milk yield and milking frequency. Although milk conductivity change might be useful in detecting mastitis, it is not a reliable or sensitive parameter for conclusive diagnosis (Hovinen, Aisla & Pyörälä, 2006) on its own because of the high number of false positives.

1.4. Biomarker evaluation

A biomarker is a characteristic that can be measured and evaluated as an indicator of normal biological processes, pathological processes, or pharmacological responses to therapeutic interventions (Boehmer, 2011). To be considered a “good” biomarker, the indicator must be specific for a disease and should remain unchanged by unrelated disorders. Likewise, reliable and reproducible biomarker quantification must be demonstrated (Issaq & Blonder, 2009).

As with the aforementioned ions, enzymes are also released into milk as a result of an animal’s immune response against infection and changes in vascular permeability. The enzymes dealing with milk synthesis tend to decrease, while the enzymes related to inflammation tend to increase (Pyörälä, 2003). The enzymes originating from phagocytes increase exponentially. Such enzymes include N-acetyl-d-glucosaminidase (NAGase), β -glucuronidase, and catalase. The activity of other enzymes originating in blood also increases, including plasminogen, which is locally activated as plasmin, a proteolytic enzyme that degrades fibrin and casein (Pyörälä, 2003). Several enzymes could be used as

biomarkers for mastitis diagnosis, including NAGase (Kitchen, Middleton & Salmon, 1978), serum amyloid A (SAA), haptoglobin (Hp), and lactate dehydrogenase (LDH), a cytoplasmic enzyme (Hiss, Mueller, Neu-Zahren & Sauerwein, 2007). A previous study (Åkerstedt, Forsbäcka, Larsena & Svennersten-Sjaunja, 2011) showed that LDH was the biomarker with the lowest variation between milkings in clinically healthy cows when compared with SAA, Hp, and NAGase. These authors assert that whatever the method used, several measurements over time could be a viable approach as well as information on the normal biomarker variation in clinically healthy udder quarters. Colorimetric and fluorimetric assays have been developed for measuring milk enzyme concentrations, which increase during the early stages of mastitis, including NAGase (Kitchen et al., 1978) and LDH (Larsen, 2005).

Milk proteins may be submitted to proteolysis caused by bacteria or endogenous proteases during episodes of mastitis. Peptide biomarkers of milk could thus be used in the diagnosis of mastitis and could discriminate between bacterial causes (Mansor et al., 2013). These authors used capillary electrophoresis, liquid chromatography, and mass spectrometry to reveal a biomarker panel of 47 peptides, with a sensitivity of 75% and specificity of 100% (Mansor et al., 2013). Immunoassays have also been used in the diagnosis of bovine mastitis to detect acute phase proteins Hp and SAA, which increase in milk during inflammation (Grönlund, Hultén, Eckersall, Hogarth & Waller, 2003), but could be ≤ 1 and ≤ 0.3 $\mu\text{g/ml}$, respectively, in healthy milk samples (Åkerstedt, Waller, Larsen, Forsbäck & Sternesjö, 2008). An ELISA has been developed for Hp with a detection limit of $0.07 \mu\text{g/ml}$ in milk and serum (Hiss, Mielenz, Bruckmaier & Sauerwein, 2004), and a commercially available solid-phase sandwich ELISA has been developed for SAA (Szczubiał, Dąbrowski, Kankofer, Bochniarz & Albera, 2008). A previous study (Welbeck et al., 2011) used an automated optical biosensor-based immunoassay to detect NAGase in milk. The limit of detection for the assay was $1 \mu\text{g/ml}$. Nevertheless, other researchers (Boehmer et al., 2010) assert that while ELISAs feature accuracy and specificity, antibody-based strategies are restricted by the ability to detect and quantify 1 protein at a time and by a reliance on the availability of species-specific antibodies. ELISAs, therefore, have little application to the discovery of novel inflammatory

mediators, as currently only a limited number of bovine-specific antibodies are available.

2. Discussion

Phenotypic methods continue to be more frequently used than genotypic methods for the identification of mastitis pathogens. However, we are faced with a few problems and challenges. One problem is the large proportion of milk samples submitted to bacteriological analysis from mastitis cases that lead to no-growth results (Taponen et al., 2009). These results are generally recognized as false negatives corresponding to detection failure of IMI causative agents (Koskinen et al., 2009).

Therefore, a considerable number of infected cows may remain undetected without a concomitant increase in SCC (Schwarz et al., 2010) and mastitis pathogen control and eradication in herds may be compromised (Cremonesi et al., 2009). Consequently, phenotypic identification is being supplemented with genotypic methods. A recent study (Raemy et al., 2013) supports the combination of conventional microbiology as first identification for triage and multiplex PCR use for rapid identification of bacteria associated with IMI. Molecular detection assays are a promising avenue in resolving false-negative issues, and several assays have already been developed that can provide solutions to this problem (Taponen et al., 2009).

On the other hand, phenotypic methods are usually considered less expensive than genotypic methods (Zadoks & Watts, 2009). Whether or not this is true, depends in part on the number of samples processed per time unit. In some laboratories, phenotypic tests are used with such high frequency that an investment in automation for test reading could become profitable (Ieven, Verhoeven, Pattyn & Goossens, 1995). Regardless of sample number, additional testing may be needed to obtain conclusive results from phenotypic methods. The potential increase in cost and turnaround time of phenotypic testing may narrow or eliminate the cost and time differences between phenotypic and genotypic identification (Ieven et al., 1995).

In addition, the cost of inaccurate results must also be taken into consideration (Zadoks & Watts, 2009). Ultimately, several genotypic methods require investment in equipment that is usually very expensive, which limits their use in routine diagnosis.

3. Future trends

Development prospects for new bovine mastitis diagnosis methodologies point to new biomarkers and technological advances for high sensitivity and specificity, fast and efficient devices that can offer a “cow-side” use. More recently, transcriptome and proteome analyses have been introduced to the biomedical research field. Such tests allow for the identification of biomarkers, gene expression profiles, and the understanding of complex molecular mechanisms in cell physiology and pathology (Klopfleisch & Gruber, 2012). Advances in relevant proteomic techniques such as 2-dimensional gel electrophoresis and mass spectroscopy (Smolenski et al., 2007) have led to the identification of several new proteins involved in mastitis. Progress in microbial proteomics has been achieved with the availability of whole genome sequences for a number of bacterial groups (Cash, 2000), including proteome profiles of mastitis-causing pathogens, which, combined with newly available information on toxins, enzymes, and metabolites produced in the udder, could lead to their identification in milk (Viguier et al., 2009). Proteomic studies performed for several mastitis pathogens have led to information on protein expression pattern, which can be applied to the discovery of new therapeutic targets (Lippolis & Reinhardt, 2010) (e.g., bacterial immunogenic proteins for vaccines) and new diagnostic biomarkers.

Biosensors are fast becoming the next generation of tools in analyzing areas such as environmental research, medicine, biodefense, agriculture, and food control (Lazcka, Del Campo & Muñoz, 2007). Biosensors use biological receptor molecules (e.g., antibody, enzyme, and nucleic acid) combined with a transducer to produce a signal that shows a specific biological event (e.g., an antibody–antigen interaction). Nanotechnology-based pathogen detection has created an array of technologies that have advanced detection, diagnosis, and imaging of

biomarkers of disease pathogenesis (Driskell & Tripp, 2009), shortening the time span between sample uptake and results. Portability of biosensors has been explored over the past 15 years through lab-on-chip platforms, incorporating electronics, sampling, and detection modules necessary for a fast, accurate, and low-cost analysis. Several types of these biochips have been demonstrated, using several detection principles: chemical (Pinijsuwan, Rijiravanich, Somasundrum & Surareungchai, 2008), mechanical (Gfeller, Nugaeva & Hegner, 2005), optical (Gunnarsson, Jönsson, Marie, Tegenfeldt & Höök, 2008), electrical (Gonçalves, Prazeres, Chu & Conde, 2008) and magnetic (Martins et al., 2010).

4. Conclusion

A variety of mastitis diagnostic tests are routinely used to evaluate microbiological milk quality in dairy farms. The successful choice for a test that evaluates milk requires methodological knowledge and diagnostic capabilities for each test currently available. The suitability of a detection method for routine diagnosis depends on its specificity, sensitivity, cost, amount of processing time, and suitability for a large number of milk samples. New technical advances in mastitis diagnosis still require specialized training and experience to interpret results. The personnel responsible should be aware of the strict compliance of each step in the process for good quality control in obtaining reliable data.

PCR and conventional bacteriological culture are the most common tools used for pathogen detection and represent reliable diagnostic methodologies for veterinarians and farmers. The sensitivity of culture tests may be complemented by PCR analysis and are often combined together to yield more robust results. However, to make treatment decisions, this combination does not allow for a timely answer. Proteomic research for reliable biomarkers is viable for the early detection of mastitis and drug efficacy, and to discover potentially novel targets for the development of alternative therapies. However, these innovations are still not possible to use for routine diagnosis. In conclusion, the demands for an alternative, fast, and accurate diagnostic procedure for mastitis is rising as farms increase in size, cows produce more milk, and milking techniques such as automatic milking systems become more common.

CHAPTER II

Specific antibodies selection.

The author contributed to the conception and design of the study and conducted the experiments.

1. Introduction

A comprehensive understanding of the pathogenicity of bovine mastitis is the key for the development of appropriate detection techniques (Viguier et al., 2009). Mastitis is a multifactorial disease usually caused by a microbial infection. Once inside the teat, bacteria must also elude the cellular and humoral defense mechanisms of the udder and if they are not eliminated, they start multiplying in the mammary gland (Sordillo & Streicher, 2002).

An antibody (Ab) or immunoglobulin (Ig), is a glycoprotein produced by plasma B-cells. There are five different isotypes of antibodies with different organism distributions and functions: IgM, IgG, IgD, IgA and IgE. The IgD is present on B-cell surface as antigen receptor, IgA is a secretory antibody found as dimer in secretions and IgE is involved in allergenic responses (Tizard, 2009). The complement system is a part of the immune system that enhances (complements) the ability of antibodies and phagocytic cells to destroy pathogens from an organism. Only IgM and IgG antibodies have the ability to trigger and interact with the complement cascade system.

Natural antibodies are produced in the complete absence of external antigenic stimulation and are a component of innate humoral defenses. The term humoral immune response refers to immunological action of antigen-specific antibodies, which are secreted by activated B cells. Antibodies produce an immune response through three main mechanisms: neutralization, opsonization, and activation of the complement cascade (Tizard, 2009). Neutralization simply refers to the process by which antibodies prevent pathogens from entering into host cells by binding to its surface proteins. Opsonization occurs after antibodies coat the surface of the pathogen, binding to the antigen (cell wall protein) so that the antigen molecules can be recognized and destroyed by phagocytes. The complement cascade itself has two possible outcomes: pathogen opsonization by certain complement proteins and direct killing of the invading pathogen by the formation of a pore in the plasma membrane (Janeway, Travers, Walport, & Shlomchik, 2001) through which polymorphonuclear neutrophils pass to engulf and destroy it.

As far as mastitis-causing bacteria are concerned, cows have opsonic antibodies in their serum. In rather low concentrations, opsonic antibodies belong to the IgG2 and IgM isotypes (Guidry, Berning & Hambleton, 1993), but much of the

opsonic antibodies in adult serum and milk of cows are IgM (Hill, Heneghan & Williams, 1993). Nevertheless, bacteria are opsonized as soon as inflammation develops and plasma is released in milk. This is true in animals without previous history of mastitis. The spontaneous and general occurrence of Ab, particularly in the IgM class, suggests that these are natural Ab. They provide immediate, early and extensive protection against pathogens, before adaptive antibodies are developed in the course of infections (Rainard & Riollot, 2006).

Bacteria at different growth states may preferentially express different sets of molecules to allow their growth and virulence factors to be under precise control (Beier & Gross, 2006; Bronner, Monteil & Prévost, 2004). Bacteria even undergo antigenic variations to escape the hosts' surveillance (Loughman et al., 2008; van der Woude & Bäumler, 2004). Phase and antigenic variation result in a heterogenic phenotype of a clonal bacterial population, in which individual cells either express the phase-variable protein(s) or not, or express one of multiple antigenic forms of the protein, respectively (Barbour, 2002). This form of regulation has been identified mainly for a wide variety of surface structures in animal pathogens and is implicated as a virulence strategy (van der Woude & Bäumler, 2004).

Proteomics techniques (high resolution two-dimensional electrophoresis and protein characterization) are widely used for microbiological research to analyze global protein synthesis as an indicator of gene expression (Aebersold, Rist & Gygi, 2006). Western Blotting is an example of a rapid and sensitive method for characterizing purified proteins or complex mixtures of proteins. Western blotting consists in the separation of proteins by gel electrophoresis [usually with the high resolution of SDS-polyacrylamide gel electrophoresis technique (SDS-PAGE)] followed by the transfer of these proteins to a membrane to obtain a blot. Immunoblotting combines this technique with the specificity and sensitivity of immune detection.

The present study supports the immunological recognition achieved during dynamic detection of bacterial cells in raw milk performed by the mastitis diagnosis method henceforth developed and extensively described in this thesis. Therefore, it was critical to know if immunogenic cell wall proteins of selected target pathogens were recognized by commercially available antibodies. The selected immunoglobulins G and M were from animal species other than bovine

to avoid immunological cross reactivities with those present in cow's milk, which potentially recognize different epitopes of the bacterial cell wall proteins (Tizard, 2009). Adding to this, these two immunoglobulins have binding affinity to protein A (Ljungberg et al., 1993) which was useful for nanoparticles functionalization because nanoparticles' bonding molecules to antibodies are 2 to 5 protein A around its surface.

To mimic immunological recognition with whole cells in the developed magnetic detection method, ELISA trials were performed. Only one of the four selected primary antibodies was used for guidance of further magnetic labelling cell.

The main goal of this study was to verify antigen identification by each antibody tested, and also to measure the antibodies' specificity in immunoblotting and sensitivity in the ELISA tests performed.

2. Material and Methods

This study included three reference strains from ATCC and CECT culture collections including *Staphylococcus aureus* (ATCC 29213), *Streptococcus agalactiae* (CECT 183) and *Streptococcus uberis* (CECT 994), and three other bovine mastitis isolates, *Staphylococcus chromogenes* (10Q1397LH1) and *Staphylococcus epidermidis* (5M3129LF) both previously identified genotypically (Bexiga et al., 2014) and *Streptococcus dysgalactiae* (79_04) identified phenotypically by a commercial identification system (API 20 Strep®, bioMérieux).

All strains mentioned were stored in aliquots at -80°C and kept in buffered peptone water (Scharlau, 02-277-500).

2.1. Staphylococci protein extraction

The extraction of cell wall proteins for selected staphylococci strains was based on the adapted protocol of Bedidi-Madani, Greenland & Richard (1998), as briefly described herein.

Each thawed staphylococci strain was plated onto an agar plate with 5% of sheep blood (Oxoid, CM854) and kept at 37°C, during 24h. After confirmation of culture purity, all the colonies were collected and inoculated onto 25 ml of BHIB

for incubation at 37°C, for 24h until evidence of growth for further protein extraction.

The previous microbiological cultures were centrifuged in three cycles, the first at 4500 rpm, for 15 min at 4°C, the second at 3500 rpm, for 15 min at 20°C and the last at 4000 rpm, for 5 min at 20°C. Between cycles, each remaining bacterial pellet, after discarding of the supernatant, was washed with sterile deionized water and centrifuged again. The resulting pellet was resuspended in 0.7 ml of sterile deionized water and submitted to strong manual agitation. That suspension was transferred to a 1.5 ml sterile micro centrifuge tube, to which 30 µl of a 10 mg/ml of lysostaphin (Sigma, L-7386) was added. After agitation, the suspension in the micro tube was incubated in a water bath at 37°C, overnight (16 h maximum). After that, 50 µl of a 20% SDS (sodium dodecyl sulfate) solution was added. To finish bacterial lysis, suspensions were boiled for 10 min in a dry bath (QBD2, Grant) and were further centrifuged at 7000 rpm for 15 min, at 20°C. Sterile supernatant collection was performed with a syringe and finally filtered through a porous membrane with 0.2 µm diameter (Acrodisc 4192, Gelman). The protein extracts obtained were preserved in aliquots at -20°C until immunoblotting trials.

2.2. Streptococci protein extraction

The extraction of cell wall proteins for streptococcal strains was based on the adapted protocol from Cole, Djordjevic & Walker (2008), as follows.

The thawed streptococci strains were plated onto an agar plate with 5% of sheep blood (Oxoid, CM854) at 37°C, during 24h. After confirmation of culture purity, all the colonies were collected and inoculated in 2 ml of TSB (tripticasein soy broth) (Pronadisa, 1224.00) and incubated at 37°C, for 24h until evidence of growth. To the previous bacterial suspension, a higher volume of 98 ml of sterile TSB was added and a 24h of incubation at 37°C was followed for further protein extraction.

Each previous overnight culture was transferred to a sterile centrifuge tube and the bacterial cells were harvested by centrifugation at 4200 rpm for 20 min, at 4°C. The remaining pellet, after discarding the supernatant, was placed on ice for 5 min and then resuspended in 5 ml of chilled TE (Tris-EDTA) buffer containing 1 mM PMSF (phenylmethylsulphonyl fluoride) (Sigma, P7626), by pipetting

successively while avoiding the formation of foam and until no bacterial clumps were visible. This bacterial suspension was centrifuged twice at 4200 rpm for 20 min, at 4 °C and the supernatant was discarded. Then, the pellet was resuspended in 1.15 ml of ice-cold mutanolysin mix by pipetting successively. This suspension was transferred to a sterile micro centrifuge tube and incubated for 2h at 37°C under agitation. After incubation, the suspension was centrifuged at 8000 rpm for 5 min, at room temperature (RT) and the supernatant was collected (solubilized cell wall-associated proteins) by aspiration. The obtained protein extracts were stored in aliquots at -20°C until immunoblotting trials.

2.3. Protein quantification

The amount of cell wall-associated proteins in bacterial extracts was determined by Bicinchoninic Acid (BCA) Protein Assay Kit (Sigma). The principle of the BCA assay relies on the formation of a Cu^{2+} -protein complex under alkaline conditions, followed by reduction of the Cu^{2+} to Cu^{1+} , forming a purple-blue complex. The amount of reduction is proportional to the protein present and can be monitored at absorbance 562 nm (Smith et al., 1985).

2.4. Selected antibodies

The following primary antibodies were used: rabbit anti-*Staphylococcus aureus* ScpA polyclonal antibody (ab92983, Abcam) which recognizes the extracellular cysteine proteinase staphopain A (ScpA), a putative virulence factor; mouse anti-*Staphylococcus aureus* ATCC 29740 monoclonal antibody (MCA 5793, AbDSerotec) which recognizes the peptidoglycan of *S. aureus*, protein A-negative *S. aureus* and *S. epidermidis* and generally referred to as anti-*Staphylococcus* spp.; rabbit anti-*Staphylococcus aureus* polyclonal antibody (AB-T161, Advanced Targeting Systems) which recognizes all cell wall proteins of *Staph. aureus*; rabbit anti-*Streptococcus* B polyclonal antibody (8435-2000, AbDSerotec) which reacts with type specific carbohydrate of group B *Streptococcus*); and finally, mouse anti-*Streptococcus agalactiae* monoclonal antibody (MA1-10871, ThermoScientific) which specifically detects *S. agalactiae*.

All dilutions of primary antibodies were performed in PBST solution and incubated 2 or 3h according to manufacturers' instructions at user improved concentrations.

The following HRP-conjugated antibodies were used: donkey F(ab) anti-rabbit IgG (H&L) antibody (ab102283, Abcam); goat anti-mouse IgM antibody (PA1-85999, Thermo Scientific); goat anti-rabbit IgG antibody (STAR 124P, AbDSerotec); donkey anti-rabbit IgG (H&L) antibody (ab7083, Abcam) and a rabbit anti-mouse IgM antibody (31456, Thermo Scientific).

For immunoblotting analysis, HRP-conjugated secondary antibodies were incubated during one hour period at user improved concentrations in PBST.

2.5. Immunoblotting

Three different strains, by bacterial genus, were tested simultaneously. The protein extracts from each isolate were properly diluted in deionized water to achieve good protein resolution (1 µg of protein per 1 µl of sample). Further addition of Laemmli buffer and a boiling pre-treatment step of 1-3 min were necessary to assure protein denaturation. Clarified protein cell wall fractions were then resolved by SDS-PAGE (Laemmli, 1970) and electroblotted onto a 0.45 µm pore diameter PVDF membrane (IPVH 00010, Millipore), according to Towbin, Staehelin & Gordon (1979) methodology. Blots were further blocked with PBS plus 0.05% Tween 20 (PBST buffer) containing 5% of nonfat dry milk (w/v), during 1h at RT, and later incubated with specific primary antibodies during 2 or 3h, depending on specific Ab. After three 10-min wash steps with PBST buffer, immunoblots were exposed to HRP-conjugated secondary antibodies (1h at RT) followed by chromogenic detection through a dark brown reaction resulting from DAB (3,3'-diaminobenzidine, D4293, SigmaFast) oxidation by peroxidase enzyme.

The PVDF membrane contained triplicates of the protein blot profiles of the three strains, and was divided to obtain the antigenic detection test (incubation with both primary Ab and HRP-conjugated one) and two negative controls (unique incubation with primary Ab or with HRP-conjugated Ab).

2.6. Direct ELISA

An enzyme-linked immunosorbent assay (ELISA) was performed with *Streptococcus agalactiae* (CECT 183), *Streptococcus uberis* (CECT 994) and *Streptococcus dysgalactiae* (79_04) whole cells, with the antibodies rabbit anti-*Streptococcus* Group B (IgG) (8435-2000, AbDSerotec) and goat anti-rabbit IgG (STAR 124P, AbDSerotec), according to Hudson & Hay (1989) and AbDSerotec (2013) protocols.

For each bacterial isolate, plates were coated with serial dilutions of bacterial cells and a cross-titration was performed with serial dilutions of the selected antibodies, in order to establish the optimum antigen coating and antibody concentrations.

Bacterial cells were grown separately onto Columbia agar supplemented with 5% sheep blood (bioMérieux, 43021) and incubated at 37°C, overnight. Four colonies of each isolate were selected and re-suspended onto 4 ml of Trypticase Soy Broth over 24 hours at 37°C. Subsequently, the bacterial cells were collected through centrifugation (15 minutes, 17°C, 2700 rpm) and re-suspended in PBS 1X (pH 7.2) to allow optical density measurement (at 600 nm) (BECKMAN DU-68 Spectrophotometer) and for colony-forming unit estimation. A bacterial suspension with a known concentration of 10⁸ CFU/ml was the starting point to get different bacterial dilutions for each species, in carbonate-bicarbonate buffer: 1/2; 1/5; 1/10; 1/25; 1/50 and 1/100.

Both antibodies were diluted in PBST buffer (1/500; 1/1000 and 1/5000 dilutions for rabbit anti-*Streptococcus* Group B antibody, and 1/50000; 1/75000 and 1/100000 dilutions for the goat anti-rabbit IgG antibody). All antibodies and bacterial dilutions were tested in triplicate per microtiter plate, and negative controls included wells with only or without bacteria and wells with only or without antibodies.

Briefly, microtiter plate wells (3361 Costar, Corning Incorp, USA) were coated with 100 µl of three different bacterial concentrations diluted in carbonate-bicarbonate buffer and incubated overnight at 4°C. After discarding the remnant buffer, wells were coated with 250 µl of blocking solution (PBS + 1% BSA (w/v) for 1h and washed once with PBST. The incubation with different concentrations of primary Ab (100µl/ well) was performed at RT for 2h. After three 10-min wash steps with PBST buffer, the wells were coated with 100µl of conjugated Ab

solution at different concentrations and incubated at RT for 1h. After another three 10-min wash steps with PBST buffer, the targeted bacterial cells were incubated with 100µl of TMB (eBioscience Cat. No. 00-4201, LabClinics) substrate solution, protected from light for 20 min. Afterwards, each well was filled with 100µl of 2M H₂SO₄ to stop colorimetric reaction. Finally, absorbance was read at 450nm.

3. Results and Discussion

3.1. Immunoblotting

To achieve optimal conditions for specific immune detection by the antibodies it was necessary to vary experimental conditions (Abcam, 2011), changing sequentially the concentration (acrylamide/ bisacrylamide amount in the resolving gel, immunogenic proteins and antibodies); voltage values [electrophoresis (85-120V for stacking gel, 195-250V for resolving gel) and protein transfer (25-30V)]; time [electrophoresis (5-8h), protein transfer (16-18h) and antibodies incubation (1-3h)]; and also the temperature [protein transfer (coil of cold water) and antibodies incubation (4-25°C)].

Immunoblotting results are evidenced on Figures 1 to 4 and translate the final optimal conditions for antigenic recognition and blot visualization for protein quantities, primary and secondary antibodies concentrations, incubation times and temperature. Antigenic recognition was achieved for selected primary antibodies and conjugated pairs followed.

For rabbit anti-*Staphylococcus aureus* antibody (IgG) (1.5 µg/ml, 3h, RT) and donkey F(ab) anti-rabbit IgG (HRP) antibody (0.2 µg/ml, 1h, RT), 40µg of protein for *Staph. aureus*, *Staph. epidermidis* and *Staph. chromogenes* extracts were used to achieve optimal recognition and visualization. Three narrowed blots were evidenced in *Staph aureus* protein profile (Figure 1) showing immunogenic proteins weights between 48 and 60 kDa, but also three faded blots were evidenced between 35 and 48 kDa. These results were achieved after changing temperature and incubation time of primary and HRP-conjugated antibodies from overnight at 4°C to a few hours at RT showing that higher temperature was necessary by these antibodies for efficient immunological detection. On the other hand, the variation of primary antibody concentration from 1 to 3 µg/ml and of

protein extracts amounts from 20, 40, 50 and 60 µg, helped to assess the final clear blot pattern on PVDF membrane.

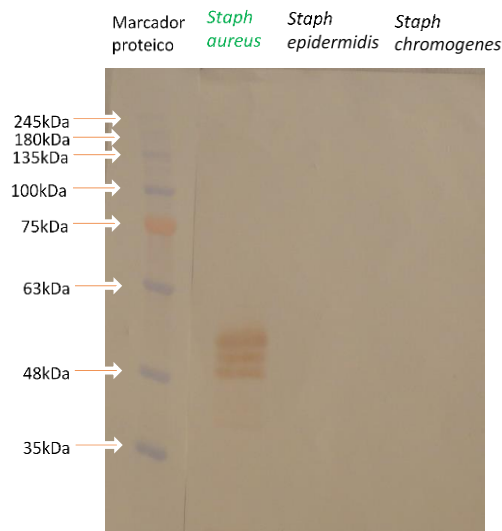


Figure 1. Immunogenic proteins from *Staphylococcus aureus* identified by rabbit anti-*S. aureus* ScpA (ab 92983) are evidenced as dark brown blots. Molecular weights (kDa) of evaluated proteins are indicated on the left of immunoblot images.

Regarding the mouse anti-*Staphylococcus* spp antibody (2.25 µg/ml, 3h, RT) and goat anti-mouse (HRP) antibody (0.25 µg/ml, 1h, RT), the same 40µg of protein for each three staphylococci strain extracts were used to achieve optimal recognition and visualization. One slight blot with 60 kDa was observed for *Staph. aureus* and another one with 17 kDa was evidenced for *Staph. epidermidis* (Figure 2). These results were achieved after varying both antibodies concentration from 2 to 2.25 µg/ml and from 0.11 to 0.25 µg/ml, respectively, which helped to assess the final clear blot pattern on PVDF membrane. Adding to that, the decrease of the resolving gel pore size, corresponding to higher percentage of acrylamide/bisacrylamide content (15% instead of previous 12% gel's used), caused a decreasing rate of protein migration and better separation of smaller and lighter immunogenic proteins.

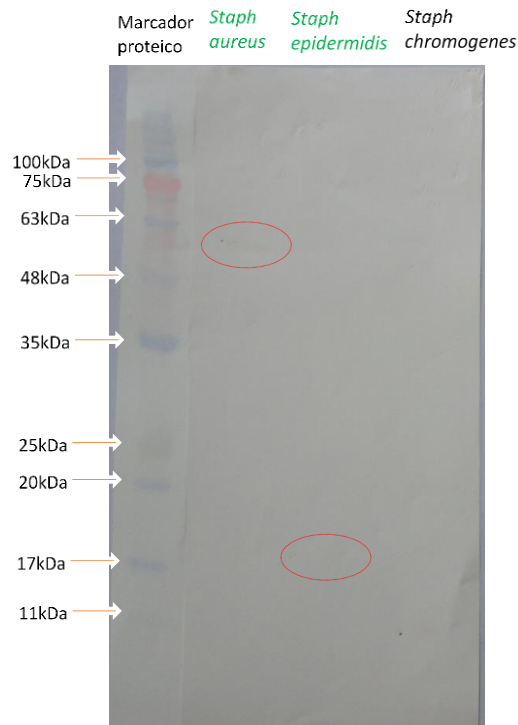


Figure 2. Immunogenic proteins from *Staphylococcus aureus* and *Staphylococcus epidermidis* identified by mouse anti-*Staphylococcus* spp. (MCA 5793) are evidenced as dark brown blots. Molecular weights (kDa) of evaluated proteins are indicated on the left of immunoblot images.

Concerning rabbit anti-*Streptococcus* Group B antibody (IgG) (2 μ g/ml, 3h, RT) and goat anti-rabbit IgG (HRP) antibody (0.2 μ g/ml, 1h, RT), 40 μ g of protein for *Strep. agalactiae*, 50 μ g of protein for *Strep. uberis* and 40 μ g of protein for *Staph. chromogenes* extracts were considered to lead to optimal recognition and visualization. Several narrowed blots above 100kDa weight were shown in the *Strep. agalactiae* protein profile and also other faded immunogenic proteins between 23 and 75 kDa weight. On the other hand, two immunogenic proteins from *Strep. uberis* were evidenced around 30 kDa and 40 kDa (Figure 3). These results were obtained after varying HRP-conjugated antibody concentration from 0.5 to 0.2 μ g/ml and protein extracts amounts differentiation from an equal amount of 30 μ g for all three strains protein extracts, with increased time of boiling pre-treatment step from 1 to 3 min to ensure protein denaturation and to assess the final clear blot pattern on PVDF membrane.

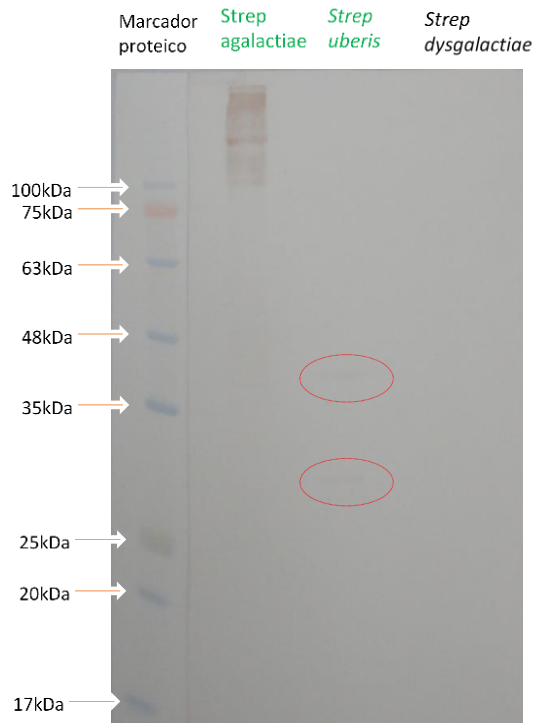


Figure 3. Immunogenic proteins from *Streptococcus agalactiae* and *Streptococcus uberis* identified by rabbit anti-*Streptococcus* Group B (8435-2000) are evidenced as dark brown blots. Molecular weights (kDa) of evaluated proteins are indicated on the left of immunoblot images.

For mouse anti-*Streptococcus agalactiae* antibody (IgM) (2 $\mu\text{g/ml}$, 3h, RT) and goat anti-mouse IgM (HRP) antibody (0.11 $\mu\text{g/ml}$, 1h, RT), 100 μg of protein for *Strep. agalactiae*, 50 μg of protein for *Strep. uberis* and 65 μg of protein for *Staph. chromogenes* extracts were considered to lead to optimal recognition and visualization. Several narrowed blots above 135 kDa weight were evidenced in the *Strep. agalactiae* protein profile (Figure 4). These results were achieved after decreasing *Strep. agalactiae* protein extract amount from 55 to 40 μg , which helped to assess the final clear blot pattern on PVDF membrane. Adding to that, the increase of the resolving gel pore size, corresponding to lower percentage of acrylamide/bisacrylamide content (7.5% instead of previous 12% resolving gel's used), allowed an increased rate of protein migration and better individualization of bigger and heavier immunogenic proteins, as shown in Figure 4.

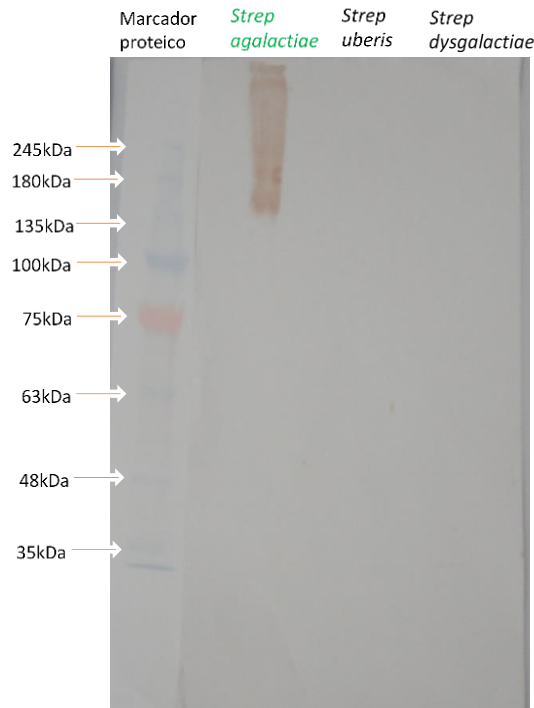


Figure 4. Immunogenic proteins from *Streptococcus agalactiae* identified by mouse anti-*Streptococcus agalactiae* (MA1-10871) are evidenced as dark brown blots. Molecular weights (kDa) of evaluated proteins are indicated on the left of immunoblot images.

The three remaining antibodies tested, such as the primary rabbit anti-*Staph. aureus* antibody (AB-T161, Advanced Targeting Systems) and the two HRP-conjugated antibodies, donkey anti-rabbit IgG (H&L) antibody (ab7083, Abcam) and rabbit anti-mouse IgM antibody (31456, Thermo Scientific), evidenced lack of specificity to our targeted proteins.

The primary antibody mentioned (AB-T161, Advanced Targeting Systems) was used with the donkey anti-rabbit IgG (H&L) antibody (ab7083, Abcam) and did not recognize any of the staphylococcal cell wall proteins used in our experiments.

Both HRP-conjugated antibodies (ab7083, Abcam; 31456, Thermo Scientific) evidenced nonspecific bounding to immunogenic cell wall proteins of *Staph. aureus* and of *Strep. dysgalactiae*, respectively, shown on PVDF controls incubated only with the HRP-conjugated antibody and without the correspondent primary antibody. The first HRP-conjugated antibody (ab7083, Abcam) was tested with both rabbit anti-*Staph. aureus* ScpA antibody (ab92983, Abcam) and rabbit anti-*Staph. aureus* antibody (AB-T161, Advanced Targeting Systems), and

the second one (31456, Thermo Scientific) was tested only with the mouse anti-*Strep. agalactiae* monoclonal antibody (MA1-10871).

To avoid *Staph. aureus* recognition by the HRP-conjugated antibody (ab7083, Abcam) instead of rabbit anti-*Staph. aureus* ScpA antibody (ab92983, Abcam), the first one was replaced by an incomplete HRP-conjugated immunoglobulin G with only antigen binding fragment (F(ab)) (ab102283, Abcam). This fact eliminated the probability of higher binding affinity to staphylococcal protein A, by the IgG' Fc fraction (Ljungberg et al., 1993), translated on better results as shown in Figure 1.

3.2. Direct ELISA

To achieve optimal conditions for ELISA trials based on previously described protocol (section 2.6.), it was necessary to vary experimental conditions, especially washing times, blocking conditions (with BSA instead of nonfat dry milk), concentration of bacterial cells and antibodies, time of incubation and detection, and temperature (KPL, 2013).

Nevertheless, the minimum concentration of both whole cells of *Strep. agalactiae* and *Strep. uberis* bounded to rabbit anti-*Streptococcus* Group B antibody was 10^3 CFU/ μ l (10^6 CFU/ml), and the correspondent concentrations observed for primary and HRP-conjugated Ab, to detect both streptococci immunogenic proteins were 1 μ g/ml (1/1000 dilution) and 0.0133 μ g/ml (1/75000 dilution), respectively.

Comparing our ELISA test sensitivity (10^6 CFU/ml) to detect streptococci cells to a sandwich ELISA test recently patented (Libing et al., 2012) to detect *Staph. aureus* in artificially contaminated milk, a lower detection limit of 10^5 CFU/ml was found. Also, a previous study (Heller, Berthold, Pfützner, Leirer & Sachse, 1993) using *Mycoplasma bovis* cells in milk samples, obtained the same sensitivity (10^5 CFU/ml) through an ELISA test employing a monoclonal antibody.

4. Conclusions

The four primary antibodies mentioned, evidenced affinity to correspondent immunogenic cell wall proteins of *Staphylococcus aureus*, *Staphylococcus epidermidis*, *Streptococcus agalactiae* and *Streptococcus uberis* in the described immunoblotting conditions. This information was necessary for the quantification analysis of the magnetic detection methodology, concerning to the expected number of immunogenic cell wall proteins to be identified on each bacterial strain, as detailed in chapters III, V and VI of this thesis.

Despite the higher sensitivity of ELISA trials, its results were the working basis to start nanoparticles functionalization experiments, necessary for bacterial magnetic labelling. The *Strep. agalactiae* was the first species to be tested in the biosensor with a concentration used in sterile milk of 10^3 CFU/ μ l and a concentration of the primary antibody (rabbit anti-*Streptococcus* Group B antibody) of 1 μ g/ml. Moreover, the nanoparticle functionalization was based on antibody number (number/ volume) instead of concentration (weight/ volume). Briefly, a phosphate buffered saline (PBS) and ethylene diamine tetra acetic acid (EDTA) mix with known number of nanoparticles with primary antibody was added to milk samples, containing the minimal detectable concentration of bacterial cells found in ELISA trials, and subsequently analyzed by the biosensor, as explained in the next chapters.

CHAPTER III

Lab-on-chip cytometry based on magnetoresistive sensors for bacteria detection in milk.

A.C. Fernandes, *C.M. Duarte, F.A. Cardoso, R. Bexiga, S. Cardoso, P.P. Freitas
(2014). *Sensors*, 14, 15496-15524.

* The author contributed to the conception and design of the study, conducted the experiments and drafted the manuscript.

Abstract

Flow cytometers have been optimized for use in portable platforms, where cell separation, identification and counting can be achieved in a compact and modular format. This feature can be combined with magnetic detection, where magnetoresistive sensors can be integrated within microfluidic channels to detect magnetically labelled cells. This work describes a platform for in-flow detection of magnetically labelled cells with a magneto-resistive based cell cytometer. In particular, we present an example for the validation of the platform as a magnetic counter that identifies and quantifies *Streptococcus agalactiae* in milk.

Keywords: cytometer; microfluidic; magnetoresistive sensor; milk; *Streptococcus agalactiae*.

1. Introduction

Flow cytometry is a technique that enables the measurement of morphological, biochemical and functional characteristics of microscopic particles (cells, viruses, bacteria, yeast, intracellular organelles, aerosol particles or microbeads (from 0.2 μm to 150 μm diameter) suspended in a stream of fluid. It allows the characterization and quantification of a population at high rates and with a high-throughput (Groisman & Simonnet, 2006). The multiparametric analysis of the particles can be performed by light scattering or staining the particles with fluorophores (fluorescent conjugated antibodies or absorption dyes) or quantum dots and presenting the particles, one by one, to a laser beam of a single wavelength or arc lamp (Groisman & Simonnet, 2006 ; Yu, Kim, Niessner & Knopp, 2012; Piyasena & Graves, 2014).

For the past three decades, advances in sample pre-treatment, flow handling, precision technologies, synthesis of emitting particles, data handling techniques and bioinformatics have allowed the introduction of this sophisticated analytical tool into routine clinical and laboratory use in cell/molecular biology fields (Harding, Lloyd, McFarlane & Al-Rubeai, 2000; Boeck, 2001; Rieseberg, Kasper, Reardon & Scheper, 2001), formulation and biotesting of compounds (Mach et al., 2011; Edwards, Oprea, Prossnitz & Sklar, 2004), disease diagnosis (Stein, Korvick & Vermund, 1992; Fenili & Pirovano, 1998; Schmid, Tinguely, Cione, Moch & Bode, 2011), immunology (Gabriel & Kindermann, 1995; Garratty & Arndt, 1999), genetics (Wedemeyer & Pötter, 2001), industrial bioprocesses (Díaz, Herrero, García & Quirós, 2010), and environmental monitoring (Yu et al., 2012; Dubelaar, Gerritzen, Beeker, Jonker & Tangen, 1999; Hammes et al., 2008). In addition to detection and enumeration, some flow cytometers have the ability to sort cells at high speeds based on detected signals without loss of viability or particle-specific characteristics (Piyasena & Graves, 2014).

Although conventional state-of-the-art flow cytometry systems provide rapid and reliable analytical results, and despite the considerable recent technological advances, these devices are still bulky, expensive and complex. Over the past years, the drawbacks of conventional flow cytometers have encouraged efforts to take advantage of microfabrication technologies and advanced microfluidics to

achieve smaller, simpler, more innovative and low-cost instrumentation with enhanced portability for on-site measurements. This miniaturization approach has in general made use of inexpensive polymers such as polydimethylsiloxane (PDMS) (Huh, Gu, Kamotani, Grotberg & Takayama, 2005) and detection techniques easily integrated with electronics (Chung & Kim, 2007), such as optical fibers (Frankowski et al., 2013), CCD cameras (Yang et al., 2006), diode lasers (Kim et al., 2009; Akagi et al., 2013), PIN photodiodes (Kettlitz, Valouch, Sittel & Lemmer, 2012), electrodes (Hassan, Watkins, Edwards & Bashir, 2014) and magnetoresistive sensors (Loureiro et al., 2011). Approaches such as label-free electrical impedance-based ones (Kemna, Segerink, Wolbers, Vermes & van den Berg, 2013; Esfandyarpour, Javanmard, Koochak, Harris & Davis, 2013), while quantitative and high throughput, present high sensitivity to the sample matrix, being affected by components in the sample other than the target, specifically their charges, which greatly hinders these devices' use in off-laboratory locations. This could also occur in fluorescent applications (Spencer, Elliott & Morgan, 2013), due to non-specific adsorption of fluorophores or self-fluorescence of sample components (Freitas et al., 2012). Some platforms present a static detection (²Fernandes et al., 2014) where labels complementary to the target are immobilized on sensor's surface. This approach, while sensitive and quantitative, is limited by the sensor's surface area and number of immobilized labels/targets, further requiring careful selection of sample flow rate.

Other sample focusing techniques have also been applied (Chung & Kim, 2007; Frankowski et al., 2013; Kim et al., 2009; Piyasena et al., 2012). Along with detection and enumeration, high speed sorting has been an important theme in the development of micro fabricated flow cytometers and for other applications (Fu, Spence, Scherer, Arnold & Quake, 1999; Fu, Chou, Spence, Arnold & Quake, 2002; Kruger et al., 2002; Voldman, Gray, Toner & Schmidt, 2002; Wolff et al., 2003; Fu, Yang, Lin, Pan & Lee, 2004). Several strategies have been applied to this effect (Piyasena & Graves, 2014; Chung & Kim, 2007; Gossett et al., 2010; Autebert et al., 2012; Yang & Soh, 2012; Wang et al., 2013; Ozkumur et al., 2013 ; Tan, Kee, Mathuru, Burkholder & Jesuthasan, 2013). Regardless of the use of solid-state devices to reduce the volume of the whole system, these micro fabricated systems require external equipment for the detection and enumeration of cells/particles (Freitas et al., 2012).

This work describes the development, characterization and application of a magnetic detection device for the identification and quantification of *Streptococcus agalactiae* in a complex matrix (milk), based on a previously developed platform (Loureiro et al., 2011; Freitas et al., 2012), schematically depicted in Figure 5. This device comprises magnetoresistive (MR) sensors, namely spin-valve sensors (SVs), integrated with a microfluidic platform and connected to an amplification and acquisition setup. The sensors have excellent spatial resolution (on the micrometer range) and are sensitive to the magnetic field created by magnetized beads flowing in microchannels above the sensors. The detection scheme used in this platform relies on the MR sensor's sensitivity to count individual cells in flow, contrary to other approaches (Mujika et al., 2009) while providing information on nanoparticles' magnetization direction along the flow process. Therefore, no additional cell culture is needed. In addition, this platform is compatible with complex matrixes without the need of intricate sample pre-processing, while using a detection principle (magnetic) non-existent in Nature (thus greatly reducing biological background noise and false positives). The use of magnetoresistive sensors also simplifies connection with electrical equipment while still allowing coupling with other detection techniques (e.g., fluorescence or a laser-irradiated magnetic bead system (LIMBS)) if needed. This work, unlike other platforms (Helou et al., 2013; Qiu, Zhou, Chen & Lin, 2009; Golberg et al., 2014) provides a simple approach for single cell detection, without the need for cell guiding mechanisms of hydrodynamic focusing approaches, targeting at a broader area of application - such as bacterial detection in food and water samples. To be competitive to other bulk cytometers, however, this approach should be able to accept large volumes of samples, operating with high flow rates (cm/s at least), and using multiple channels in a parallel sampling architecture.

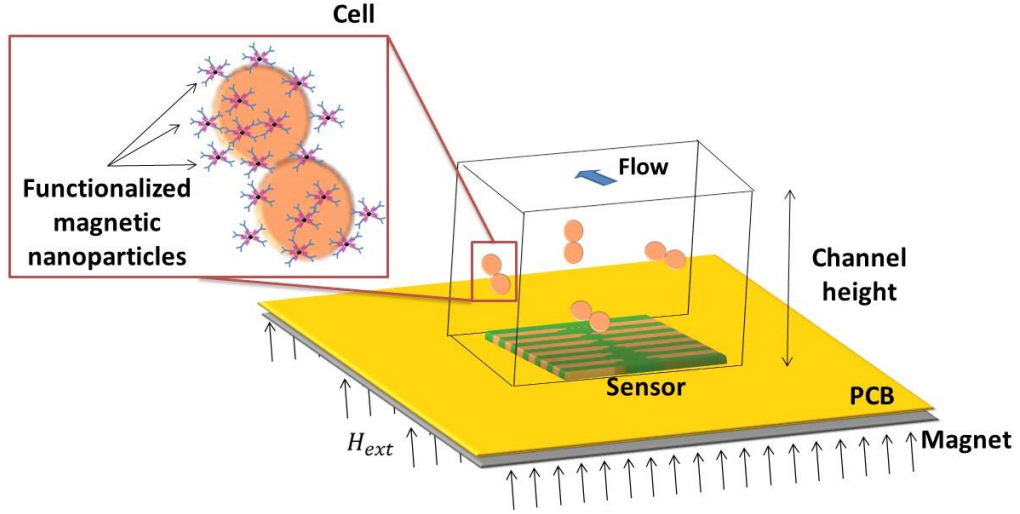


Figure 5. Schematics of magnetic detection device for identification and quantification of cells.

2. Sensor Design and Detection Scheme

Spin-valves (SV) are magnetoresistive sensors (Baibich et al., 1988; Dieny, 1994) composed of a non-magnetic (NM) metal between two layers of ferromagnetic (FM) metals, one of which (the pinned layer) has its magnetization fixed by an adjacent antiferromagnetic layer, while the other (the free layer) is free to rotate (Figure 6). Under an external magnetic field, it is possible to switch the relative magnetic orientations of the FM layers from parallel to antiparallel, therefore changing the sensor resistance, linearly with the cosine of the relative angle between the pinned layer and the free layer ($\theta_p - \theta_f$), according to Equation (1), where ΔV is the variation in potential obtained at electric current I due to sensor's resistance change. Here, MR is the sensor magnetoresistance ratio (Equation (2)) and $\langle \cos(\theta_p - \theta_f) \rangle$ is averaged over the active area of the sensor (between contacts):

$$\Delta V = -\frac{1}{2} \left(\frac{R_{AP} - R_P}{R_P} \right) \times R \times \frac{l}{w} \times I \times \langle \cos(\theta_p - \theta_f) \rangle \quad (1)$$

$$MR = \frac{R_{AP} - R_P}{R_P} \quad (2)$$

where, R is the square resistance of the sensor, l the length of the sensor, w the width of the sensor, I the current applied to the sensor, R_{AP} the resistance of the

sensor when $\theta_p - \theta_f = \pi$ and R_P the resistance of the sensor when $\theta_p - \theta_f = 0$.

To achieve a linear behavior (2), the free and pinned layer easy axes should be orthogonal. The linearization can be obtained by inducing an orthogonal magnetization direction between pinned and free layers during deposition or by patterning the SV with a large aspect ratio so that orthogonal magnetizations are facilitated by the demagnetizing fields (Loureiro et al., 2011; Freitas et al., 2012; Wang & Li, 2008).

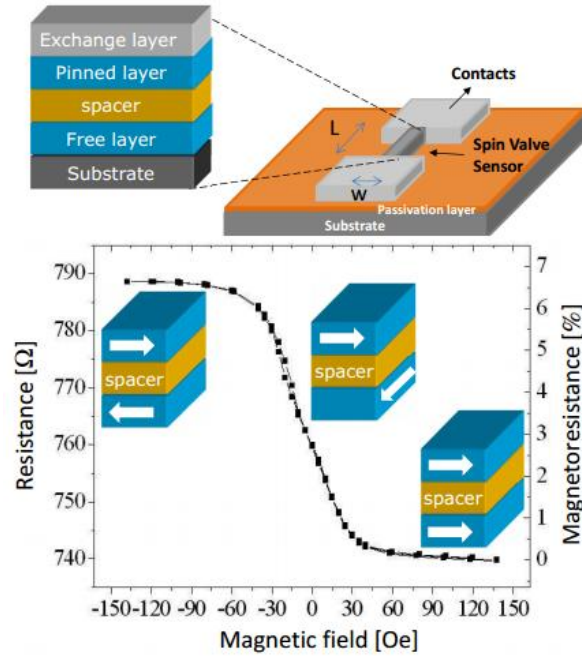


Figure 6. Resistance vs. magnetic field transfer curve of a linear spin-valve at a given sense current.

The dimensions of the SV sensors are optimized taking into account final sensor application. In biological applications, the detection targets have sizes ranging between few nm (molecules such as DNA, RNA and various proteins) to tens of μm (cells can vary in size from $1\mu\text{m}$, like the target cell described in this paper, to $100\mu\text{m}$, size of a big plant eukaryotic cell). Detection is performed through magnetic labeling of these biological targets with nano- or micrometer superparamagnetic particles, which under a magnetic field acquire a magnetic moment. This creates a fringe field that can be detected by the sensor, through a change in its resistance. Using Equation (1), if one considers a coherent magnetization model for the free layer rotation, then:

$$\langle \cos(\theta_p - \theta_f) \rangle = \frac{(H_{ext} + H_{bias} + H_{coupling})}{H_k + H_{demag}} \quad (3)$$

where H_{ext} is the external field, H_{bias} is the bias field used to center the SV transfer curve, $H_{coupling}$ is the sum of the ferromagnetic Néel coupling between the free and pinned layers, H_k is the free layer anisotropy field and H_{demag} is the demagnetizing field.

Therefore the sensor output (Equation (1)) can be written as Equation (4) below:

$$\Delta V = -S \times R_p \times I \times (H_{ext} + H_{bias} + H_{coupling}) \quad (4)$$

where $S = \frac{MR}{2(H_k + H_{demag})}$ is the sensitivity of the sensor, $R_p = R \times \frac{l}{w}$ is the resistance of the sensor when $\theta_p - \theta_f = 0$.

Here, H_{ext} represents the external magnetic field, averaged over the sensor area. In our case this is the fringe field created by the magnetic labels (Freitas et al., 2000; Freitas et al., 2012; Freitas, Ferreira, Cardoso & Cardoso, 2007).

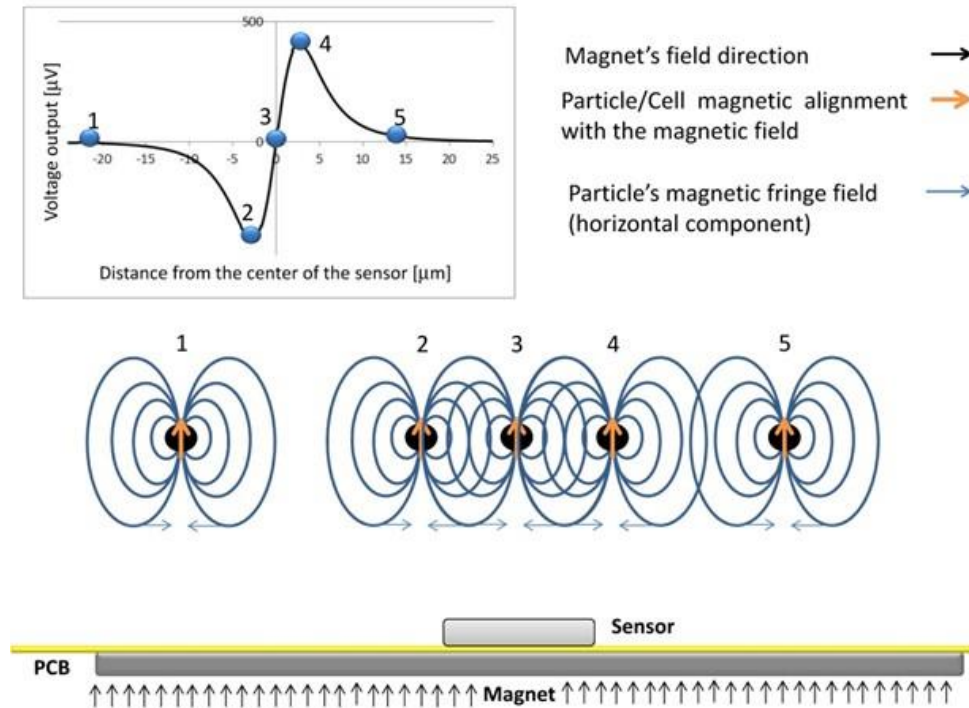


Figure 7. Schematics of MR sensor detection of magnetically labeled targets flowing above the sensor, from the left (position 1) to the right (position 5).

The dynamical detection approach employed in this work involves the application of a magnetic field perpendicular to the sensors in order to magnetize the beads labeling the cells, with minimum impact on the in-plane sensing direction of the sensor (as will be described in Section 3.4). The dynamic detection mechanism is illustrated in Figure 7, where a vertically magnetized particle is injected through a microchannel and generates a variable field over the sensor. In position 1, because the large distance to the sensor, the fringe field produced by the particles is negligible. As the particle approaches the sensor, the free layer will sense the right-side component of the particles fringe field, which changes the sensor resistance (position 2). When the particle is in the center of the sensor, the average fringe field of the particle is equal to zero vanishing the signal (position 3). Finally, as the particle passes the sensor (position 4), the free layer magnetization is affected by an opposite fringe field component when compared to position 2. When the cells go away, the signal goes back to zero since no fringe field is sensed (position 5). As a result, a bipolar peak is the signature of the passage of a perpendicularly magnetized particle over the SV sensor.

In a dynamical approach, sample acquisition velocity depends on the electronics, thus allowing a high throughput and direct number of cells to number of signals relation. A dynamical acquisition requires magnetic labels with a high magnetic moment under an applied external magnetic field in order to obtain a large detectable fringe field, significantly larger than the noise background level. However, label selection needs to be carefully done, as these should possess a non-remnant moment in order to avoid particle clustering during the labeling process of the cells, which can result in cell clustering originating an underestimation on the cell counting. A reduced label size is also important in order to avoid the detection of isolated particles (Freitas et al., 2012; Wang & Li, 2008).

3. Experimental Methods

One general differentiation of the Streptococci is the Lancefield groups based on serological grouping determined by the antigen C-substance that is a group-specific cell wall polysaccharide. *Streptococcus agalactiae* belongs to Lancefield Group B. Before using the selected rabbit polyclonal antibody (pAb) anti-Lancefield Group B Streptococci (8435-2000, AbDSerotec) against

Streptococcus agalactiae cells, we have done several western blotting (WB) trials and ELISA tests for specificity and sensibility confirmation.

As known, western blotting identifies with specific antibodies proteins that have been separated from one another according to their size by gel electrophoresis. The blot is a membrane, almost always of nitrocellulose or polyvinylidene fluoride (PVDF). In our case, we have used hydrophobic PVDF membranes because it exhibits better binding efficiency of blotted proteins and have high sensitivity. Then, the gel is placed next to the membrane and application of an electrical current induces the proteins in the gel to move to the membrane where they adhere. The membrane is then a replica of the gel's protein pattern, and is subsequently stained with an antibody.

The proteins used in our WB trials were cell wall proteins of bovine field isolates of Streptococci species (*S. agalactiae* (Lancefield Group B), *S. uberis* (ungroupable) and *S. dysgalactiae* (Lancefield Group C)) and also from bacteria standards (as CECT 183 for *Streptococcus agalactiae* and CECT 994 for *Streptococcus uberis*). Results proved specificity of this pAb at 2 µg/ml concentration for 3 h of incubation at RT), to *Streptococcus agalactiae* cell wall proteins. Blots were probed with 0.2 µg/ml of goat anti-rabbit antibody conjugated to horseradish peroxidase (HRP) (STAR 124P, AbDSerotec) after one incubation hour at RT. Consequently, we have obtained stained immunogenic proteins of molecular weight higher than 100 kDa (and also two distinct immunogenic proteins around 30 and 41 kDa of molecular weight belonging to *Streptococcus uberis*).

The enzyme-linked immune sorbent assay (ELISA) is a commonly used technique to detect antibodies or antigens in samples using the specific reaction of antibodies to their antigens (Lequin, 2005). For pAb sensibility quantification, we have performed ELISA tests. We have used standard and field isolates of bacterial cells suspensions (*S. agalactiae*, *S. uberis* and *S. dysgalactiae*) and once more, specificity was evidenced and sensitivity obtained: the minimal pAb concentration of 1 µg/ml still identifies 10³ CFU/µl of *Streptococcus agalactiae* cells (and also 10³ CFU/µl of *Streptococcus uberis*).

In this work, magnetic particles are used as labels of polyclonal antibodies anti-Group B Streptococci (probes) which are going to recognize (via biomolecular recognition) bacterial *Streptococcus agalactiae* cells (targets) in the sample.

Biological affinities between nanobead surface protein A, IgG Fc fraction and the antibodies and Lancefield Group B Streptococci cell wall immunogenic proteins are illustrated in Figure 8. After labeling, the cells are introduced in a microfluidic channel and the SV sensor detects the fringe field of the magnetic labels bound around the target cell.

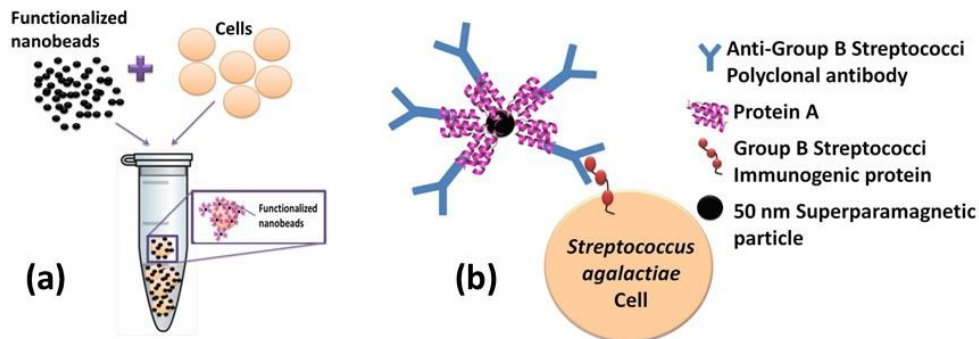


Figure 8. Schematics of immuno-magnetic functionalization of cells (a) Incubation of functionalized beads with *Streptococcus agalactiae* cells and (b) biological affinities between beads protein A, polyclonal IgG antibodies and bacterial cell wall epitopes.

The sensors and microfluidic channels were microfabricated and optimized at INESC-MN for this application, using an acquisition setup adapted from a previous work (Loureiro et al., 2011). The tests using raw milk in microchannels were carried out at INESC-MN. The cell culture and magnetic functionalization and labeling protocols were performed at CIISA, according to manufacturer protocols.

3.1. Beads Functionalization

Nanomag®-D-spio 50 nm particles (79-20-501, Micromod Partikeltechnologie GmbH, Rostock, Germany) were selected because they have protein A at surface and can bind up to five IgG. The calculation of beads number and the amount of pAb anti-Group B Streptococci (8435-2000 AbDSerotec, Kidlington, UK) was based on the *Streptococcus agalactiae* (CECT 183) concentration in samples and considering 400 times more beads than the estimation for cell surface area saturation (1600 particles/cell calculated based on bead and cell surface areas) with 50 nm nanoparticles. The nanoparticles number for cell surface saturation (1600) was estimated according to Wolfram Mathematica 7.0 calculations. A magnetic particles concentration of 6.4×10^9 particles/ μl was prepared for each sample in order to ensure the cells full coverage.

Particles were coated with 10.6 μl of pAb anti-Group B Streptococci (1 $\mu\text{g}/\text{ml}$) at room temperature (RT) incubation (25°C), during 50 min. assisted with rolls plate agitation. Functionalized particles were magnetically separated by magnetic separation (MS) column (130-042-201 Miltenyi, Bergisch Gladbach, Germany) according to Miltenyi Biotec protocol.

3.2. Bacterial Cells Magnetic Labeling

Streptococcus agalactiae cells (CECT 183) were grown at 37 °C overnight on blood agar plates and resuspended in trypticasein soy broth (TSB) over 24 h at 37°C [(Cole et al., 2008), adapted protocol]. After cell pellet collection through 2700 rpm centrifugation at 17 °C during 15 min. (HERMLE Z 383K centrifuge, Wehingen, Germany) and discarding the supernatant, PBS 1X (pH 7.2) buffer was added to absorbance reading at 600 nm (DU-68 Spectrophotometer, Beckman, Pasadena, CA, US) and for CFU/ml estimation. For incubation of 200 μl of magnetic particles with pAb anti-Group B Streptococci, milk and PBS volumes were prepared for final samples amount of 600 μl , and bacteria concentration of 10^4 CFU/ μl . Incubation was performed at RT for 50 min assisted with rolls plate agitation.

3.3. Milk Samples Preparation

Raw milk for experiments was collected aseptically from a healthy cow. As known, milk is a natural buffer with pH between 6.6 and 6.8 (National Mastitis Council [NMC], 1999). Conventional microbiological tests were performed accordingly with NMC (1999) protocols, to confirm no bacterial growth. Briefly, a raw milk drop (10 μl loop) was smeared on a COS blood agar plate (43021, Biomerieux, Craponne, France) and a MacConkey agar plate (610028, Liofilchem Diagnostic, Roseto degli Abruzzi, Italy) made in the laboratory and both submitted to 37 °C during 48 h.

To achieve defatted milk samples, raw milk samples were frozen at -20 °C over 24 h and then defrosted. During freezing, fat “cold agglutination” occurs forming a top layer of crystallized fat globules at milk surface. This layer was removed and milk underneath was used as “defatted” one.

3.4. Sensor Fabrication

3.4.1. MR sensor fabrication

The chips fabricated in this work comprised 4 sets of rectangular SVs disposed in a line. Each SV set includes seven sensors with 3 μm width, and length varying from 20 to 100 μm (measured between contact leads), according with Figure 9. Sensor geometry was optimized to promote a linear, hysteresis-free transfer curve upon patterning into micrometric dimensions (sensor dimensions and shape definition). Additionally to individual sensors, we have included also four SV sensors connected in series. These configurations were designed to cover the width of the microchannel to be included above the chip. The sensors were fabricated on a 150 mm-diameter silicon wafer passivated with a 50 nm-thick Al_2O_3 film deposited by Physical Vapor Deposition (PVD). The bottom-pinned SV thin film stack was deposited by Ion Beam Deposition (IBD) on a Nordiko 3000 device (Hampshire, UK) with the following structure (thickness in nm, compositions in atomic %): Ta 2.0/ $\text{Ni}_{80}\text{Fe}_{20}$ 2.5/ $\text{Co}_{80}\text{Fe}_{20}$ 2.3/ Cu 2.2/ $\text{Co}_{80}\text{Fe}_{20}$ 3.3/ $\text{Mn}_{76}\text{Ir}_{24}$ 7.0/ Ta 10.0 (Gehanno et al., 1999). During the deposition, a 3mT magnetic field was applied in order to induce a parallel anisotropy simultaneously for the free layer ($\text{Ni}_{80}\text{Fe}_{20}/\text{Co}_{80}\text{Fe}_{20}$) and pinned layer ($\text{Co}_{80}\text{Fe}_{20}$) easy axis. Then, a 15nm of $\text{Ti}_{10}\text{W}_{90}(\text{N}_2)$ passivation layer was deposited by PVD in a Nordiko 7000 tool. SV definition was performed by direct write laser (DWL) lithography and ion milling in a Nordiko 3600 tool. The metallic contacts were defined by lithography and liftoff of a 300 nm-thick $\text{Al}_{98.5}\text{Si}_{1.0}\text{Cu}_{0.5}$ / 15nm-thick $\text{Ti}_{10}\text{W}_{90}(\text{N}_2)$ layer deposited by PVD in a Nordiko 7000 tool. Deposition of 300 nm-thick Si_3N_4 passivation layer was carried out in Electrotech Delta Chemical Vapor Deposition System. Via definition was performed by lithography and reactive ion etching in LAM Rainbow Plasma Etcher 4400. After wafer microfabrication, dicing of the individual dies was done by a Disco DAD 321. Prior to sensor characterization, the wafer was submitted to a magnetic annealing at 250 $^\circ\text{C}$ for 15 min, in vacuum and cooled down under a 1 Tesla magnetic field.

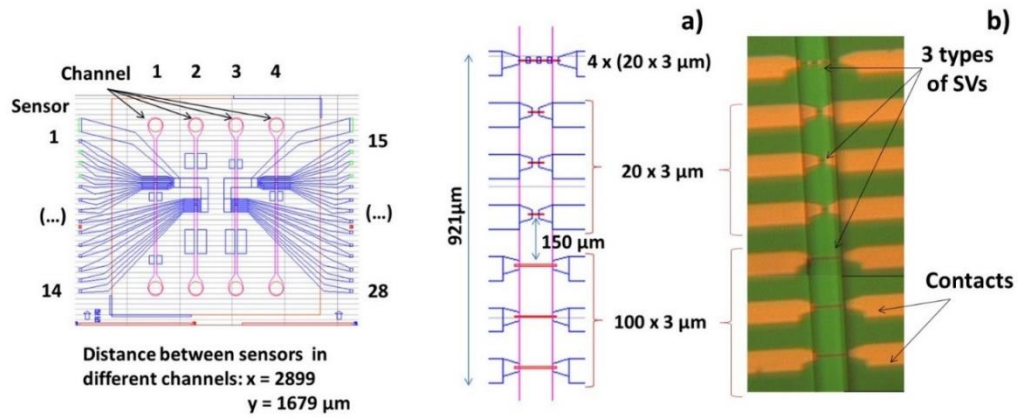


Figure 9. (a) Device CAD mask and sensor dimensions; (b) Microscope photo of one set of seven microfabricated SVs.

3.4.2. Microfluidic channels fabrication

A channel geometry of four single parallel channels with $100 \mu\text{m}$ height, $100 \mu\text{m}$ width and 1 cm length was considered. The inlets have a tear shape to ease cell entrance in the channels. Channels were made of poly (dimethylsiloxane) (PDMS) and fabricated by cast-molding, following a procedure similar to Yeo & Friend (2010) work. A hard-mask used to expose channels' mold was made of $\text{Al}_{98.5}\text{Si}_{1.0}\text{Cu}_{0.5}$ 150 nm thick layer deposited on Corning glass by PVD in a Nordiko 7000 tool, patterned by DWL lithography and chemically etched with a solution of acetic acid (3.3%), nitric acid (3.1%) and phosphoric acid (3.0%). Channels' mold was fabricated by contact microlithography (Figure 10) of a $100 \mu\text{m}$ thick SU-8 50 photosensitive negative resist spun onto a silicon wafer and it was observed for defects in a DEKTAK 3030ST profilometer. In order to cast PDMS channels with a controlled thickness and shape and inlet/outlet aligned with microchannel, three 2 mm -thick poly(methylmethacrylate) (PMMA) plates were micromachined with a CNC TAIG Micro Mill tool. The resist mold was mounted on the bottom plate with Kapton tape, then the middle plate defined PDMS (2 mm) shape and thickness and the top plate defined inlet and outlet holes (1 mm). The two top plates possess alignment holes (2 mm).

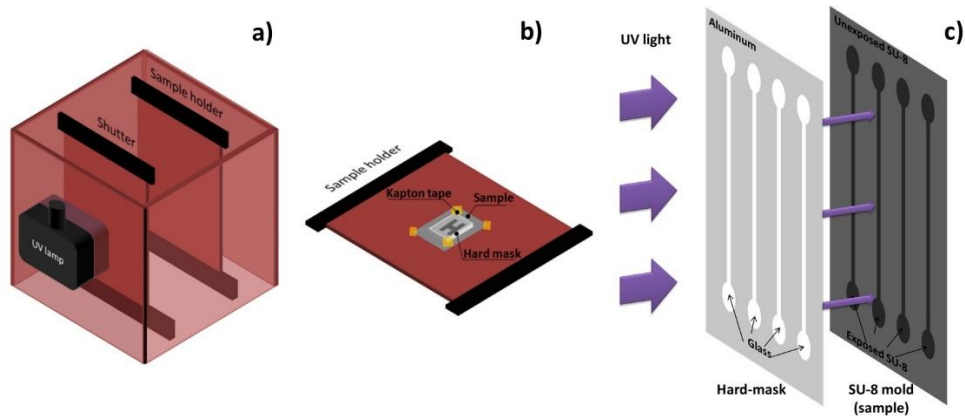


Figure 10. Schematics of the contact microlithography steps: (a) UV exposure setup; (b) Sample holder with hard-mask assembled over SU-8 substrate; (c) SU-8 negative resist exposure process.

3.4.3. Bonding and encapsulation

Silicon chip integration with PDMS microchannels was achieved through irreversible bonding of the Si_3N_4 and PDMS surfaces by ultraviolet/ozone (UVO). Both surfaces were treated in a UVO Cleaner (Jelight, USA) for 15 min and immediately submerged in deionized water. Chip and microchannels were then mounted face-to-face, aligned on a microaligner with an x, y and theta direction stages under a microscope, using ethanol to delay bonding until complete alignment (Figure 9b). After drying at room temperature, the bonded device was kept at RT, overnight, to complete irreversible bonding. Encapsulation was performed by mounting and gluing the bonded device on a Printed Circuit Board (PCB). The connection to the microfabricated sensors was done by wire-bonding the contact pads with the PCB. Finally, the wires were covered with silicone gel for protection. Figure 11 shows the final assembled device.

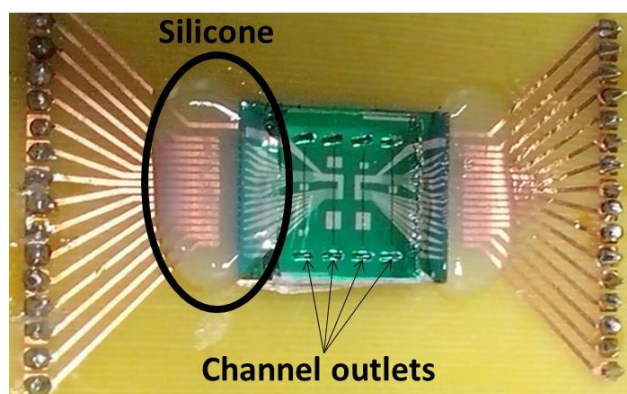


Figure 11. Wire-bonding silicon-protected assembled device.

3.5. Samples Measurement

Sensor output signals were obtained using the electrical scheme shown in Figure 12. A 3 mA current was supplied to the sensor by two 9 V batteries in series (~18 V), 1 k Ω resistance (R_R), a potentiometer (R_{pot}) set at 5 k Ω (R_R and R_{pot} together have a higher resistance than the sensor's average resistance, $R_S \sim 555 \Omega$). The output of the sensor was connected to acquisition setup composed by (a) an amplifier (Stanford Research Systems SR560, California, US) operating for gains of 10,000x, (b) high-pass and low-pass filters of 300 (to filter the DC and part of low frequency noise) and 10,000 Hz (to avoid aliasing), respectively and (c) a 16 bit analogue to digital converter (ADC) board DT9836-12-2-BNC (20 kHz acquisition frequency), which was connected to a laptop, where a home-made software was used to acquire sensor output vs. time (Figure 12b, c).

Each test required channel inlet sample introduction through capillary tubes (BTPE-90 polyethylene tubes, Instech Laboratories, Inc., Pennsylvania, PA, USA) plugged into a 1 ml syringe (Codan, Cat: 621640, LuerStubs LS20, Pennsylvania, PA, USA). Fluid flow was controlled by an automated syringe pump (NE-300 model, New Era Pump Systems, Inc., New York, NY, USA), and the sample was collected from the outlet by another capillary tube to a disposable Eppendorf.

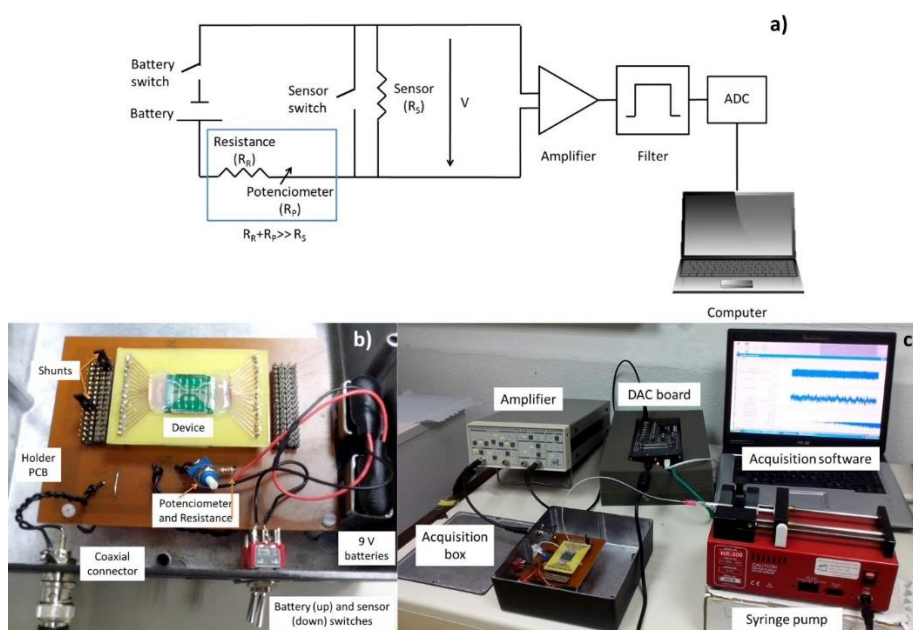


Figure 12. Acquisition Setup. (a) Electrical circuit of the acquisition setup; (b) Biasing box; (c) Acquisition setup assembly.

4. Results and Discussion

In order to be able to understand experimental data, it is important to perform simulations of the signals varying the positioning of cells and relative positioning of cells inside the channel. It is also important to understand the variations of the signals for different directions of the magnetic moment.

4.1. Sensors characterization and magnet calibration

The sensors' transfer curve (resistance versus DC magnetic field up to 140 Oe) was characterized. Figure 13 shows a representative example of a $100 \times 3 \mu\text{m}^2$ sensor, showing a linear range of 65 Oe, a sensitivity (S) of 0.24%/Oe, offset field (H_{coupling}) of -0.35 Oe and coercivity (H_c) of 0.40 Oe. A summary of the dispersion obtained over the 28 sensors measured on the chips fabricated is depicted in Table 1. From the table, one can confirm that connecting the sensors in series reduces the dispersion in all parameters because it averages the individual SV characteristics.

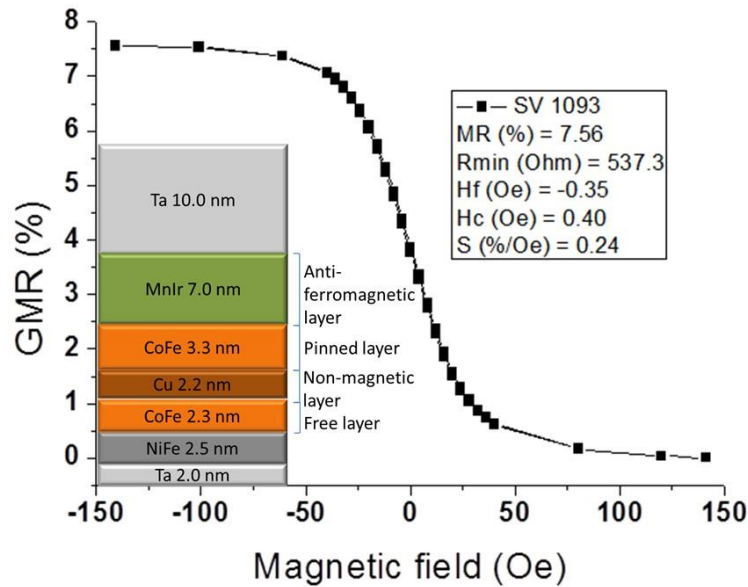


Figure 13. Transfer curve for a selected sensor with an area of $100 \times 3 \mu\text{m}^2$. Inset shows the multilayer structure used for these sensors.

Sensor dimensions [μm^2]	MR (%)	R_{\min} (Ω)	H_f (Oe)	H_c (Oe)	S (%/Oe)
100 × 3	7.59 ± 0.28	554.61 ± 20.65	1.01 ± 2.07	0.81 ± 0.74	-0.24 ± 0.03
20 × 3	6.58 ± 1.74	179.05 ± 39.31	-1.74 ± 2.98	2.79 ± 3.01	-0.19 ± 0.09
In series	7.51 ± 0.11	608.83 ± 4.79	-3.59 ± 0.47	2.40 ± 0.34	-0.18 ± 0.04

Table 1 - Results of SVs transport characteristics [28 sensors measured].

To set a vertical magnetic field to magnetize the nanoparticles, a permanent magnet block (dimensions $20 \times 20 \times 3 \text{ mm}^3$, NdFeB, Supermagnete, Gottmadingen, Germany) with $\sim 6.29 \times 10^4 \text{ A/m}$ was mounted below the PCB with the bonded device. As the SV are only sensitive to an in-plane, if well aligned, the magnet will not affect the sensitivity of the sensor. However, a small tilting of the magnet can create magnetic field components in the sensor plane and therefore affect the sensor's sensitivity. The impact of the magnet positioning on the sensor transfer curve is illustrated in Figure 14. With a well aligned magnet, the sensor transfer curve is centered on zero external fields, with maximum sensitivity (Figure 14a). A slight tilt of the magnet creates fields in the longitudinal and/or sensing direction that shift the sensor transfer curve and/or decrease the sensor sensitivity, respectively (Figure 14b). Therefore, combining magnet positioning and transfer curve measurements, it was possible to achieve a magnet position that did not degrade the sensor sensitivity.

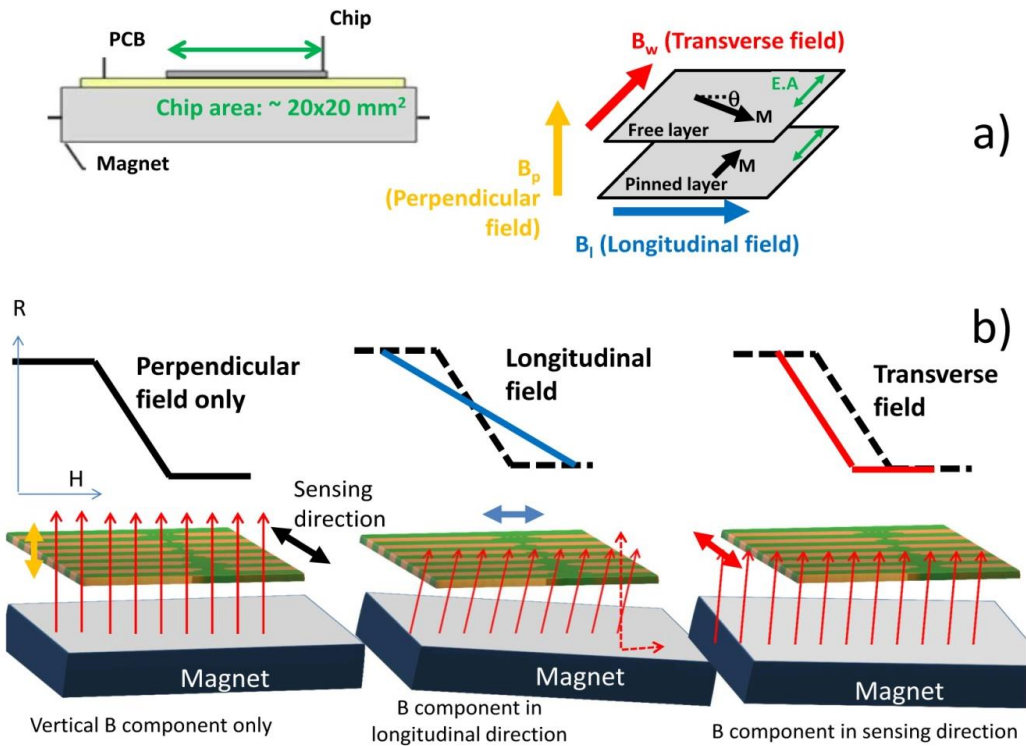


Figure 14. (a) Schematics of the geometry used for the nanoparticle magnetization using an external permanent magnet underneath the sensor and the magnetic field components (transverse, perpendicular and longitudinal) with respect to the free and pinned layer magnetization orientations; (b) Impact on the sensor response of each magnetic field component (set by magnet position) transfer curves.

4.2. Sensors magnetic behavior, signal amplitude and shape

In this work, several sensor dimensions were tested in order to ascertain the best configuration for dynamic single cell detection in a wide range of concentrations in terms of signal intensity and noise level (signal-to-noise ratio). Three different sensors were fabricated: four $20 \times 3 \mu\text{m}^2$ sensors in series, a sensor with a large detection area ($100 \times 3 \mu\text{m}^2$) and a sensor with a small area ($20 \times 3 \mu\text{m}^2$). Both sensors in series and the large area sensor allow increasing the detection area available with a higher signal intensity, however are probably unable to distinguish between two or more cells flowing over the sensor simultaneously. In terms of magnetic labels, the chosen 50 nm superparamagnetic particles have a very low individual moment ($\sim 2.7 \times 10^{-18} \text{ A}\cdot\text{m}^2$) and so cannot be individually detected, while having a magnetic moment sufficient for detection of a completely covered cell. Their small dimension reduces the probability of several cells to bind to a single particle causing cell aggregation.

Magnetic Detection Simulations

In order to assess the expected signal that would be obtained with each sensor dimension, a simulation of their sensing behavior and sensitivity to magnetic labeled cells was performed in Wolfram Mathematica 7.0. To simulate the magnetically labeled cells' behavior over sensor's free layer we considered that each particle labeling the cell could be approximated to a magnetic dipole centered on the geometrical center of the particle, which was considered a sphere (Figure 15).

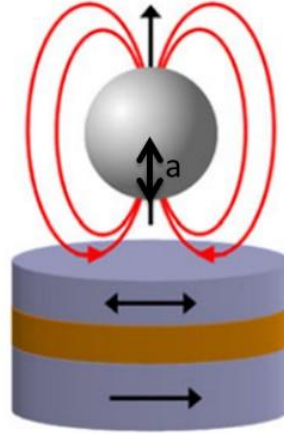


Figure 15. Out-of-plane magnetic field application for magnetic label sensing measurement schematics.

Dipole's magnetic field created at the position a from dipole center is given by Equation (5):

$$H(a) = \frac{1}{4\pi} \left(\frac{3(a \cdot m)a}{|a|^5} - \frac{m}{|a|^3} \right) \quad (5)$$

As SVs used in this work are only sensitive to transverse in-plane component of beads' fringe field, only the magnetic field parallel to sensor plane (x-component of fringe field) for particles with a magnetic moment (m) was calculated. The field below a particle at position (x, y, a) when it is magnetized perpendicularly to the sensor plane (z direction), is thus given by:

$$H_x^{perp}(x, y, a) = \frac{m_z}{4\pi} \frac{3xa}{(x^2 + y^2 + a^2)^{5/2}} \quad (6)$$

As SVs are sensitive to the average fringe field generated by magnetically labeled cell, the field of each particle has to be averaged over the sensor, which can be achieved by integrating Equation (6) over the sensor area and divide the result by

sensor's area. In the specific case of this work, the fringe field of a cell (H_x^{perp}) with $1\mu\text{m}$ diameter fully covered with 50 nm superparamagnetic particles (1600 nanoparticles per cell) was calculated considering spherical cell and each particle occupying a circle area equivalent. Since each *S. agalactiae* cell is composed by pairs of $1\mu\text{m}$ coccus, simulations were performed for pairs of spheres. The simulation was performed considering the geometry presented in Figure 16 with axis positioned in each sensors center and assuming sensors positioned in the center of the channel.

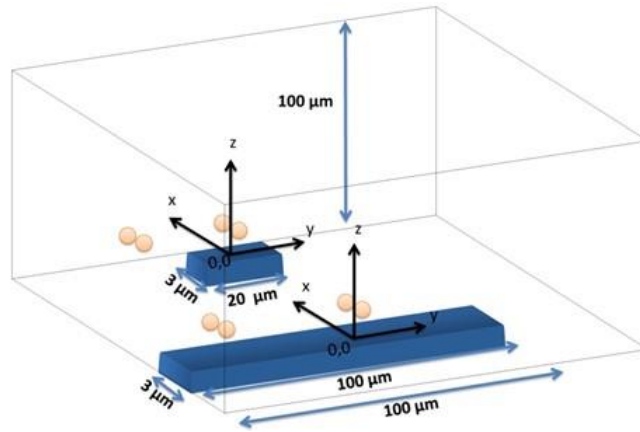


Figure 16. Schematics of sensor and channel geometry considered for output signal simulation in Wolfram Mathematica 7.0.

In this simulation, the fringe field generated by a single particle was calculated considering its position on the cell (Equation (7), where c is the cell's radius, θ is the angle within the x/z plane and φ is the angle within the x/y plane) (Figure 17), which was assumed as a pair of spheres flowing in the middle of the channel (Figure 18):

$$\begin{aligned}
 x &= c \times \sin \varphi \times \cos \theta \\
 y &= c \times \sin \varphi \times \sin \theta \\
 z &= c \times \cos \varphi
 \end{aligned}
 \tag{7}$$

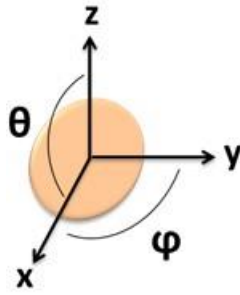


Figure 17. Axis and angles considered for Wolfram Mathematica 7.0 simulations.

Cells' fringe field was obtained for 62 different positions of x ($0.8 \mu\text{m}$ apart covering a range from $-25 \mu\text{m}$ and $25 \mu\text{m}$ in the x axis, considered the flow direction) and plotted against its corresponding position relative to sensor's center. In order to obtain simulated signals similar to experimental ones, cells' fringe field was transformed into electrical signal (ΔV) using Equation (4), considering $H_{ext} = H_{cell}$, $H_{bias} = H_{coupling} = 0$, $I = 3 \text{ mA}$ and the sensors characteristics of Figure 18. Initially, signal simulations were performed considering one or two cell pairs oriented according to one of the axis (Figure 18) and at different height above the sensor.

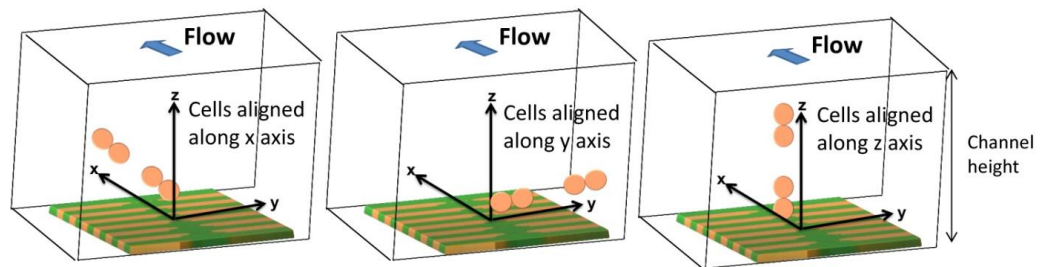


Figure 18. Schematics of cell orientations along x , y and z axis considered for cells in flow (x axis direction) in Wolfram Mathematica 7.0 simulations.

Accordingly with simulations, different signal shapes and intensities were observed if the cell pair is oriented along x , y or z axis. In Figure 19a, when compared to the x and z orientation, an intensity increase of $200 \mu\text{V}$ was observed for y axis orientation. This is due to the fact that pair of cells was aligned along the length of the sensor and therefore the observed signal corresponds to two $1 \mu\text{m}$ cells. This is not the case for the other two orientations since in one case, the $1 \mu\text{m}$ cells are flowing one after the other (x orientation) and, in the other case, one of the $1 \mu\text{m}$ cells is more apart from the sensor leading to a signal attenuation. Nevertheless, these signals shape remain very similar and for simplification, only the pair of cells aligned in the x direction will be further analyzed. In Figure 19b,

the signal variation with channel height for a cell pair is shown. It can be observed that the higher the cell flows along the channel the lower is the signal intensity. The amplitude of the bipolar peak above a height of 10 μm is below 15 μV . Since the sensor noise is 10–15 μV (Freitas et al., 2012), we can conclude that cells passing at a height above 10 μm are unable to be detected.

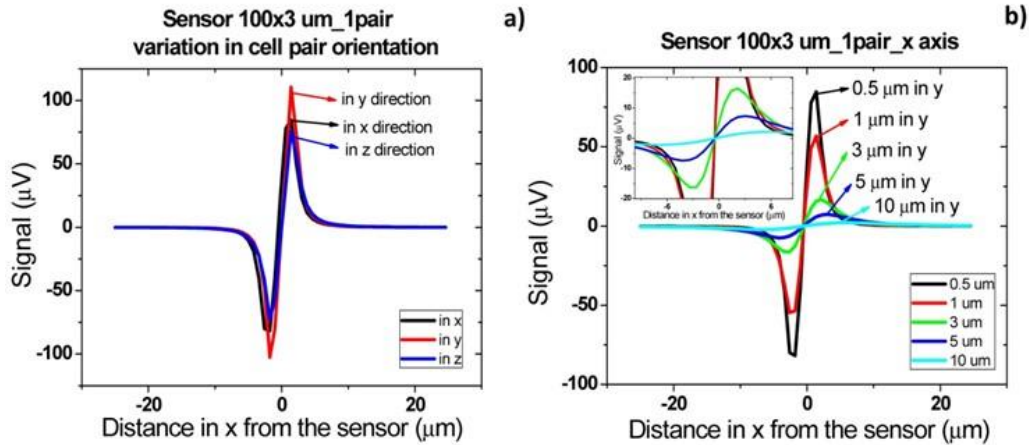


Figure 19. Signal simulation for *Streptococcus agalactiae*. (a) Pair of cells oriented according with each axis; (b) Signal variation with height from the sensor according with x axis.

Besides the specific cells presence detection, the final goal of this device will be also to set known cells concentration in samples. It is therefore important to understand which signal shapes are obtained when two pairs of cells are flowing one after the other, side by side or one on top of the other.

Figure 20b shows the signal of two pairs of cells flowing one after the other over the sensor with a separation of 2 and 10 μm . For a cell pair distance of 2 μm , a bipolar signal is observed with a slight slope variation near zero and no variation in the amplitude when compared to a single pair of cells. For a distance of above 10 μm between each pair, the signal of each cell is already decoupled and two bipolar peaks are observed. These signatures allow the identification of two pairs of cells passage one after the other. Furthermore, by increasing the height of the cells, as expected, the signal amplitude is reduced (Figure 20c). As discussed previously, for heights above 10 μm , the signal is below the expected sensor noise and therefore the sensors are unable to detect it.

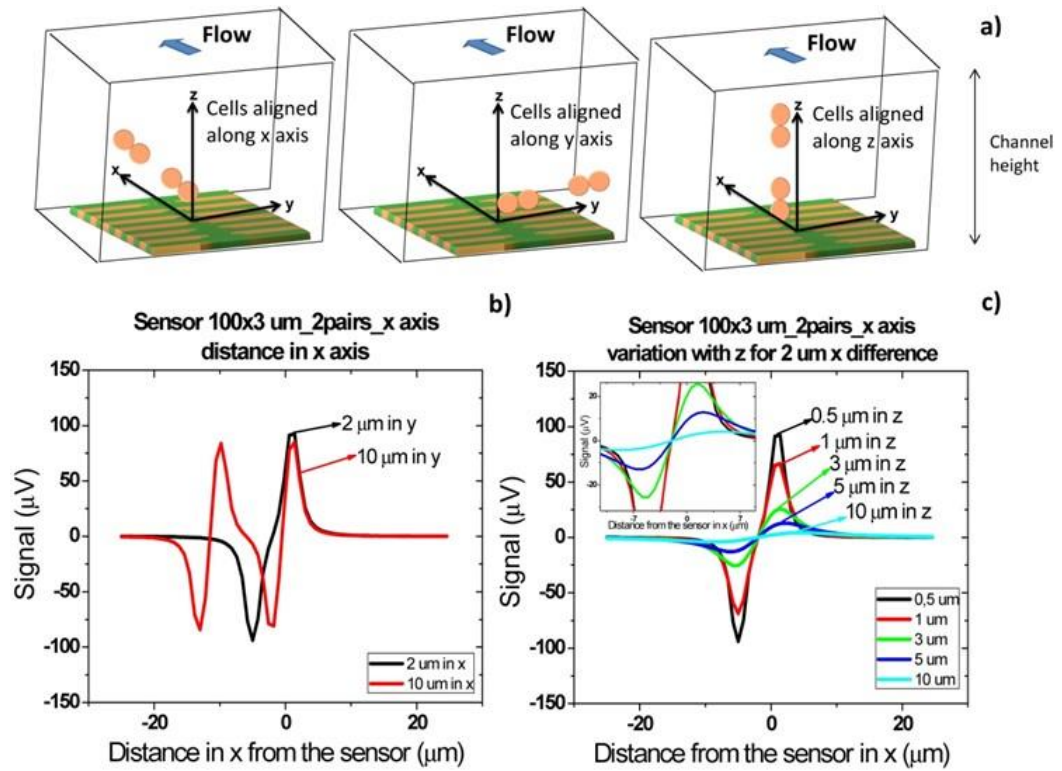


Figure 20. Signal simulation for two *Streptococcus agalactiae* along x axis. (a) Schematics of cell pair's orientation considered for simulation; (b) Cells at a given distance along x axis; (c) Signal variation with height from the sensor for cells at 10 μm distance from each other along x axis.

For cells flowing simultaneously above the sensor at different heights (Figure 21) similar peaks are observed. As can be observed in Figure 21a, for separations larger than 30 μm , there is an attenuation of 200 μV . This is due to the fact that in this case only the cell closer to the sensor generates a fringe field high enough to be detectable. Again, as expected, when the two pairs of cells (2 μm separated from each other) flow at a height above 10 μm , the signal is within the sensor's noise enabling it to detect the cells.

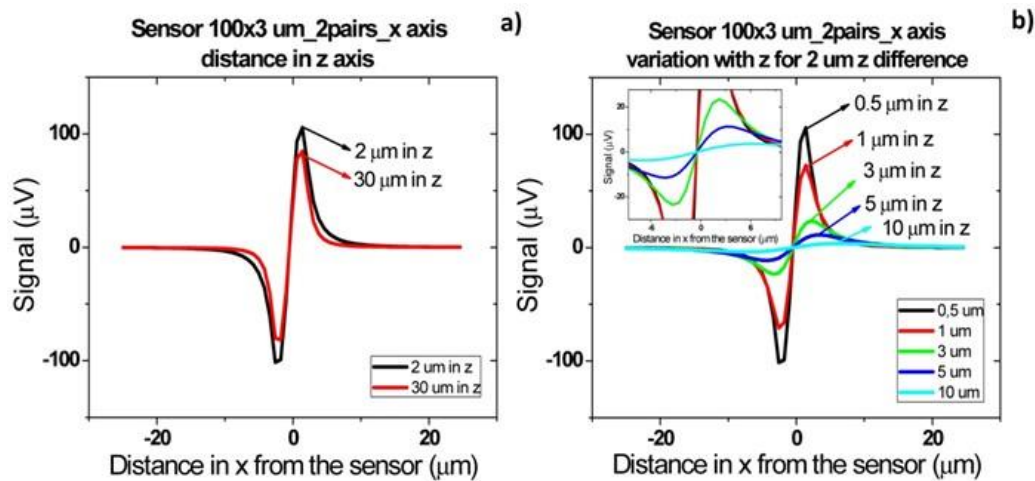


Figure 21. Signal simulation for two *Streptococcus agalactiae* along z axis. (a) Cells at a given distance along z axis; (b) Signal variation with height from the sensor for cells at 2 μm distance from each other along z axis.

Finally, when cells flow simultaneously through sensor at different positions in y direction (Figure 22), a signal increase corresponding to sum of each individual cell signal (Figure 22a) is observed. As sensor is 100 μm long, which corresponds to channel's width, the signal will remain independent of cells separation distance in y direction. As in previous cases, the amplitude of bipolar peaks will be attenuated as cells flow more apart from sensors.

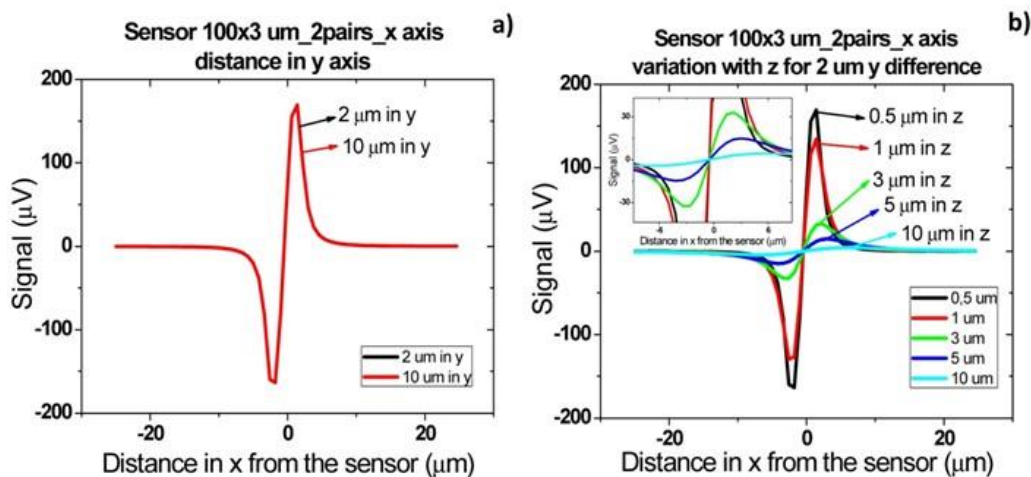


Figure 22. Signal simulation for two *Streptococcus agalactiae* along y axis. (a) Cells at a given distance along y axis; (b) Signal variation with height from the sensor for cells at 10 μm distance from each other along y axis.

Sometimes, in real data it is not easy to distinguish if two cells are flowing side by side in y direction, since a large signal can correspond to several cells flowing simultaneously at a specific height or to a single cell pair flowing at a lower

height. This fact would lead to an underestimation of detected cells number. To avoid this, one can spread several small sensors over the channel's width and measure them in parallel. Assuming that one of these sensors would have an area of $20 \times 3 \mu\text{m}^2$, simulations were carried out for two pairs of cells separated by 2 and $10 \mu\text{m}$ in y axis. As expected from Equation (4), a lower signal is obtained for these sensors than for $100 \times 3 \mu\text{m}^2$ sensor in the same conditions (Figure 23). Plus, due to sensor's smaller length than the channel, there is a decrease in signal detection outside sensor area due to dilution of cell magnetic fringe field with distance. Thus, cell pairs flowing outside $20 \times 3 \mu\text{m}^2$ sensors sensitive/ detection will not be observed. Spreading the small sensors would therefore give more reliable results than using a single sensor occupying the channel's width. However, from the electronics point of view, a more complicated system would be required, to allow acquisition of several sensors in parallel.

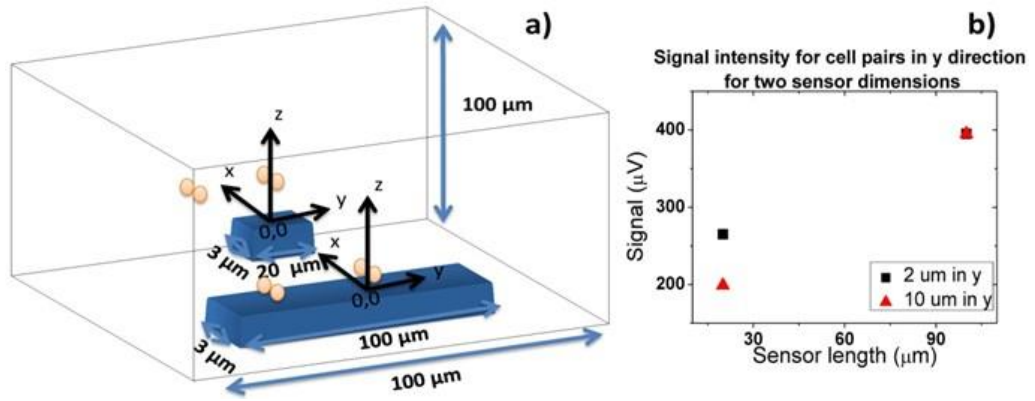


Figure 23. (a) Schematics of cell flow over two types of SVs; (b) Signal amplitude for two types of SVs obtained from simulations for two pairs of cells oriented along y axis and separated by 2 and $10 \mu\text{m}$.

Finally, it has previously been observed that cell rotation due to flow or non-vertical magnetization direction influences signal peak shape observed (Loureiro et al, 2011). Thus, the influence of a magnetic moment component in the x direction (Figure 24) was analyzed by introducing Equations (8) and (9) in the simulation:

$$H_x^{tot} = \frac{m_z}{4\pi} \frac{3xa}{(x^2 + y^2 + a^2)^{5/2}} - \frac{m_x}{4\pi} \left(\frac{3x^2}{(x^2 + y^2 + a^2)^{5/2}} - \frac{1}{(x^2 + y^2 + a^2)^{3/2}} \right) \quad (8)$$

$$m_z = m_s \times \sin \beta \quad (9)$$

$$m_x = m_s \times \cos \beta$$

Where m_s is the particle's saturation magnetic moment, which for the 50 nm particles used in this work, corresponds to $m_s = 2.7 \times 10^{-18} \text{A.m}^2$.

The Figure 25 presents signal variation with angle β , between perpendicular and parallel magnetization directions. It is possible to observe that the introduction of parallel component of fringe field is translated as an asymmetric bipolar signal, which intensity decreases with higher β , since the contribution of perpendicular component decreases. When the magnetization direction is parallel to x axis a unipolar peak is observed.

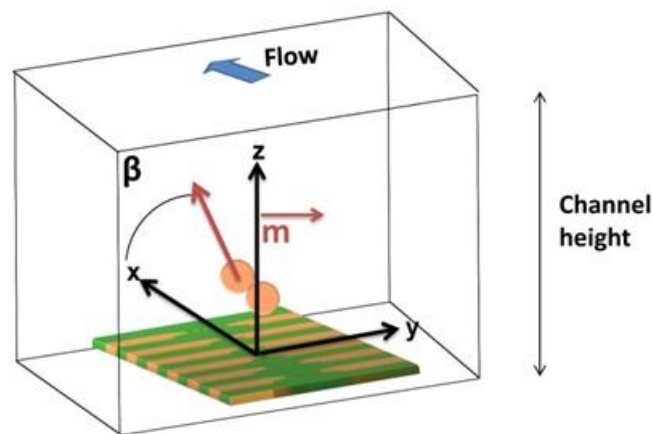


Figure 24. Schematics of axis and configuration considered for simulation in Mathematica 7.0 on the signal influence by both perpendicular and parallel components of fringe field.

In summary, analyzing peaks shape and amplitude, it is possible to determine the magnetic moment orientation and cell's number, as well as cell's height when flowing over the sensor.

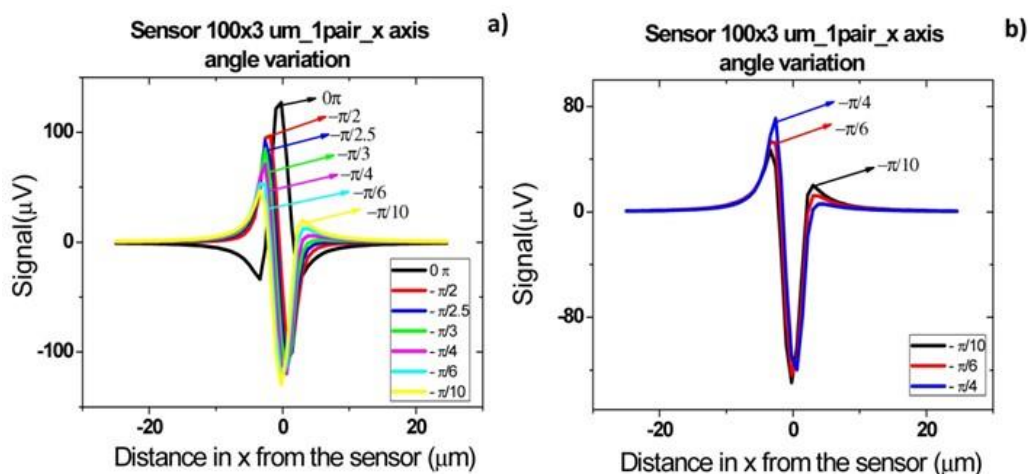


Figure 25. Signal simulation for detection of a *Streptococcus agalactiae* cell using a $100 \times 3 \mu\text{m}^2$ sensor (a) oriented along x axis considering different magnetic moment angles relative to the x axis; (b) Selection of simulated angles.

4.3. Detection of *Streptococcus agalactiae* cells

For a first experiment, three samples were considered:

- (i) raw milk as collected;
- (ii) milk spiked with 200 μl of functionalized nanoparticles (6.4×10^9 particles/μl for 10^4 cells/μl detection) (after magnetic separation of buffer solution with 145 μl of magnetic nanoparticles and 10.6 μl of pAb anti-GB *Streptococci*, per sample);
- (iii) Similar to (ii) and also spiked with 4.6 μL of *Streptococcus agalactiae* cells suspension (1.28×10^6 cells/μl). The samples were first incubated for 50 min and injected inside the microfluidic channel at a 50 μl/min flow rate. Results presented were obtained from repeated trials (three times for each sample) and with at least ten measurements for each flow rate.

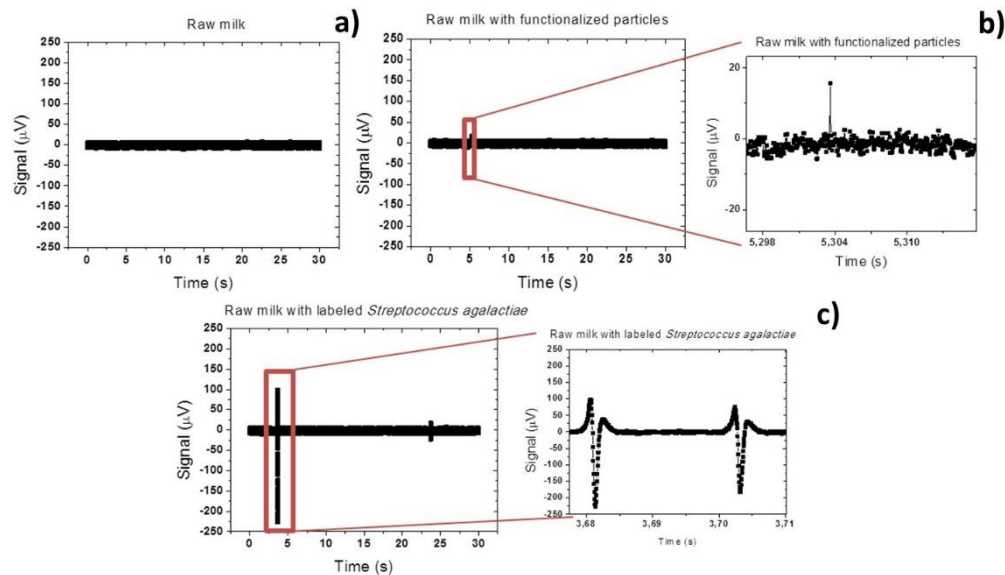


Figure 26. Acquired signal for raw milk samples (a) as collected; (b) spiked with functionalized nanoparticles and (c) spiked with magnetically labeled *Streptococcus agalactiae* cells at 50 µl/min.

This Figure 26a shows that (i) sample has no peaks observed and only the background noise of the sensor was observed. A peak-to-peak noise of 20 µV was measured. On the other hand, on sample (ii), where only functionalized magnetic particles were added to raw milk, sporadically small peaks (< 40 µV) appeared (Figure 26b). This may be explained by small particles agglomeration due to applied magnetic field or due to adsorption of particles to milk constituents. From this point, all peaks above 40 µV of peak-to-peak amplitude were considered as a positive bacterium detection peak. In fact, on samples (iii) including magnetically labeled *Streptococcus agalactiae* cells, large peaks (~ 325 µV) were observed proving a positive detection of cells. As can be observed in Figure 26c, the measured peaks were unipolar. This indicates that magnetic moment of magnetic particles was almost oriented in the x direction ($\beta \sim \pi/10$). This seems contradictory since a vertical magnetic field is applied during the experiment. In fact, this phenomenon was already observed in the past for magnetic particles (Loureiro et al., 2011) in a similar system and was associated to rolling of the magnetic particles over the sensor surface. However, this was the first time that such behavior was observed in cells.

Analyzing the literature, several works reported that in square or rectangular channels cells tend to focus on four equilibrium regions centered at channel edge as shown in Figure 27 (Di Carlo, 2009; Papautsky & Zhou, 2013).

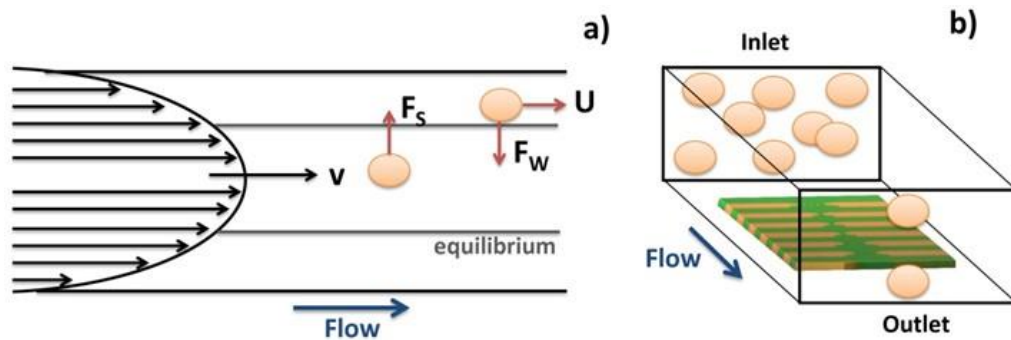


Figure 27. Schematics of inertial focusing in square microchannels. (a) Two lift forces in action, wall-induced F_w and shear-induced F_s lift forces; U is the migration velocity of cell; (b) In square channels randomly distributed particles or cells focus into four equilibrium positions at the wall centers.

This is valid for dilute suspensions of particles or cells flowing at moderate Reynolds numbers (Di Carlo, 2009). Considering that in this work, cells are magnetically labeled and the magnet is positioned below sensors, there may be a magnetic force pushing cells downwards. This small magnetic force associated to the equilibrium regions will therefore pull cells towards sensor surface. The surface drag force associated to the parabolic liquid velocity will further cause rolling of cells over the sensor.

On other trials, more symmetric peaks were observed (Figure 28) and with a lower amplitude. This demonstrates that in some cases cells flow above the sensor without rolling over the surface. When compared to the simulations of Section 4.2 (Figure 19b), peaks amplitude of $111 \mu\text{V}$ and $143 \mu\text{V}$ indicate cells positioning of $3\text{--}5 \mu\text{m}$ above sensor. Furthermore, peaks observed in Figure 28a are superimposed showing that at least two cells are flowing very close to each other but still far enough to distinguish two bipolar peaks. Comparing to simulations (Figure 20b) this indicates that cells are flowing one after the other at a separation ranging from 5 to $10 \mu\text{m}$. This fact may be explained by some cell agglomeration at the inlet and consequent sporadic magnetic labeled cells release, generating peaks with these characteristics.

Based on the peak analysis, it is possible to estimate the concentration of bacteria in solution. Assuming an average of four peaks per acquisition of 30 s , a flow rate

of 50 $\mu\text{l}/\text{min}$ (meaning 25 μl of sample volume) and that each peak corresponds to a single cell, a bacteria concentration of 0.14 cells/ μl is obtained. This value is far below the concentration of the input sample (10^4 CFU/ μl). This fact reinforces the assumption that there is a strong agglomeration of cells at channel's inlet and that only few cells are released into the channel and measured. This agglomeration could be explained by the large vertical (z direction) magnetic gradients created by magnet at channel's inlet. Some cells could only be released by the Stoke force created by a large flow rate (50 $\mu\text{l}/\text{min}$). Therefore, further optimizations of the system could include new inlet geometry, more homogeneous external magnetic field and/or higher flow rates aiming at reduction of magnetic agglomeration at the inlet.

The platform's quantitative detection limit still requires further testing, however a limit of 10 CFU/ μl has already been attained in a yes/no answer format as described in our subsequent work (Duarte et al., 2015).

A quantitative output of the platform can be obtained, through correlation between experimental and simulated peaks. One example can be seen in Figure 29, where one experimental peak from raw milk with bacteria could be compared with the simulation assuming a $-\pi/10$ rotation (in x direction).

The amplitude of 60 μV was achieved by considering that two *S. agalactiae* cells were contributing to the detected signal.

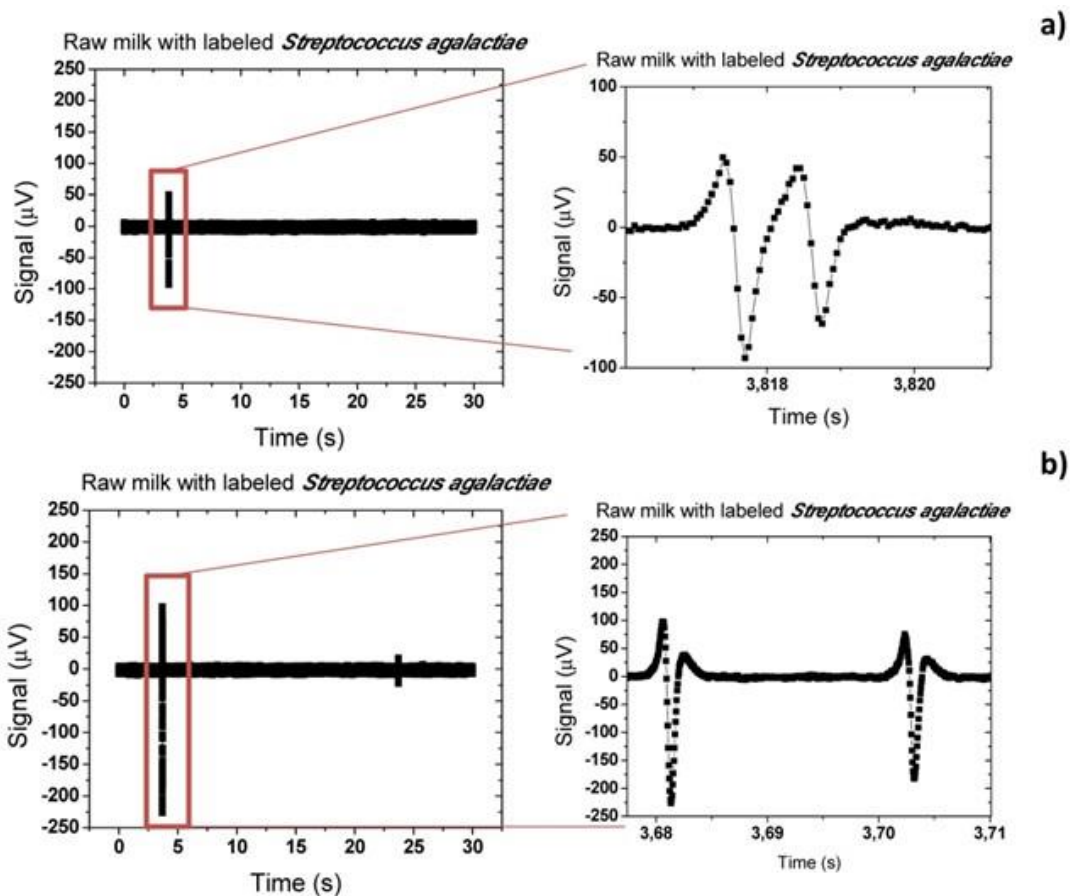


Figure 28. Acquisition signal for raw milk samples with magnetically labeled *Streptococcus agalactiae* cells at 50 $\mu\text{l}/\text{min}$.

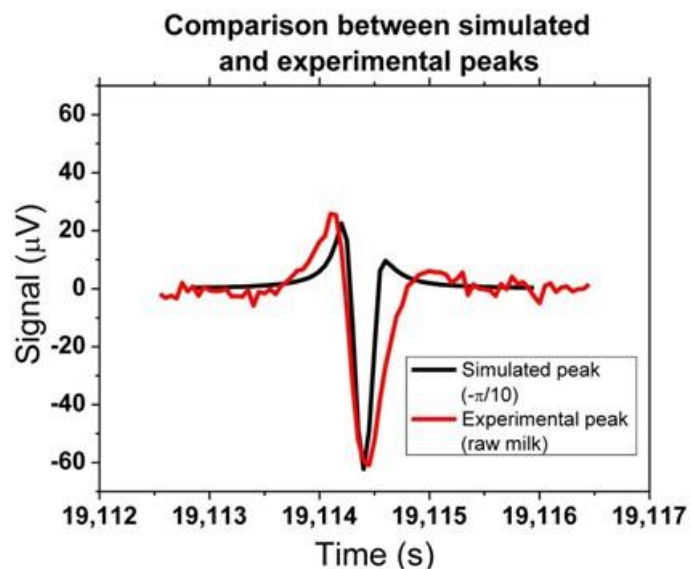


Figure 29. Direct comparison of experimental and simulated peaks. The simulation considered two *Streptococcus agalactiae* cells flowing at 50 $\mu\text{l}/\text{min}$, with a rotation of the magnetization by an angle of $-\pi/10$ with respect to the vertical.

Finally, a study comparing measurements in raw milk and defatted milk samples was performed. As observed in Figure 30b,c, the peaks' shape in defatted and raw milk are very similar and, as discussed previously, indicate that cells are rolling over sensor's surface. However, peaks in defatted milk show almost twice the amplitude than peaks in raw milk. This can be explained by the fact that raw milk is a more complex solution than defatted milk and therefore its constituents (fat globules, casein, etc.) can be blocking the binding of magnetic nanoparticles to bacteria. This fact leads to a lower load of magnetic nanoparticles on bacteria inside raw milk and thus lower signals are measured.

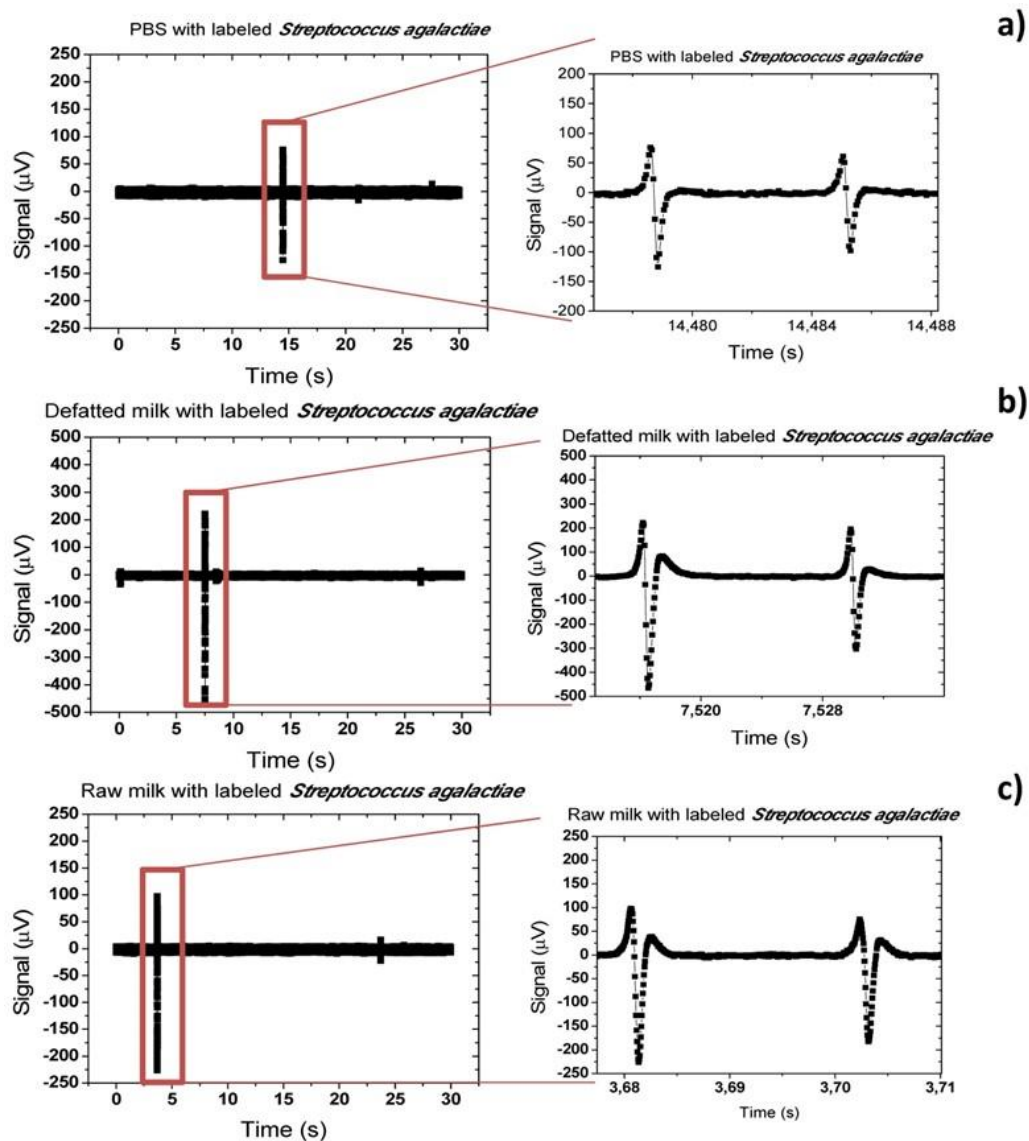


Figure 30. Acquisition signal of (a) PBS; (b) defatted and (c) raw milk samples spiked with magnetically labeled *Streptococcus agalactiae* cells at $50 \mu\text{l}/\text{min}$.

On the other hand, PBS solution presents smaller amplitude peaks than milk samples (Figure 30a). Meaning probably that bacterial cells have less magnetic particles bonded. It is coherent with its simpler saline composition, unlike milk complexity, explaining more individualized bacteria cells. However, milk samples larger peaks show us that sensor might detect bacteria cells agglomerations due to favorable immunological bonding conditions existing in milk.

5. Conclusions/Outlook

This work describes a platform for in-flow detection of magnetically labelled cells with a magnetoresistive based cell cytometer, as an inexpensive and portable alternative to current flow cytometry in bio-applications. Sensor output response to cells and particles were simulated to obtain the impact of their position in the microchannel with respect to the sensor. Simulations indicated that the analysis of the different peaks' amplitudes and shapes can infer the position of the cells inside the channel and eventual simultaneous passage of two cells over the sensor. Experiments performed in raw milk, defatted milk and PBS buffer demonstrated specific detection of *Streptococcus agalactiae* cells. The results indicate that raw milk constituents (fat globules, casein, etc.) inhibit the bonding of nanoparticles to the bacteria leading to lower signal amplitudes. On the other hand, quantification is still an output to be improved since the cells seem to agglomerate at channel's inlet due to a strong magnetic gradient. To overcome this limitation, a different inlet/channel design, more homogeneous external magnetic field and/or higher flow rates, could reduce this cells agglomeration and deliver more reliable quantification values.

CHAPTER IV

Magnetic counter for Group B Streptococci detection in milk.

C.M. Duarte, A.C. Fernandes, F.A. Cardoso, R. Bexiga, S. Cardoso, P.P. Freitas
(2015). *IEEE Transactions on Magnetics*, 51(1). doi
10.1109/TMAG.2014.2359574

* The author contributed to the conception and design of the study, conducted the experiments, participated in the data analysis process and drafted the manuscript.

Abstract

Identification of bovine mastitis pathogens is necessary to control the disease, reduce the risk of chronic infections, and target the antimicrobial therapy to be prescribed. Development prospects for new bovine mastitis diagnosis methodologies go also through rapid and efficient devices that can offer a cow-side use, meaning that raw milk collected for analysis should have limited pretreatment. This paper aims at developing a magnetic counter that identifies the presence of *Streptococcus agalactiae* (a Group B Streptococci) in raw milk. The detection is done with an integrated microfluidic platform, where 50 nm magnetic beads attached to *Streptococcus agalactiae* are dynamically detected by magnetoresistive sensors. This device allows the analysis of raw milk without bridging the microfluidic channels, making this integrated platform very attractive for fast bacteriological contamination screening.

Index Terms: Cytometer, magnetic detection, microfluidic channels, milk, *Streptococcus agalactiae*.

1. Introduction

Bovine mastitis is an inflammation of the mammary gland, most often of infectious origin. It is the most frequent disease of dairy cattle and one of the main reasons for culling dairy cows (Gröhn, Eicker, Ducrocq & Hertl, 1998; Hortet & Seegers, 1998; Hovi & Roderick, 1999). Dairy farm management focusing on animal health and hygiene improvement program implementation, contributes to control mastitis. The timely identification of etiologic agents is necessary to control the disease, reduce the risk of chronic infections and target the antimicrobial therapy to be used. *Streptococcus agalactiae* (a Lancefield Group B Streptococci) is one of the major mastitis pathogens (Bradley, 2002) that can be found in milk.

This work describes the application of a magnetic detection device for identification and quantification of *Streptococcus agalactiae*, present in milk samples. Our portable device is composed of magnetoresistive (MR) sensors, namely spin-valve sensors (SVs), integrated with a microfluidic platform and connected to an amplification and acquisition setup. The sensors are sensitive to the magnetic field created by magnetically labeled cells flowing in microchannels above the sensors. This dynamic detection is based on immunoassay methodology since these antibodies anti-Group B (GB) Streptococci (probes) recognize immunogenic proteins on bacteria cell walls (targets). The SV sensor detects the fringe field of the magnetic labels bound around the target cell through the specific probe. In our previous work (¹Fernandes et al., 2014), the platform is described in detail, and a proof of concept is demonstrated, for milk samples. Here we reduce the functionalized nanoparticles quantity to the limits where one can distinguish magnetic signal amplitude between milk control samples and milk samples with known bacterial concentrations.

2. Material and methods

All device fabrication steps (sensors and microfluidic channels) and milk sample trials were performed at INESC-MN (¹Fernandes et al., 2014), using acquisition setup adapted from a previous work (Loureiro et al., 2011). The cell culture, magnetic functionalization and labeling protocols were performed at CIISA, according to preexisting and manufacturer protocols.

2.1. Sensor fabrication

The integrated cytometer used here was fabricated according to a previously developed geometry (Loureiro et al., 2011). The chips fabricated comprised four sets of rectangular SVs disposed in a line. Each SV set includes seven sensors with $3\mu\text{m}$ width, and length varying from 20 to $100\mu\text{m}$ (measured between contact leads), according to Figure 31. Sensor geometry was optimized to promote a linear, hysteresis-free transfer curve upon patterning. Additionally to individual sensors, we have included also 4 sensors connected in series. In this work we have selected results obtained with the $100 \times 3\mu\text{m}^2$. These configurations were designed to cover the width of the PDMS microchannel to be included above the chip.

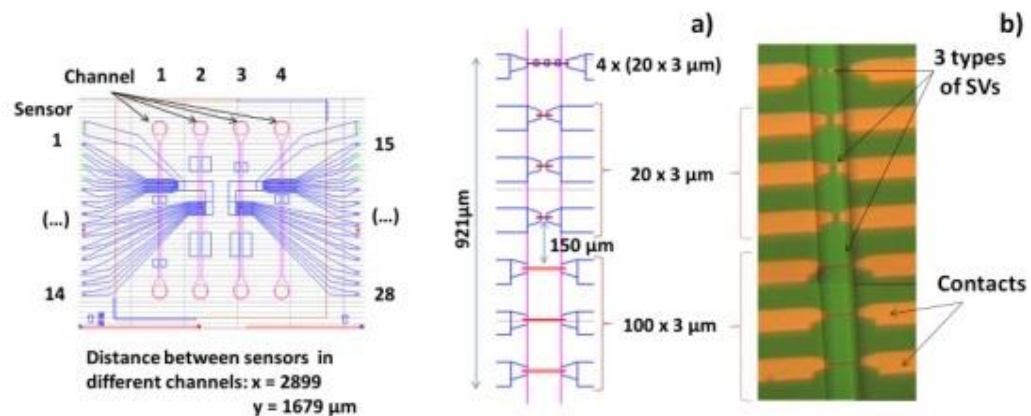


Figure 31. a) Device CAD mask showing microfluidic channels, sensors and sensor contact leads. Each channel crosses several sensors, b) Microscope photo of one microchannel aligned over 7 microfabricated SVs.

The sensors were fabricated on a 150 mm-diameter silicon wafer passivated with a 50 nm-thick Al_2O_3 film. The SV thin film stack was deposited by Ion Beam deposition in Nordiko 3000 tool with the structure (thickness in nm, atomic % of composition): Ta 2.0/ $\text{Ni}_{80}\text{Fe}_{20}$ 2.5/ $\text{Co}_{80}\text{Fe}_{20}$ 2.3/ Cu 2.2/ $\text{Co}_{80}\text{Fe}_{20}$ 3.3/ $\text{Mn}_{76}\text{Ir}_{24}$

7.0/ Ta 10.0 (Gehanno et al., 1999). During the deposition, a 3mT magnetic field was applied in order to induce a parallel anisotropy simultaneously for the free layer (Ni₈₀Fe₂₀/Co₈₀Fe₂₀) and pinned layer (Co₈₀Fe₂₀) easy axis. SV definition was performed by direct write laser (DWL) lithography and Ion Milling in a Nordiko 3600 tool. The metallic contacts were defined by lithography and liftoff of a 300 nm-thick Al_{98.5}Si_{1.0}Cu_{0.5}/15 nm-thick Ti₁₀W₉₀(N₂) layer deposited by PVD (Physical Vapor Deposition) in a Nordiko 7000 tool. A passivation layer of 300 nm-thick Si₃N₄ was deposited. Via definition was performed by lithography and reactive ion etching in Rainbow Plasma Etcher 4400. After dicing and before characterization, all individual dies were submitted to a magnetic annealing at 250°C for 15 minutes, in vacuum and cooled down under a 1 Tesla magnetic field.

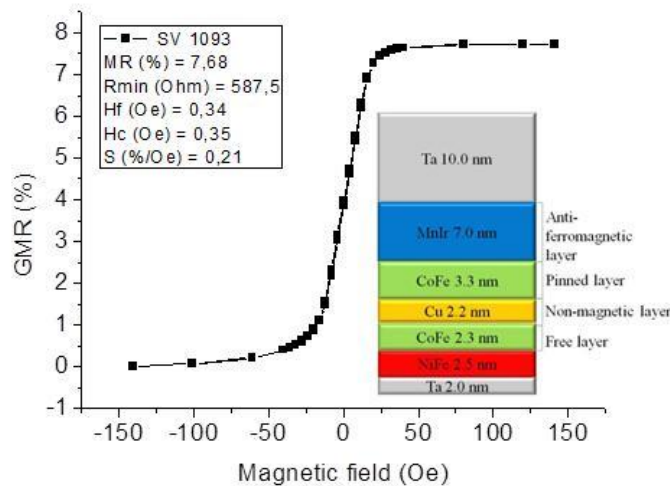


Figure 32. Selected transfer curve for a SV sensor with 100 x 3μm².

The sensors' electrical transport (resistance versus DC magnetic field) was characterized at INESC-MN. The resistance variation with magnetic field, normalized by the minimum resistance is defined as magnetoresistance, $MR = \frac{R_{max} - R_{min}}{R_{min}}$. Figure 32 shows a representative example of the sensor transfer curve, for a sensor with dimensions of 100 x 3μm², showing a linear range of 65 Oe, a sensitivity (S) of 0.21 %/Oe, offset field (Hf) of 0.34 Oe and coercivity (Hc) of 0.35 Oe.

2.2. Microfluidic channel fabrication

The microchannels (Figure 31.a) were fabricated in poly(dimethylsiloxane) (PDMS), with 100 μ m x 100 μ m cross section. A hard-mask used to expose channels' mold was first made of Al_{98.5}Si_{1.0}Cu_{0.5} 150 nm thick layer deposited on Corning glass by PVD in a Nordiko 7000 tool, patterned by DWL lithography and chemically etched with a solution of acetic acid (3.3%), nitric acid (3.1%) and phosphoric acid (3.0%). Channels' geometry was defined by contact microlithography using 100 μ m thick SU-8 50 photosensitive negative resist (soft-baked for 10 min at 65°C, followed by 30 min at 95°C). After exposing for 56 s with a 320-405 nm UV light (600 mJ/cm²) the resist was developed with PGMEA. This mold was mounted on a plate where PDMS was injected (1:10 curing agent and elastomeric base, with 1 hour degassing), aiming a final thickness of 2 mm. The PDMS was then cured for 1 hour at 70°C. Silicon chip integration with PDMS microchannels was achieved through irreversible bonding of the Si₃N₄ and PDMS surfaces. Both surfaces were exposed to ultraviolet/ ozone (UVO Cleaner (Jelight, USA) for 15 min., and then mounted face-to-face and manually aligned. Finally, the bonded device was kept at RT, overnight, for irreversible bonding.

2.3. Readout electronics

Sensor output signals were obtained using a 3 mA bias current, supplied by two 9 V batteries in series (~18 V), using a layout described in Loureiro and coworkers (2011) research. The output of the sensor was connected to an acquisition setup composed by a) an amplifier (Stanford Research Systems SR560) operating for gains of 10 000x, b) high-pass and low-pass filters of 300 (to filter the DC and part of low frequency noise) and 10 000 Hz (to avoid aliasing), respectively and c) a 16 bit analogue to digital converter (ADC) board DT9836-12-2-BNC (20 kHz acquisition frequency), which was connected to the computer.

2.4. Particles' functionalization

Nanomag®-D-spio 50 nm particles (79-20-501, MicromodPartikeltechnologie GmbH) were selected because they have protein A on the surface and can bind up to five IgG. The calculation of beads number and the amount of polyclonal antibody (pAb) anti-GB Streptococci (8435-2000, AbD Serotec) was based on

the *Streptococcus agalactiae* concentration in samples and considering 10 and 100 fold more than one cell surface area saturation (1600 particles) with 50 nm nanoparticles (baseline estimated according to Wolfram Mathematica 7.0 calculations). Particles (7.27 μ l of original vial) were coated with 0.53 μ l of pAb anti-GB Streptococci (1 μ g/ml) at RT incubation, during 50 min. assisted with rolls plate agitation. Functionalized particles were magnetically separated by MS (Magnetic Separation) column (130-042-201 Miltenyi) according to MiltenyiBiotec protocol. A suspension of 4x10⁸ functionalized beads/ μ l was obtained for further dilution according to different concentrations of nanobeads and target bacteria. Biological affinities between nanobead surface protein A, IgG Fc fraction and *Streptococcus agalactiae* cell wall immunogenic proteins are illustrated in Figure 33.

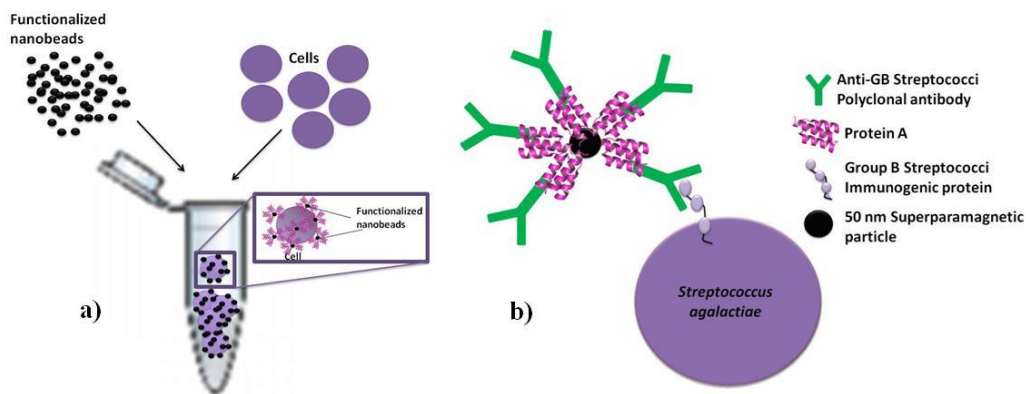


Figure 33. Schematics of immuno-magnetic functionalization of cells a) Incubation of functionalized beads with bacteria cells and b) biological affinities between beads protein A, polyclonal IgG antibodies and bacterial cell wall epitopes.

2.5. Bacterial cells magnetic labeling

Streptococcus agalactiae (CECT 183) cells were grown at 37°C overnight on sheep blood agar plates and resuspended in TSB (trypticasein soy broth) over 24 hours at 37°C ((Cole et al., 2008) adapted protocol). After cell pellet collection through 2700 rpm centrifugation at 17°C during 15min. and discarding of the supernatant, PBS (Phosphate Buffered Saline) 1X (pH 7.2) buffer was added for absorbance reading at 600 nm (BECKMAN DU-68 Spectrophotometer) and for (Colony-Forming Unit) CFU/ml estimation.

For incubation of 100 μ l of magnetic particles with pAb anti-GB Streptococci, milk and PBS volumes were prepared for a final sample volume of 500 μ l, and

bacteria concentrations of 100 CFU/ μ l. Incubation was performed at room temperature (RT) for 50 min assisted with rolls plate agitation.

2.6. Milk samples preparation

Raw milk for experiments was collected aseptically from a healthy cow. Conventional microbiological tests were performed according to NMC (1999) protocols, to confirm no bacterial growth. Briefly, a raw milk drop (10 μ l loop) was smeared on a sheep blood agar plate (Biomerieux, 43021) and in a MacConkey agar plate and both incubated at 37°C for 48 hours. To achieve defatted milk samples, raw milk was frozen at -20°C during 24h and then thawed. During freezing, fat “cold agglutination” occurs forming a top layer of crystallized fat globules at the milk surface (Walstra, Wouters & Geurts, 2006). This layer was removed and milk underneath was used as defatted one.

2.7. Sample measurement

According to our previous work (¹Fernandes et al., 2014), experiments were made at the fastest flow rate (50 μ l/min) and with milk with the least fat content, namely defatted milk. PBS and defat milk samples were tested under the following conditions:

(i) alone;

(ii) with only functionalized particles, further called “controls”. The concentration of beads was set as 10x and 100x 1600 beads/ cell. Calculations take into account that samples could have three different bacteria concentrations;

(iii) with functionalized particles incubated with different bacterial concentrations. Here the number of beads is calculated as previously but now with bacterial cells (100 CFU/ μ l) for each quantity of functionalized beads (10x and 100x).

As an example, a defatted milk sample with 10x1600 functionalized particles and with 100 CFU/ μ l of *Streptococcus agalactiae* concentration, had a volume of 10 μ l of the suspension of 4x10⁸ functionalized beads/ μ l obtained from MS column, diluted in 90 μ l of PBS (100 μ l on total). This is posteriorly added to 400 μ l of defatted milk with bacterial cells. These 400 μ l are composed by 397 μ l of defatted milk and 3 μ l of the suspension of cells with 1,82x10⁴ CFU/ μ l. After 50 minutes incubating in rolls plate agitation at RT, sample was injected through microfluidic channel for SV measurement.

The PDMS microchannel above the SV sensors was washed with 70% ethanol (90 μ l/min, 10 min) and deionized water (90 μ l/min, 10 min) between experiments. This minimizes contaminations between tests with control samples, samples with bacteria, PBS samples and milk ones.

3. Results and discussion

A. Typical signals

Figure 34 shows typical signals obtain in PBS or defatted milk samples: without beads or bacteria, with beads and bacteria and with a cleaning solution. On one hand, the noise measured (+ 20 μ V) was mostly independent of the solution flowing over the sensor. This was expected since the magnetoresistive sensors are only sensitive to magnetic fields and, both PBS and defatted milk solutions by nature have no magnetic content inside.

On the other hand, peaks ranging from 50 to 500 μ V only appear in solutions where beads and bacteria were added. This means that the observed signals are undoubtedly from magnetic origin, i.e. caused by magnetic particles passage. However, when flowing a solution with bacteria and beads during a period of time of 300s, it can be observed that the presence of peaks is inhomogeneous overtime. In particular, in the PBS solutions, magnetic signals were only observed during a small time span of ~30s. This indicates that there is an agglomeration of magnetic beads at channel's inlet and only once in a while there is a release of beads. Magnetic beads agglomeration can be explained by strong vertical magnetic forces generated by the magnet under the chip which capture the magnetic labels at channel's inlet. A more homogeneous magnetic field needs to be implemented in order to minimize this effect.

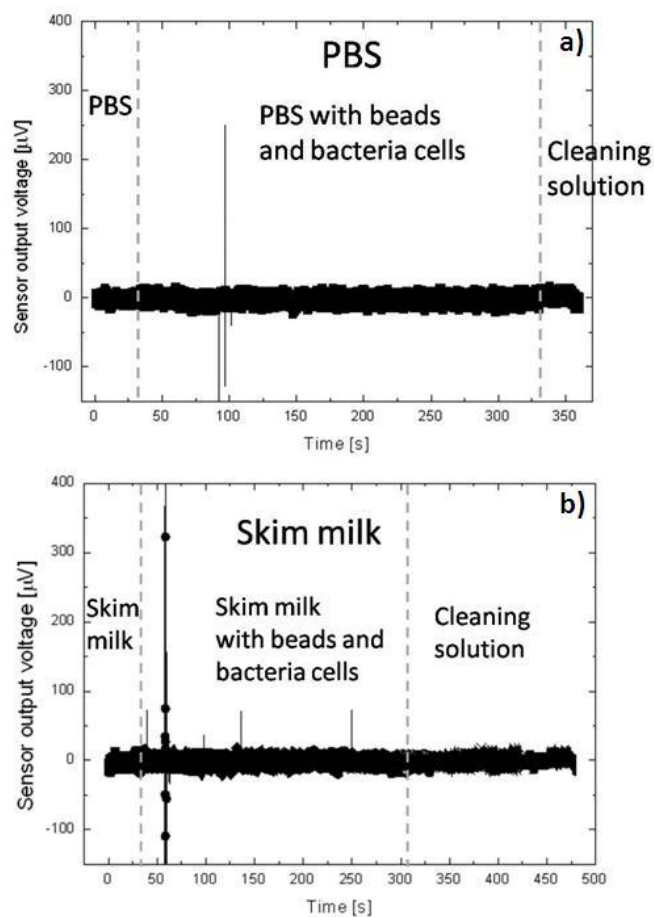


Figure 34. Dynamic detection and differences between sensor signals on the passage of: a) PBS, PBS with beads (10x) and *Streptococcus agalactiae* cells (100 CFU/ µl) and a cleaning solution; b) defatted milk, defatted milk with beads (10x) and *Streptococcus agalactiae* cells (100 CFU/ µl) and a cleaning solution.

B. Quantification results

In order to evaluate the labeling efficiency, different concentration of magnetic beads (x10 and x100) were used in PBS and defatted milk spiked with and without 100 CFU/ µl of *Streptococcus agalactiae* cells. The solutions without bacteria were the control ones. As observed in experiments, all the control solutions showed no peak whatsoever. This indicates that all observed peaks are due to several beads bonded to *Streptococcus agalactiae* immunogenic proteins and therefore due to specific detection of these bacteria. However, as observed in figure 35 b), c), d) and e), peaks amplitude may vary between 50 to 500 µV. Assuming that each peak corresponds to an agglomeration of magnetically labeled cells, the large discrepancy in peaks amplitude can be explained by cells number variation in each agglomerate. On the other hand, these agglomerates can

be flowing at different heights above the sensor having also an influence in peak amplitude (¹Fernandes et al., 2014). Therefore, at this stage, only a qualitative analysis of these results can be performed. In fact, if bacterial cells are present, peaks can be correlated to the presence of *Streptococcus agalactiae* cells in the solution because of polyclonal antibody specificity.

Figure 35a) shows a relationship between the number of peaks and the amount of particles used for labeling bacteria. In both defatted milk and PBS solutions, an increase of peaks number can be observed as more magnetic beads are used for labeling *Streptococcus agalactiae* cells. This increase is consistent with the fact that binding efficiency of magnetic beads to bacteria is below 100% and that more diluted magnetic beads may be unable to “find” a small amount of cells in solution, remaining unbound.

On the other hand, the best functionalized particles labeling performance shown in PBS can be explained by the fact that defatted milk is a complex solution and that some of its constituents may hinder the antibodies binding to the *Streptococcus agalactiae* cells.

Nevertheless, although a lower amount of peaks was observed in defatted milk solutions, a low concentration (100 CFU/ μ l) of *Streptococcus agalactiae* cells was successfully detected directly in milk.

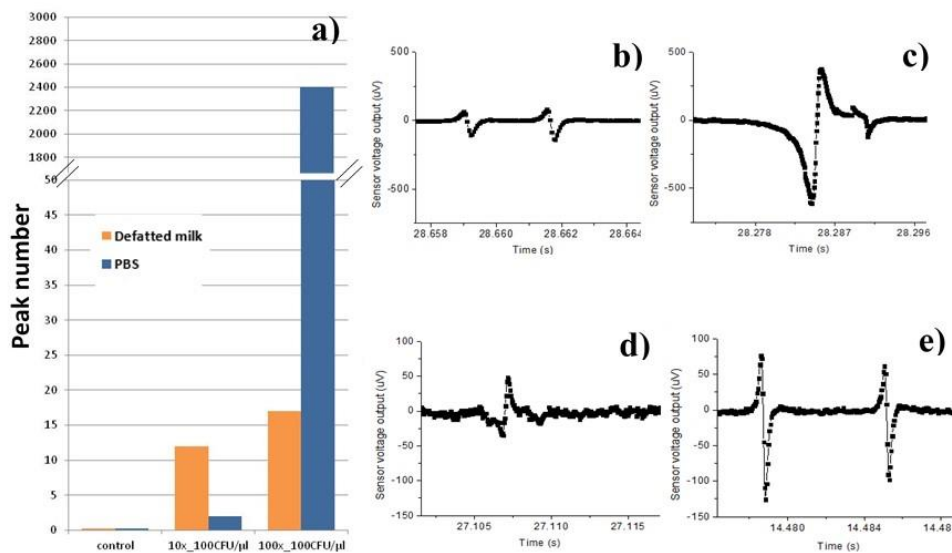


Figure 35. Differences between a) peak numbers in defatted milk and PBS samples with 100 CFU/ μ l of *Streptococcus agalactiae* and different concentrations of functionalized beads. Peak details in b) defatted milk with lower (10x) and c) higher concentration (100x) of functionalized beads and in PBS samples with d) lower (10x) and e) higher (100x) concentration of functionalized beads.

4. Conclusions

In conclusion, this work proposes an integrated technique for qualitative detection of *Streptococcus agalactiae* cells in raw milk using an integrated cytometer. *Streptococcus agalactiae* cells labeled with 50nm magnetic particles are detected in raw milk samples by magnetoresistive sensors without need of sample treatment. This is a huge advantage when compared with optical detection approaches that always require a previous sample preparation step to remove all milk constituents which interfere with optical detection of cells, or long time to get the results (cell culture). The quantification of bacteria is limited by the fact that magnetically labeled bacteria agglomerate at channel's inlet due to strong magnetic forces, therefore the detected signals indicate the presence of particle clusters. Furthermore, a less efficient binding of magnetic particles in milk was demonstrated when compared to PBS. On-going improvements in the homogeneity of magnetic field and labeling will allow in the near future the quantification of cells. However, even a qualitative analysis can be used in dairy farms to rapidly identify bovine causing bacteria and consequently target the antimicrobial therapy to be used, aiming a more efficient cow treatment and disease control.

CHAPTER V

Semi-quantitative method for Streptococci magnetic detection in milk.

C.M. Duarte, T. Costa, M.S. Piedade, C. Carneiro, R. Soares, A. Jitariu, S. Cardoso, R. Bexiga, P.P. Freitas. *Biosensors*, 6 (2), 19. doi 10.3390/bios6020019

* The author contributed to the conception and design of the study, conducted the experiments, participated in the data analysis process and drafted the manuscript.

Abstract

Bovine mastitis is the most costly disease for dairy farmers and the most frequent reason for the use of antibiotics in dairy cattle, thus control measures to detect and prevent mastitis are crucial for dairy farm sustainability. The aim of this study was to develop and validate a sensitive method to detect magnetically *Streptococcus agalactiae* (a Group B streptococci) and *Streptococcus uberis* in raw milk samples. Mastitic milk samples were collected aseptically from 44 cows with subclinical mastitis, from 11 Portuguese dairy farms. Forty six quarter milk samples were selected based on bacterial identification by conventional microbiology. All samples were submitted to PCR analysis. In parallel, these milk samples were mixed with a solution combining specific antibodies and magnetic nanoparticles, to be analyzed using a lab-on-a-chip magnetoresistive cytometer, with microfluidic sample handling. This paper describes a point of care methodology used for detection of bacteria, including analysis of false positive/negative results. This immunological recognition was able to detect bacterial presence in samples spiked above 100 cfu/ml, independently of antibody and targeted bacteria used in this work. Using PCR as a reference, this method correctly identified 73% of positive samples for streptococci species with an anti-*S. agalactiae* antibody, and 41% of positive samples for an anti-GB Streptococci antibody.

Keywords: magnetoresistive sensors, magnetic nanoparticle (NP), *Streptococcus agalactiae*, *Streptococcus uberis*, milk, immunogenic recognition, microfluidic

1. Introduction

Bovine mastitis, the inflammation of the mammary gland most often with infectious origin, is the most costly disease for dairy farmers and the most frequent reason for the use of antibiotics in dairy cattle, thus control measures to prevent mastitis are crucial for farm sustainability. The identification of contagious bacteria that cause mastitis is necessary to control the disease in the herd, reduce the risk of chronic infections and target antimicrobial therapy. *Streptococcus agalactiae* (a Lancefield Group B Streptococci) and *Streptococcus uberis* (no Lancefield group) are major mastitis pathogens (Bradley, 2002) that can be transmitted from cow to cow in the milking parlor in a contagious way (Zadoks, Middleton, McDougall, Katholm & Schukken, 2011). Their identification is currently performed most often through conventional bacteriology, by growth of bacteria in culture media, isolation and identification based on phenotypic features. This methodology is time-consuming, with results taking between 48 and 72 hours to be obtained, and can lead to no-growth results corresponding to false negatives. In these cases, phenotypic identification is being supplemented with genotypic methods, as Polymerase Chain Reaction (PCR) (Raemy et al., 2013) for more accurate identification of bacteria associated with intramammary infections.

The suitability of a detection method for routine diagnosis as “cow-side use” depends mainly on time to produce results, sensitivity and specificity. Immunological identification of mastitis pathogens has been reported (Hicks et al, 1994; Bourry & Poutrel, 1996). These authors suggested that the diagnosis of clinical mastitis cases could be considerably enhanced if samples showing no growth on culture media could be subjected to an enzyme-linked immunosorbent assay (ELISA), because of the antibodies' observed ability to detect soluble as well as insoluble antigens, independently of intact bacterial cell presence in milk. The basis for a true positive result in immunological analysis is the confidence on the specificity of the selected antibody. As mentioned in previous work (Fernandes et al., 2014), Western Blotting assays using a polyclonal anti-GB Streptococci antibody evidenced two stained immunogenic proteins in *Streptococcus uberis* cell wall proteins' pattern besides the expected immunogenic protein set of *Streptococcus agalactiae*. According to Groschup,

Hahn and Timoney (1991), some *Streptococcus uberis* strains can also react with Lancefield group B serum.

The use of portable platforms to detect bacteria has been optimized (Driskell & Tripp, 2009) allowing for cell separation, identification and counting to be achieved in a compact and modular format. This feature can be combined with magnetic detection, where magnetoresistive (MR) sensors can be integrated within microfluidic channels to detect magnetically labelled cells, being promising as one emerging technology for magnetic biodetection (Lazcka et al., 2007; Loureiro et al., 2011).

The aim of this study was to develop and validate a sensitive method for magnetic detection of *Streptococcus agalactiae* and *Streptococcus uberis* in raw milk samples. For both magnetic detection and conventional microbiology methods, sensitivity, specificity and positive predictive value (PPV) were calculated in comparison with the PCR reference method.

2. Material and methods

2.1. Method principles

This dynamic detection is based on the detection of the fringe field created by magnetic particles attached to the bacterial cells. By selecting the suitable antibodies, it is possible to perform immunological recognition of Group B Streptococci (including *Streptococcus agalactiae*) and of *Streptococcus uberis* immunogenic proteins (Figure 36A, B). A polyclonal anti-GB Streptococci IgG (8435-2000, AbD Serotec) and one monoclonal anti-*Streptococcus agalactiae* IgM (MA1-10871, Thermo Fisher), were used separately. The antibodies were expected to attach to protein A of Nanomag®-D-spio 50 nm particles (79-20-501, MicromodPartikeltechnologie GmbH), by the Fc fraction in immunoglobulins G and by the joining chain (J chain) in immunoglobulins M (Figure 36C). Antibodies and bacterial cells dimensions are shown in Figure 36.

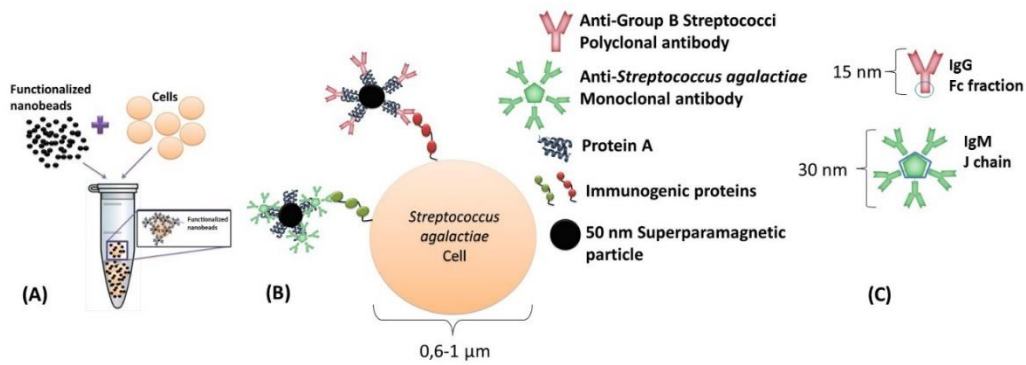


Figure 36. Schematics of immuno-magnetic detection of cells. (A) Incubation of functionalized NPs with bacteria cells and (B) biological affinities between different functionalized NPs with bacterial cell wall immunogenic proteins. (C) Predictable protein A binding site to each antibody.

The bio-functionalization of nanoparticles was achieved by the addition of 7.27 μl from nanoparticles original vial, to 0.53 μl of polyclonal anti-GB Streptococci antibody (1 mg/ml) (or to 5.5 μl of monoclonal anti- *Streptococcus agalactiae* antibody (0.5 mg/ml)) in 492.2 μl (or 487.2 μl) of PBS. The incubation step required 1 hour at room temperature (RT) and continuous agitation. Final functionalized particles were magnetically isolated by MS column (130-042-201 Miltenyi) according to MACS MiltenyiBiotec protocol and eluted with phosphate buffered saline (PBS) + 0.5% bovine serum albumin (BSA) + 2 mM ethylene diamine tetra acetic acid (EDTA) buffer after removal of the MS column from the magnet. A volume of 2 μl of this final suspension was added to each PBS or milk sample.

2.2. Biosensor fabrication

Following a previously reported work for magnetic particle detection (Loureiro et al., 2011; Freitas et al., 2012), an integrated cytometer platform was used, consisting of magnetoresistive sensors and readout/acquisition electronics and a microfluidic channel where the milk was injected. The device geometry and physical principles of operation are described (Fernandes et al., 2014), and are based on spin valves (SV) deposited by Ion Beam Deposition on a Nordiko 3000 tool with the following structure: Si/Al₂O₃ 60/ Ta 1.5/ Ni₈₀Fe₂₀ 2.5/ Co₉₀Fe₁₀ 2.0/ Cu 2.1/ Co₉₀Fe₁₀ 2.0/ Mn₇₆Ir₂₄ 6.0/ Ta 5.0 (Gehanno et al., 1999; Freitas et al., 2007) (thickness in nm, compositions in atomic %), patterned with 3 μm x 100 μm active dimensions (measured between the AlSiCu 300 nm thick contact

leads), according to Figure 37. Passivation was done with a 300 nm thick Si_3N_4 layer deposited by PECVD (electrotech delta chemical vapor deposition system). Sensors were annealed at 250°C for 15 min, in vacuum, and cooled down under 1 Tesla magnetic field.

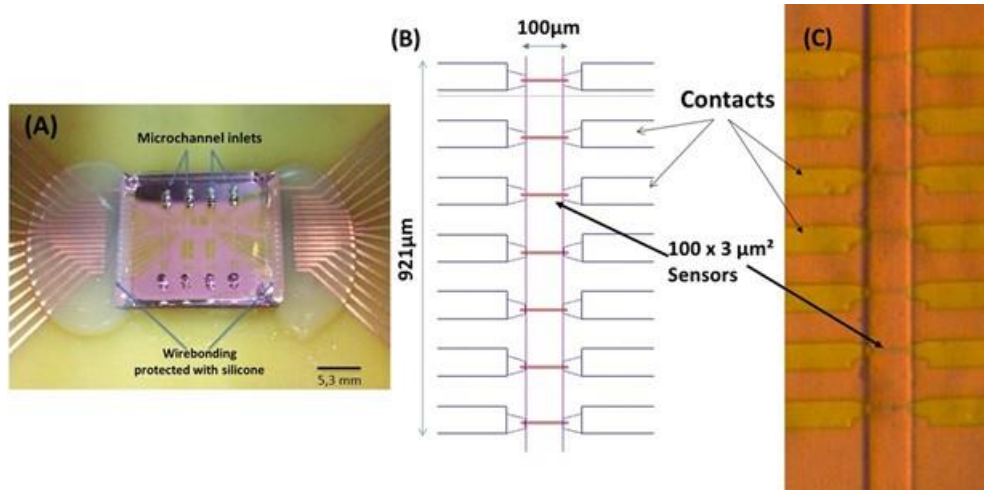


Figure 37. (A) Final device with the magnetoresistive chip bonded to the polydimethylsiloxane (PDMS) microchannels. The sensor's wirebonding are protected with silicone. (B) Spinvalve (SV) sensor distribution along the microchannels. (C) Microscope photo of the fabricated SVs with the PDMS micro channel over them (20X amplification).

The SV sensors electrical transport characterization (resistance versus DC magnetic field) provided information on the magnetoresistance, defined as $\text{MR} = (\text{R}_{\text{max}} - \text{R}_{\text{min}}) / \text{R}_{\text{min}}$ (where R_{max} and R_{min} are the maximum and minimum resistance levels). The sensor sensitivity is defined as the slope of the curve over the linear range of operation and ranges 0.15-0.17 % /Oe for the sensors measured across the wafer.

The magnetic detection mechanism used nanoparticles which had a superparamagnetic signature, therefore required an external magnetic field to activate their magnetization. This was done with an external vertical field created by a permanent magnet (NdFeB, 20-10-01STIC, Supermagnete) mounted below the printed circuit board (PCB). After magnet alignment below this sensor, the effect of the small components in the plane of the sensors was visible in their sensitivity decrease to 0.074% /Oe. The magnetic field at the microfluidic channel center was ~ 31 mT, so the individual nanoparticles were magnetized with a magnetic moment of 2.0×10^{-18} Am². Upon magnetization, the nanoparticles created a magnetic field fringe field at the sensor surface, therefore the particle

presence was detected through the changes in the sensor resistance (or voltage, as shown in Figure 40).

2.3. Microfluidic channel fabrication

The microchannels (Figure 37B) were fabricated in polydimethylsiloxane (PDMS), with 100 μm (length) x 50 μm (height), following the method described in Fernandes and colleagues' work (2014).

The integration of the magnetoresistive chip with the PDMS microchannels was achieved through irreversible bonding of the Si_3N_4 and PDMS surfaces. Both surfaces were exposed to ultraviolet/ ozone (UVO Cleaner, Jelight, USA) for 15 min and then mounted face-to-face and manually aligned to be kept at room temperature (RT), overnight. The ensemble was then mounted in a PCB, where the sensors were wire-bonded and the wires protected with silicone (Figure 37A). The raw milk samples constant flowing through microchannel's section of 50 μm height and 100 μm length was challenging because of its density and colloidal behavior. A surfactant addition to milk samples, namely Tween 20, was used to achieve higher dispersion of fat globules (0.1-10 μm), allowing lower interfacial tension and its dimension reduction (Walstra et al., 2006). On the other hand, we adopted the milk preparation method of dairy industries for milk homogenization, using agitation (vortex) and higher temperatures (60°C) to decrease fat globules dimension and allow its uniform distribution in the sample.

2.4. Readout electronics

The multi-channel PCB designed to interface 15 spin-valve sensors was connected to an amplifier with operating gain of 5000x, a high-pass and low-pass filters of 300Hz and 10 kHz, respectively. Each channel included a configurable DC current source, from 0.25 mA to 2 mA (Costa, Piedade, Germano, Amaral & Freitas, 2014).

In this work, only one sensor per channel was monitored. One syringe pump was attached to the system, and was the only device not operating under DC batteries (thus, introducing the 50 Hz noise from the main power grid). The sensor output signals were recorded over time by using a connection to an acquisition setup composed by a 16 bit-analog-to-digital converter (ADC board DT9836-12-2-BNC), at 50 kHz acquisition frequency. The resulting digital signals were then post-processed in a software developed in Matlab, to apply a low pass digital

filter with cut-off frequency of 2 kHz, allowing real-time noise characterization and data-storing into the hard-drive for further analysis (Figure 38). The sensors used for this work showed a noise level of 2.5-4 μ V (peak-to-peak). During the experiments, the pump operation increased the noise level to 3-4.5 μ V.

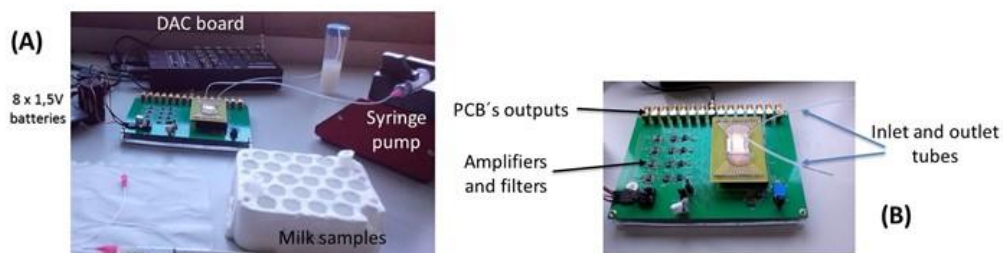


Figure 38. (A) Acquisition setup assembly and (B) multi-channel PCB connected to external electronics.

2.5. Magnetic detection method calibration

A blank sample (only PBS or sterile raw milk) and a negative control sample (PBS or sterile raw milk, with 2 μ l of functionalized NPs) were always measured prior to the measurements with contaminated milk, giving the background signal of the system.

A first calibration assay was then made with *Streptococcus agalactiae*/ pAb anti-GB Streptococci spiked on PBS sample.

Finally, *Streptococcus agalactiae*/ pAb anti-GB Streptococci; *Streptococcus uberis*/ pAb anti-GB Streptococci and *Streptococcus agalactiae*/ mAb anti-*Streptococcus agalactiae* were spiked in sterile milk samples and the correspondent calibration curves made. Each concentration point was the result of three different assays' measurements.

The calibration range between 0.1 and 20 CFU/ μ l was established taking into account the detection limit for conventional microbiology of 500 CFU/ml (0.5 CFU/ μ l).

2.6. Bacterial cells

Streptococcus agalactiae (strain CECT 183) and *Streptococcus uberis* (strain CECT 994) cells were grown separately onto Columbia agar supplemented with 5% sheep blood (bioMérieux, 43021) and incubated at 37°C, overnight. A single colony of each isolate was selected and re-suspended onto 4 ml of Trypticase Soy Broth over 24 hours at 37°C. Subsequently, the bacterial cells were collected

through centrifugation (15 minutes, 17°C, 2700 rpm) and re-suspended in PBS 1X (pH 7.2) to allow optical density measurement (at 600 nm) (BECKMAN DU-68 Spectrophotometer) and for colony-forming unit (CFU) estimation. A bacterial suspension with a known concentration of 10^4 CFU/ μ l was the starting point to get seven different bacterial concentrations for each species, in PBS or in raw milk samples: 0.1; 0.3; 0.5; 1; 2; 10 and 20 CFU/ μ l.

2.7. Sterile milk samples

Raw milk used for the definition of calibration curves experiments was collected aseptically from healthy cows. Conventional microbiological tests were performed according to NMC protocols (NMC, 1999), to confirm no bacterial growth. Briefly, a raw milk sample (10 μ l) was plated on a Columbia agar plate and on MacConkey agar plate (CM0007, Oxoid) and both were incubated at 37°C for 48 hours. The absence of growth on both plates was considered to be equivalent to the presence of no viable bacteria in the milk.

Each sample for biosensor testing had a 500 μ l volume consisting of 2 μ l of a suspension of functionalized NPs, 98 μ l of PBST, and 400 μ l of one of seven bacterial suspensions with pre-defined bacterial concentrations in PBS or sterile raw milk. The incubation of these samples was performed at RT for 3 hours, under agitation.

All raw milk samples were submitted to a pre-treatment of 15 min at 60°C in a dry bath incubator (Grant, model QBD2) and 15 min of continuous centrifugation in a vortex mixer (Labnet) after adding bacteria and PBST. Only then, 2 μ l of functionalized NPs suspension were added for final incubation step.

2.8. Mastitic milk samples

Mastitic milk samples were collected aseptically from 44 cows originating in 11 Portuguese dairy farms. Animals were selected based on the presence of subclinical mastitis, defined by evidence of a somatic cell count over 1.000.000 cells/ml. Mammary quarters to sample were selected in these cows based on a strong positive reaction on the California Mastitis Test. Bacteria identification in mastitic milk samples was performed according to NMC protocols (1999).

These mastitic milk samples were distributed in two groups of $n = 31$ samples each for biosensor analysis, of which 16 were tested by both antibodies (anti-GB

Streptococci and anti-*Streptococcus agalactiae*). The selection of quarter milk samples was based on bacteriological results which included *Staphylococcus aureus* (n = 1), *Streptococcus agalactiae* (n = 13), *Streptococcus uberis* (n = 11), *Streptococcus* spp. (n = 4), Coagulase Negative Staphylococci (CNS) (n = 2), *Enterococcus* spp. (n = 7), *Escherichia coli* (n = 3), Yeasts (n = 3) and *Prototheca* (n = 2). All mastitic milk samples were also submitted to PCR analysis.

2.9. PCR reference method analysis

PCR analysis was performed by an external laboratory (VACUNEK, SL) with the PathoProof Mastitis Complete-16® (Thermo Scientific), which allows for the detection of 16 bovine mastitis pathogens. This method is semi-quantitative, classifying the amount of bacterial cells in mastitic milk samples as “high”, “average” or “low”.

2.10. Biosensor analysis

A volume of 400 µl of mastitic milk was collected and mixed with 98 µl of PBST. Each 498 µl sample was submitted to a pre-treatment of heating (15 min at 60°C) and homogenization (15 min in vortex). After these steps, a volume of 2 µl of a functionalized NPs suspension was added to reach a final volume of 500 µl to be submitted to incubation (RT, 3h, under agitation) and further biosensor analysis. Trials were performed with each antibody set consisting of 31 mastitic samples in different assays. Therefore, the biosensor analysis was validated 62 times. Each trial day began with noise level measurement (Figure 39-1) and each sample was injected at a flow rate of 50 µl/min, through a PDMS microchannel (Figure 39-2). The microchannel was always cleaned between samples with PBST followed by deionized water, both at a 90 µl/min flow rate (Figure 39-4), until reaching noise level values again, denoting a magnetic-free microchannel filling. A blank sample and a negative control sample were measured whenever a new MR sensor was used and always before mastitic samples analysis.

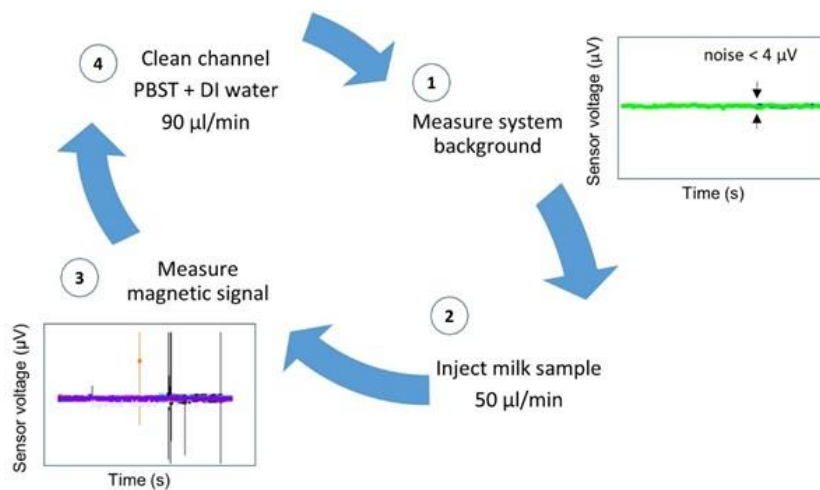


Figure 39. Biosensor analysis procedure steps.

Samples with functionalized NPs on PBS or sterile milk (negative controls) evidenced signal less than 50 µV (Figure 40A). Mastitic milk samples without the targeted bacteria (proved by PCR) and tested with NP's functionalized with chosen antibodies, also evidenced signal less than 50 µV (Figure 40B). Samples used for calibration assays spiked with bacterial cells on sterile milk showed magnetic signal upper than 50 µV (Figure 40C, D and E).

The classification of mastitic milk samples by the biosensor was based on bacterial detection (presence or absence). Consequently, the “Positive” samples were those with at least one magnetic peak above 50 µV, therefore higher than the signal found in negative control samples and in mastitic milk samples without targeted bacteria. Next, this “Positive” sample magnetic peak should evidence a bipolar or unipolar shape similar to the ones found in samples used for calibration trials as shown in Figure 5C, D and E.

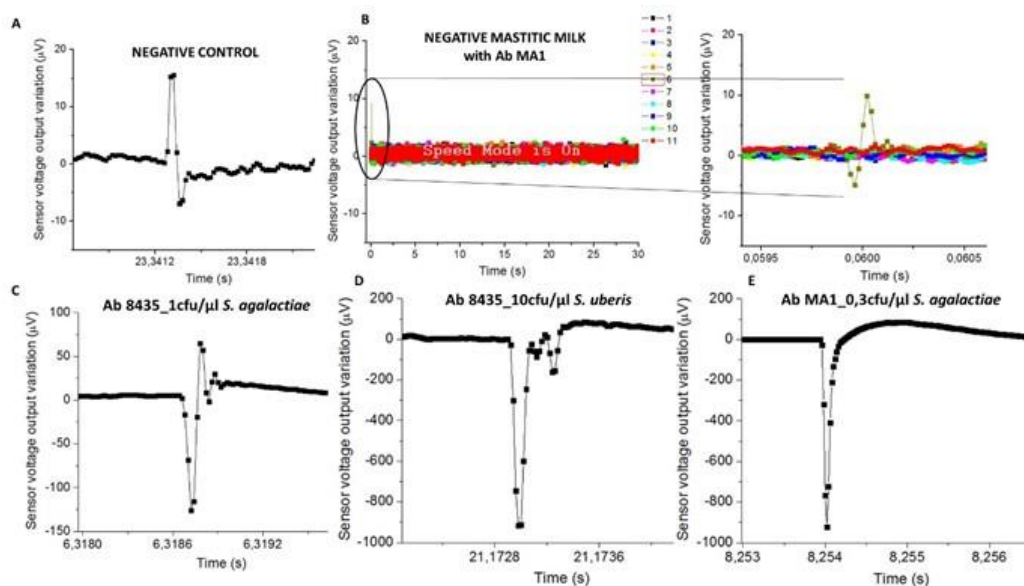


Figure 40. Sensor output for (A) negative control with the higher amplitude of 23 μV , (B) mastitic milk (without *S. agalactiae* according to the PCR) with NPs functionalized with mAb anti-*S. agalactiae* which presents an amplitude peak of 15 μV (9076AD sample code). The higher amplitude peaks found for each pair of bacteria-antibody were, (C) 193.6 μV in raw milk with anti-GB Streptococci and 1 CFU/ μl of *S. agalactiae*, (D) 917.5 μV in raw milk with anti-GB Streptococci and 10 CFU/ μl of *S. uberis* and (E) 923.7 μV in raw milk with anti-*S. agalactiae* and 0.3 CFU/ μl of *S. agalactiae*.

Biosensor analysis was a dynamic detection where a heterogeneous milk sample flowed inside the microchannel. Magnetically labelled bacterial cells were mixed randomly in milk leading to the impossibility of predicting its position above the sensor over time. Consequently, the magnetic peaks shape and time resulting from biosensor analysis were expected to be different between samples (Figure 5).

2.11. Data Analysis

Isolates were considered to be correctly identified by magnetic detection if the same species was found by the reference method, or if the magnetic detection did not identify the species it was targeting and PCR identified one of the other bacteria. For example, a correct identification referred to a *S. agalactiae* being identified magnetically in a sample that PCR had identified as *S. agalactiae*, but also when not identifying as *S. agalactiae* a sample that through PCR was identified as *Staphylococcus* spp. Regarding conventional microbiology, isolates were considered to be correctly identified if the same species was found as with the reference method. Misidentification was considered when the magnetic

detection and conventional microbiology identified a different species than the reference method. For example, a sample that was identified as *Staphylococcus* spp. by PCR and that was identified as *S. agalactiae* by magnetic detection or a sample that was identified as *S. agalactiae* by PCR and not identified as such by magnetic detection. For both magnetic detection and conventional microbiology methods, sensitivity, specificity and positive predictive value were calculated in comparison with PCR species identification. Sensitivity was calculated as the proportion of the true positive isolates that were correctly identified with the magnetic detection or microbiological tests, e.g., the proportion of *S. agalactiae* isolates based on PCR analysis that were identified as such by magnetic detection and microbiology testing. Specificity was calculated as the proportion of the true negatives that were correctly identified with the magnetic detection and the microbiological tests, e.g., the proportion of isolates other than *S. agalactiae* based on PCR analysis that were identified as something other than *S. agalactiae* by magnetic detection and by microbiological testing. Finally, PPV was calculated as the proportion of isolates identified as a specific species based on magnetic detection or on microbiological testing that truly represented that particular species, e.g., the proportion of isolates that were identified as *S. agalactiae* by magnetic detection or microbiological testing that had been identified as *S. agalactiae* based on PCR analysis.

3. Results

3.1. Evaluation of biosensor's bacterial quantification

The calibration trials outcome is shown in Figure 41. The peak's number per signal amplitude were calculated evidencing no linear correlation with increasing bacterial concentration. The milk samples with the anti-GB Streptococci antibody revealed the most exuberant signal with *S. uberis* when compared with the other two bacteria-antibody pairs (Figure 41). Only the *Streptococcus agalactiae*/ pAb anti-GB Streptococci pair evidenced no peaks higher than 200 μ V. Despite that, these MR sensors could detect *Streptococcus agalactiae* and *Streptococcus uberis* in milk samples from 0.1 CFU/ μ l (100 CFU/ml).

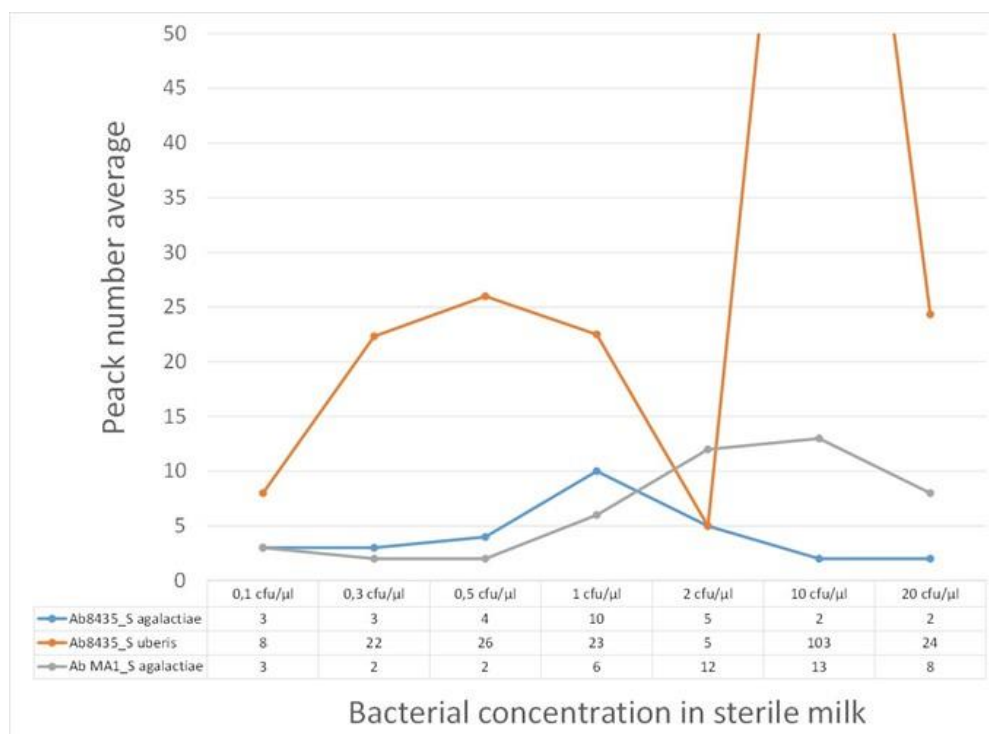


Figure 41. Calibration trials results for milk samples with seven bacterial concentrations (*S. agalactiae* or *S. uberis*) and functionalized NPs with pAb anti-GB Streptococci (Ab8435) and mAb anti-*Streptococcus agalactiae* (Ab MA1). Peak number average for each bacteria-antibody pair are counted.

The calibration curve for PBS samples with bacteria was obtained for the *Streptococcus agalactiae*/ pAb anti-GB Streptococci pair. It was evidenced that different bacterial concentrations, as in sterile milk, also presented similar amplitude peaks (under 200 μ V). Performing experimental data fitting to simulations for cell quantity estimation by peak, we obtained different results depending on considered functionalized NPs number per cell and cells cluster positioning above the MR sensor (height z) (Figure 42B, C).

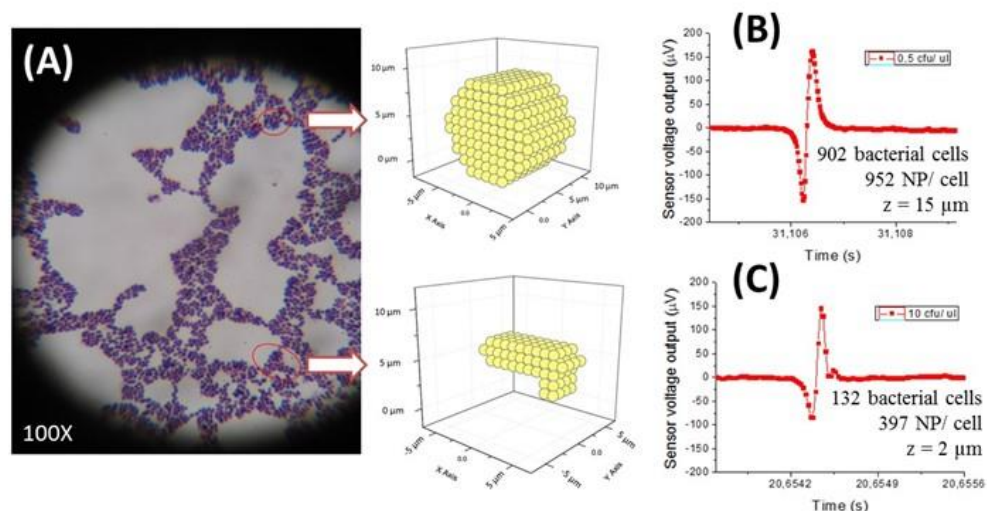


Figure 42. *Streptococcus agalactiae* cells microscopic image where a spherical cluster and an elongated cluster are evidenced (A). Experimental data fitting of the highest amplitude peaks obtained in PBS samples with different *S. agalactiae* concentrations (0.5 CFU/ μ l: 162 μ V (B) and 10 CFU/ μ l: 146 μ V (C)) during calibration curve settlement.

3.2. Validation of magnetic detection

Forty six mastitic milk samples with known bacteriology results, obtained through conventional microbiology were analyzed by PCR. A total of 160 identifications were performed by PCR for all 46 milk samples analyzed with mAb anti-*S. agalactiae* and mAb anti-GB Streptococci. The most frequently isolated species based on the PCR were *Staphylococcus* spp., *E. coli* and Yeasts followed by *S. uberis* and *S. agalactiae*. As a result of the high sensitivity of the PCR methodology, an average of 4 different pathogens were detected per mastitic milk sample, not allowing for the true causative agent of mastitis to be determined. Therefore it was decided to use the conventional bacteriology results as the basis for the true identification, confirmed by the PCR (Table 2).

The magnetic detection with the anti-*Streptococcus agalactiae* antibody tested 31 mastitic milk samples from the total of 46 analyzed by conventional microbiology, which 10 and 13 were identified as *S. agalactiae* (Table 2), respectively. However, from these 31 samples tested, 11 were identified as *S. agalactiae* by PCR and only one was not identified as such by microbiology, but as *S. uberis*. The magnetic detection with the anti-*Streptococcus agalactiae* antibody identified 8 *S. agalactiae* isolates correctly in 11 (72.7%) milk samples with this species when compared to PCR. Five mastitic milk samples did not lead to an identification by this polyclonal antibody because they did not present *S. agalactiae* according to the PCR analysis (true negatives) (Table 3). Misidentification was observed for 18 of 31 (58%) isolates in the 31 mastitic milk

samples tested with the anti-*Streptococcus agalactiae* antibody (Table 2). Only 3 misidentified *S. agalactiae* isolates were found in milk samples with this species analyzed by PCR, evidencing a failure of recognition by this monoclonal antibody (Table 2). Adding to that, 5 mastitic milk samples with *S. uberis* and/or *S. dysgalactiae* and 10 mastitic milk samples without any Streptococci species according to the PCR analysis were misidentified by biosensor analysis as having *S. agalactiae* and were all classified as false positives (Table 3). Overall a 73% sensitivity, 25% specificity and 35% PPV were found for magnetic detection with the anti-*Streptococcus agalactiae* antibody. The highest sensitivity value represents the proportion of the true positives (8) that were correctly identified with this monoclonal antibody (Table 3).

mastitic milk isolates	n	Magnetic detection						Microbiological tests		
		anti- <i>Streptococcus agalactiae</i>			anti-GB streptococci			Correctly identified		
		Correctly identified			Correctly identified			n	%	MI
<i>S. aureus</i>	1	0	0,0	0	1	100,0	0	0	0,0	1
<i>S. agalactiae</i>	13	7	70,0	3	2	25,0	6	13	100,0	0
<i>S. uberis</i>	11	3	33,3	6	5	62,5	3	8	72,7	3
Streptococcus spp.	4	0	0,0	3	2	50,0	2	1	25,0	3
Staphylococcus spp.	2	0	0,0	0	1	50,0	1	2	100,0	0
Enterococcus spp.	7	3	75,0	1	1	33,3	2	0	0,0	7
<i>Escherichia coli</i>	3	0	0,0	1	1	50,0	1	3	100,0	0
Yeasts	3	0	0,0	2	1	100,0	0	2	66,7	1
<i>Prototheca</i>	2	0	0,0	2	1	50,0	1	2	100,0	0
Total	46	13	41,9	18	15	48,4	16	31	67,4	15

Correctly identified = True Positives + True Negatives

¹ MI (misidentified) = False Negatives + False Positives

Table 2 - Identification of isolates in mastitic milk samples with both magnetic detection (mAb anti-*Streptococcus agalactiae*; pAb anti-GB Streptococci) and with conventional microbiology, compared to PCR analysis as the reference method.

Using the polyclonal anti-GB Streptococci in magnetic detection, the 31 mastitic samples tested included 16 identified equitably as *S. agalactiae* and *S. uberis* by conventional microbiology (Table 2). However, PCR analysis identified 2 more samples as *S. uberis* in the 31 analyzed by this antibody, amounting 18 bacterial target possibilities. The magnetic detection with the anti-GB Streptococci antibody identified correctly 7 streptococci isolates present in 18 (38.9%) milk samples with *S. agalactiae* and/or *S. uberis* according to PCR analysis. The microorganisms that were not identified as GB Streptococci or *S. uberis* (13/31) by the reference method in mastitic milk samples, were magnetically detected as GB streptococci and/ or *S. uberis* in those samples (5 false positives) or else, undetected as true negatives (8) (Table 3). Misidentification was observed for 16 isolates in the 31 (51.6%) mastitic samples tested. Eleven misidentified *S.*

agalactiae and *S. uberis* isolates were found in milk samples analyzed by PCR with these two streptococci, evidencing a failure of recognition by this polyclonal antibody (Table 2). Overall a sensitivity of 41%, a specificity of 57% and a PPV of 54% were found for magnetic detection with the anti-GB Streptococci antibody. The highest specificity value represents the proportion of the true negatives (8) that were correctly identified with this polyclonal antibody (Table 3).

	Magnetic detection		Microbiological tests
	anti- <i>Streptococcus agalactiae</i>	anti-GB streptococci	
True Positives	8	7	31
True Negatives	5	8	0
False Negatives	3	10	0
False Positives	15	6	15
Sensitivity	73%	41%	100%
Specificity	25%	57%	-
¹ PPV	35%	54%	67%

¹ PPV = Positive Predictive Value

Table 3 - Sensitivity, specificity and positive predictive value of the magnetic detection and the conventional microbiology, using PCR analysis as the reference method.

With regards to microbiological testing for all 46 samples considered, the highest microorganism identification, in comparison with PCR analysis, was found to be 100% for *S. agalactiae*, *Staphylococcus* spp., *E. coli* and *Prototheca*, as showed in percentage data of correct identification (Table 2). However, incomplete microbiological identifications of 67.4% (31/46) and a misidentification of 32.6% (15/46) were observed (Table 2). Microbiological tests evidenced a PPV value of 67% and a sensitivity of 100% to identify mastitis pathogens in milk samples, showing that conventional microbiology identified correctly true negatives (Table 3).

4. Discussion

Sensitivities of 73% and 41% and specificity values of 25% and 57% were obtained for magnetic identification of streptococci species with an anti-*Streptococcus agalactiae* antibody and an anti-GB Streptococci antibody, respectively. The higher PPV value (54%) evidenced for magnetic detection with the anti-GB streptococci antibody may reinforce the bonding avidity between this polyclonal antibody and the only two immunogenic cell wall proteins of *S. uberis* comparing to 10 or more antigens known in *S. agalactiae*.

Comparing sensitivity and specificity values of this magnetic detection with another study that used immunological detection of mastitis pathogens through an ELISA for detecting *S. aureus* in milk (Matsushita et al., 1990), a higher sensitivity (69-90%) and specificity values (61-97%) (Hicks et al., 1994) were observed. That ProStaph test (Proscience Corp.) had a detection limit of 10^4 – 10^5 CFU/ml, when the minimum bacterial presence detected by the present immunological recognition was 100 CFU/ml, independently of antibody and targeted bacteria used.

The microbiological misidentification ratio of 32.6% observed in our study was due to 15 wrong identifications compared with PCR analysis. The use of PCR for the identification of mastitis pathogens may have the advantage (Taponen et al., 2009) of leading to decreased false negative results, but it may also be clinically challenging. PCR's higher sensitivity leads to the identification of all milk sample pathogens and contaminants alike (Hiitiö et al., 2015), being difficult to assign mastitis causality to a particular microorganism. This was also observed in our study, with the average number of microorganisms identified per milk sample being one.

Regarding the validation of the magnetic detection method, some false positive results could be explained by NPs agglomeration by the mastitic milk matrix heterogeneity, sporadic low cleaning efficiency of the channel's inlet chamber and also due to electrical conductivity of mastitic milk samples. An effect of bovine mastitis is the ion concentration changes in the mammary gland due to increased vascular permeability resulting from inflammatory response, leading to modifications in electrical conductivity of milk (Hovinen et al., 2006). The conductance in milk causes sensor's resistivity variation translated by higher background noise. Despite a detergent (Tween 20) being in milk samples to

reduce fat globules dimensions, to distribute the bacterial cells in the milk, to improve nanoparticles mobilization and to allow a more homogeneous milk matrix, the optimization trials (not described in this manuscript) showed the need for a compromise between Tween 20 quantity and magnetic peak discrimination. Different volumes of PBST in 500 μ l of milk samples were used. The higher volumes (≥ 100 μ l) evidenced bubbles inside the microchannel which hampered milk flowing, caused nanoparticles agglomeration and did not help magnetic peaks discrimination between control samples (milk with only NPs) and samples with bacteria. On the other hand, false negatives may have occurred because of 3 circumstances. Firstly, the binding yield variations between antibodies and NPs and/or failure in bacterial cells magnetic labelling could narrow bacterial cells identification. This fact should be recognized as possible because IgM and nanoparticle's dimensions are closer, so it will be more difficult to have the same number of attached IgM when comparing with NPs functionalization with smaller IgG. Secondly, according to Henriksen, Wang and Hansen's study (2015), it is possible that the rotating nature of the magnetic dipole field of NPs magnetized by an external magnetic field, can induce signal cancelation. Therefore, the fields from two differently placed NPs can partially cancel each other. Finally, microchannel current height (50 μ m) could be reduced to improve sensor's detection by forcing bacterial cells dragging over it, but mastitic milk trials showed that milk clots hampers sample flowing and height decrease leads to microchannel obstruction, pointing out to a compromise between sensor's detection and sample fluidity.

As regards bacterial quantification data, this magnetic detection method showed some microbiological and immunological constraints. Bacterial cells group together randomly depending on growth conditions (Quinn, Carter, Markey & Carter, 1994). Each bacteria may express a different number of cell wall proteins, including the immunogenic ones (van der Woude & Bäumlér, 2004). Together, these facts limit the knowledge of how many immunogenic proteins there are per cell and consequently, how many proteins will be recognized by each specific antibody used. On the other hand, the chemical and colloidal changes of milk components in a state of inflammatory response (Walstra et al., 2006) as occurs with mastitis, prevent and reduce bacterial magnetic labelling efficacy (Duarte et

al., 2015a). Consequently, it was not possible to predict peak profiles (number, shape) for each bacterial concentration.

Although the sensitivity of the magnetic detection method is important, many additional factors must be considered, including rapidity, easy to use, flexibility, portability and costs (Mortari & Lorenzelli, 2014). This dynamic methodology showed it was possible for a mastitic milk sample to be processed until a final result was obtained in five hours, but was not suitable for processing a large number of samples (maximum of 10-12 per day). It also showed technical simplicity when established, and ease of scoring and interpreting the results. Despite the lower sensitivities obtained, both antibodies used were capable to detect bacterial cells in real milk samples. However, other antibodies could be used for further identification of different bovine mastitis pathogens, reinforcing this method flexibility.

Further studies could be done for biosensor's performance improvement as higher number of analyzed samples per day by using all the 7 SV of each microchannel's and use all of them per die. Other opportunity for better bacterial magnetic signal acquisition could be the dilution of milk samples in water or bacterial isolation from mastitic milk to be further analyzed in PBS, reducing conductance problems.

5. Conclusions

A lab-on-a-chip magnetoresistive cytometer with microfluidic sample handling, was successfully used to demonstrate the minimal detection of 100 CFU/ml of bacterial cells in raw milk. Milk samples were mixed with a solution combining specific antibodies and magnetic nanoparticles, before the analysis. This paper describes the methodology used for detection of bacteria, including analysis of false positive/negative results.

Comparison with PCR results showed sensitivities of 73% and 41%, specificity values of 25% and 57%, and PPV values of 35% and 54% for magnetic identification of streptococci species with an anti-*S. agalactiae* antibody and an anti-GB Streptococci antibody, respectively.

Magnetic detection of milk samples showed some microbiological and immunological constraints. Since bacterial cells have high variability on the

number of immunogenic proteins per cell, the number of labeled sites through the antibody is also not well defined. This affects the quantification of the magnetic method. As a consequence, it was not possible to quantify the peaks profile (number, shape) for each bacterial concentration. The method, however, allows to determine their presence, and quantification may be done within lower/upper threshold limits. Simulations of the sensor output as a function of the nanoparticle distribution over the cells (using colonies/clusters configurations compatible with the experimentally observed in microscope) can provide indication on minimum and maximum numbers. Further work would be done towards a more accurate quantification based on simulations.

Accuracy in bacterial quantification was affected by false positive results, leading to overestimation of bacteria number caused by nanoparticle agglomeration by the mastitic milk matrix heterogeneity and/or microchannel blocking. Also, undetected bacteria due to false negatives may be due to binding yield variations between antibodies and nanoparticles and/or failure in bacterial cells magnetic labelling.

This biosensor can be submitted to further improvements which may include milk pre-treatment step incorporation into the microfluidic platform and also further studies on electronics to allow multiplex analysis of several samples at a time. At this moment, this biosensor requires an external computer for system operation and displaying test results, so a fully integrated system into a single device could also be made.

CHAPTER VI

Semi-quantitative method for Staphylococci magnetic detection in milk.

C.M. Duarte, C. Carneiro, S. Cardoso, P.P. Freitas, R. Bexiga (April 2016: was submitted to Journal of Dairy Research)

* The author contributed to the conception and design of the study, conducted the experiments, participated in the data analysis process and drafted the manuscript.

Abstract

Bovine mastitis is the most costly disease for dairy farmers, therefore control measures to prevent mastitis are crucial for dairy farm sustainability. The aim of this study was to develop and validate a sensitive method for magnetic detection of *Staphylococcus aureus* and of *Staphylococcus epidermidis* in raw milk samples. Mastitic milk samples were collected aseptically from 47 cows with subclinical mastitis, from 12 Portuguese dairy farms. Forty nine quarter milk samples were selected based on bacteriological results. All samples were submitted to PCR analysis. In parallel, these milk samples were mixed with a solution combining specific antibodies and magnetic nanoparticles, to be analyzed using a lab-on-a-chip magnetoresistive cytometer, with microfluidic sample handling. This paper describes the methodology used for magnetic detection of bacteria, including analysis of false positive/negative results. This immunological recognition was able to detect bacterial presence above 100 CFU/ml, independently of antibody and targeted bacteria. Comparison with PCR results showed sensitivities of 57.1% and 79.3%, specificity values of 75% and 50%, and PPV values of 40% and 95.8% for magnetic identification of *Staphylococci* species with an anti-*S. aureus* antibody and an anti-*Staphylococcus* spp. antibody, respectively. Some constraints are described as well as the method's limitations in bacterial quantification. Firstly, false positive results could be explained by nanoparticles agglomeration by the mastitic milk matrix heterogeneity, sporadic low cleaning efficiency of microfluidic channel's inlet chamber or higher conductance in mastitic milk samples. Secondly, false negative causes may be due to binding yield variations between antibodies and nanoparticles, failure in bacterial cells magnetic labelling, or both.

Keywords: biosensor, *Staphylococcus aureus*, *Staphylococcus epidermidis*, milk, immunological recognition.

1. Introduction

Bovine mastitis is an economic burden for dairy farmers and control measures to prevent mastitis are crucial for dairy farm sustainability. The identification of etiological agents is necessary to control the disease in the herds, reduce the risk of chronic infections and target antimicrobial therapy. *Staphylococcus aureus* is considered a major mastitis pathogen due to its impact on udder health (Bradley, 2002) and coagulase-negative staphylococci are considered minor mastitis pathogens, but they are the most common agents isolated from milk samples in several large scale surveys worldwide (Tenhagen, Koster, Wallmann & Heuwieser, 2006).

Development prospects for new bovine mastitis diagnosis methodologies point to new biomarkers and technological advances for high sensitivity and specificity, fast and efficient devices that can offer a “cow-side” use (Duarte et al., 2015b). Biosensors are fast becoming the next generation of tools in analyzing areas such as environmental research, medicine, biodefense, agriculture, and food control (Lazcka et al., 2007). Biosensors use biological receptor molecules (e.g., antibody, enzyme, and nucleic acid) combined with a transducer to produce a signal that shows a specific biological event (e.g., an antibody–antigen interaction). Our previous works (Fernandes et al., 2014; Duarte et al., 2015a) describe magnetic detection of bovine mastitis pathogens based on immunological recognition of its immunogenic proteins by specific antibodies. With regards to bacterial quantification, this magnetic detection method has some microbiological and immunological constraints (Duarte et al., 2016 – chapter V of this Thesis). The knowledge that grouping of bacterial cells depends on growth conditions (Quinn et al., 1994) and that each bacteria can express different number of cell wall proteins, including the immunogenic ones to allow immune evasion during host infection (van der Woude and Bäumlner, 2004), supports the fact that it is difficult to determine how many immunogenic proteins will there be per bacterial cell and consequently, how many proteins will be recognized by each specific antibody used. On the other hand, the chemical and colloidal changes of milk components (Walstra et al., 2006) in a state of inflammatory response, as occurs with mastitic milk, prevent and reduce bacterial magnetic labelling efficacy. Accordingly, we are unable to establish a standard signal

output profile for each bacterial concentration (Duarte et al., submitted for publication – chapter V of this Thesis).

This current study provides the basis for immuno-magnetic detection of *Staphylococcus aureus* and *Staphylococcus epidermidis* cells in raw milk samples. The polyclonal antibody used for *S. aureus* identification recognizes the extracellular protease cysteine proteinase staphopain A (ScpA) which is considered a putative virulence factor (Ohbayashi et al, 2011). Regarding *S. epidermidis*, the monoclonal antibody used recognizes its cell wall peptidoglycan as well as *S. aureus* and protein A - negative *S. aureus*.

The aim of this study was to develop and validate a sensitive method for magnetic detection of *S. aureus* and *S. epidermidis* in raw milk samples. For both magnetic detection and conventional microbiology methods, sensitivity, specificity and positive predictive value (PPV) were calculated in comparison with the PCR reference method.

2. Material and methods

2.1. Milk samples

Raw milk was collected aseptically from healthy cows for biosensors calibration measurements. Conventional microbiological tests were performed according to NMC (1999) protocols, to confirm no bacterial growth. Briefly, a raw milk drop (10µl loop) was plated on Columbia agar supplemented with 5% sheep blood (43021, bioMérieux) and on MacConkey agar plate (CM0007, Oxoid) and both were incubated at 37°C for 48 hours. The absence of growth on both plates was considered to be equivalent to the presence of no viable bacteria in the milk.

Adding to this, mastitic milk samples were needed to validate biosensor detection. In these instances, milk samples were collected aseptically from cows (n = 47) of 12 Portuguese dairy farms. Animal selection was based on SCC higher than 1.000.000 cells/ml and quarter selection based on California Mastitis Test results with score 3. The quarter (n = 49) was the experimental unit considered. Bacteriological identification was performed as aforementioned. Milk sample selection was based on bacteriological results which included: *Staphylococcus aureus* (n = 9), *Streptococcus agalactiae* (n = 3), *Streptococcus uberis* (n = 1),

Streptococcus spp. (n = 1), CNS (n = 11), *Enterococcus* spp. (n = 4), *Escherichia coli* (n = 7), Yeasts (n = 6) and *Prototheca* spp. (n = 7).

PCR Analysis

Mastitic milk samples with a preservative (6.65µl of azidiol per 2 ml of milk) were submitted to PCR analysis. This validation methodology was performed by an external laboratory (VACUNEK, SL) and 16 bovine mastitis pathogens were analyzed with the PathoProof Mastitis Complete-16® assay kit (Thermo Scientific), a semi-quantitative method.

2.2. Bacterial cells

A. Suspensions. In order to distinguish biosensor signal outputs from different bacterial concentrations in raw milk samples, calibration curves were developed for the pairs: *Staphylococcus aureus*/ pAb anti-*S. aureus* ScpA; *Staphylococcus aureus*/ mAb anti-*Staphylococcus* spp. and *Staphylococcus epidermidis*/ mAb anti-*Staphylococcus* spp. The target bacteria used were ATCC 29213 for *Staphylococcus aureus* and a clinical bovine mastitis isolate of *Staphylococcus epidermidis* which identification had been previously confirmed genotypically (Bexiga et al., 2014).

Bacterial cells were grown separately on Columbia agar supplemented with 5% sheep blood (43021, bioMérieux) and incubated at 37°C, overnight. A single colony of each isolate was selected and re-suspended on 4 ml of tripticase soy broth overnight at 37°C. Subsequently, the bacterial cells were collected through centrifugation (15 minutes, 17°C, 2700 rpm) and re-suspended in PBS 1X (pH 7.2) to allow for optical density measurement (at 600 nm) (BECKMAN DU-68 Spectrophotometer) and for colony-forming unit estimation. A bacterial suspension with a known concentration of 10⁴ CFU/µl was the starting point to obtain seven different bacterial concentrations for each species, in sterile raw milk samples: 0.1; 0.3; 0.5; 1; 2; 10 and 20 CFU/µl.

B. Magnetic Labelling. The immunological recognition of Staphylococci was achieved by biological functionalization with antibodies of iron oxide nanoparticles, which could be detected by the biosensor (Duarte et al., 2015a). The antibodies were expected to attach to protein A of those nanoparticles (79-20-501, Micromod Partikeltechnologie GmbH) by the Fc fraction in

immunoglobulins G and by the joining chain (J chain) in immunoglobulins M (Figure 43). The antibodies used separately in this work were a rabbit polyclonal IgG to ScpA protein (ab92983, Abcam) and a mouse monoclonal IgM anti-*S. aureus* ATCC 29740 (MCA 5793, AbDSerotec) which recognizes the peptidoglycan of *S. aureus*, protein A-negative *S. aureus* and *S. epidermidis*, hereinafter designated as “anti-*Staphylococcus* spp.”. Antibodies (Walstra et al., 2006) and bacterial cell dimensions are shown in Figure 43.

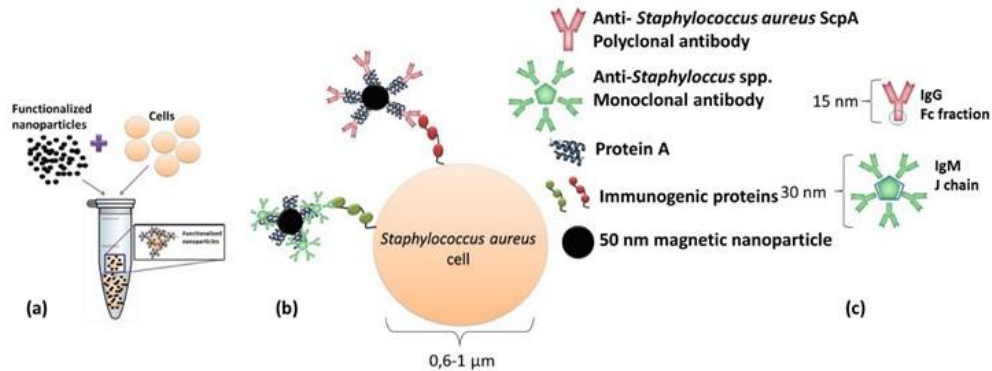


Figure 43. Schematics of immuno-magnetic detection of cells. a) Incubation of functionalized beads with bacterial cells; (b) biological affinities between different functionalized nanoparticles with bacterial cell wall immunogenic proteins; (c) predictable protein A binding site to each antibody.

As explained in our previous work (Duarte et al., 2015a), nanoparticles ($7.27\mu\text{l}$ from an original vial with 5.5×10^{13} nanoparticles per ml) were incubated with $1.08\mu\text{l}$ of pAb anti- *S. aureus* (0.5mg/ml) (or with $2.65\mu\text{l}$ of mAb anti-*Staphylococcus* spp. (1mg/ml)) in $492.2\mu\text{l}$ of PBS (or in $490.08\mu\text{l}$ for mAb), during 1 hour at room temperature (RT), under agitation. Final functionalized nanoparticles were magnetically isolated by magnetic separation (MS) column (130-042-201, Miltenyi) and eluted with buffer (PBS + 0.5% BSA + 2mM EDTA) after removal of the MS column from the magnet. A volume of $2\mu\text{l}$ of this final suspension with 8×10^6 functionalized nanoparticles was diluted in $98\mu\text{l}$ of PBST and added to each milk sample with bacteria.

2.3. Biosensor detection

This method principle is based on the detection of the fringe field created by magnetic particles attached to the bacterial cells. By selecting the suitable antibodies, it is possible to perform immunological recognition of bacteria in milk samples. As described in our previous work (Fernandes et al., 2014; Duarte et al., 2015a), an integrated cytometer platform was used, consisting on magnetoresistive sensors and readout/ acquisition electronics and a microfluidic channel where the milk was injected.

A. Calibration Trials. A blank sample (only sterile raw milk) and a control sample (sterile raw milk with functionalized nanoparticles) were always measured before samples with known bacterial concentrations. All calibration points resulted from three different days' measurements leading to three independent trials for each bacterial concentration sample.

Each milk sample with bacteria for biosensor analysis had a 500 μl volume consisting of 2 μl of functionalized nanoparticles suspension, 98 μl of PBST, and 400 μl of a bacterial suspension volume corresponding to one of seven pre-defined bacterial concentrations and the remaining volume of sterile raw milk. The incubation of these samples was performed at RT for 3 hours, under agitation.

All raw milk samples with bacteria and PBST were submitted to a pre-treatment of 15 min at 60°C in a dry bath incubator (model QBD2, Grant) and 15 min of continuous centrifugation in a vortex mixer (Labnet). Only then, the functionalized nanoparticles suspension volume was added for the final incubation step.

The calibration range between 0.1 and 20 CFU/ μl was established taking into account the detection limit for conventional microbiology of 500 CFU/ml (0.5 CFU/ μl) NMC (1999).

B. Mastitic Milk Sample Evaluation. Mastitic milk samples for evaluation were obtained by mixing 400 μl of mastitic milk and 98 μl of PBST.

Mastitic milk samples ($n = 31$) were distributed so that each trial with a different antibody (anti-*S. aureus* ScpA or anti-*Staphylococcus* spp.) could be performed independently, amounting to 62 trials for magnetic method validation. A blank

sample and a control sample were measured always before mastitic sample analysis.

Samples with functionalized NP's on PBS or sterile milk (negative controls) evidenced magnetic signal lower than $50 \mu\text{V}$ (Figure 44A). Mastitic milk samples without the targeted bacteria (proved by PCR) and tested with NP's functionalized with chosen antibodies, also evidenced magnetic signal lower than $50 \mu\text{V}$ (Figure 44B). Samples used for calibration assays spiked with bacterial cells on sterile milk showed magnetic signal higher than $50 \mu\text{V}$ (Figure 44C, D and E).

Biosensor validation was based on mastitic milk sample classification as having or not having bacteria present. Consequently, the "Positive" samples were those with at least one magnetic peak above $50 \mu\text{V}$, therefore higher than the magnetic signal found in negative control samples and in mastitic milk samples without targeted bacteria. Next, this "Positive" sample magnetic peak should evidence a bipolar or unipolar shape similar to the ones found in samples used for calibration trials as shown in Figure 44C, D and E.

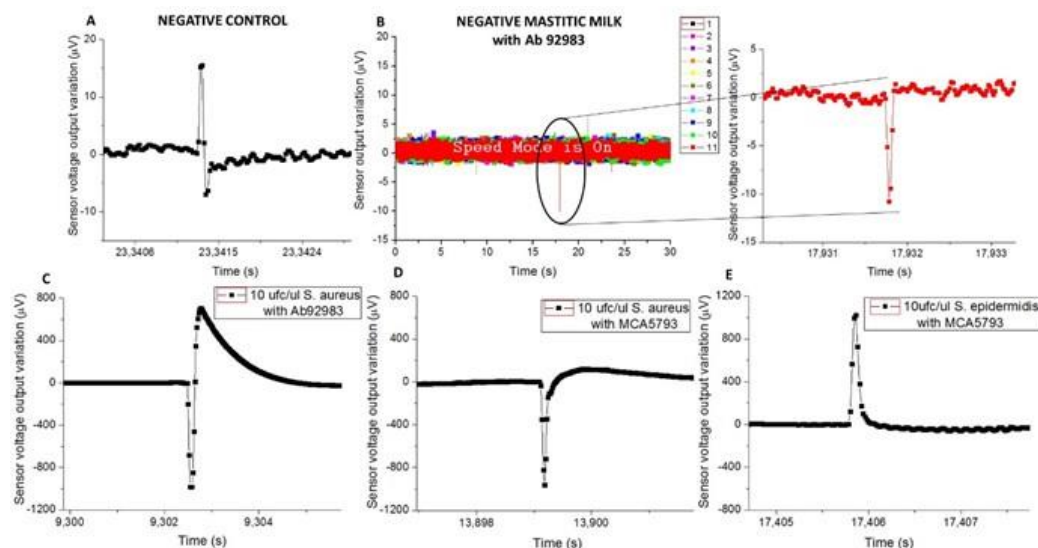


Figure 44. Sensor output for (A) negative control with the higher amplitude of $23 \mu\text{V}$, (B) mastitic milk (9077 T sample code without *S. aureus* accordingly with PCR) with NP's functionalized with pAb anti-*S. aureus* (Ab 92983) which presents an amplitude peak of $10.7 \mu\text{V}$. The higher amplitude peaks found for each pair of bacteria-antibody were, (C) $1703.4 \mu\text{V}$ in raw milk with pAb anti-*S. aureus* and $10 \text{ CFU}/\mu\text{l}$ of *S. aureus*, (D) $964.4 \mu\text{V}$ in raw milk with mAb anti-*Staphylococcus* spp. (MCA 5793) and $10 \text{ CFU}/\mu\text{l}$ of *S. aureus* and (E) $1030.5 \mu\text{V}$ in raw milk with mAb anti-*Staphylococcus* spp. and $10 \text{ CFU}/\mu\text{l}$ of *S. epidermidis*.

2.4. Data Analysis

Isolates were considered to be correctly identified by magnetic detection if the same species was found with the reference method, or if the magnetic detection did not identify as the agents it was targeting, one of the other bacteria identified as such by the PCR. For example, a correct identification referred to a *S. aureus* being identified magnetically in a sample that PCR had identified as *S. aureus*, but also when not identifying as *S. aureus* a sample that through PCR was identified as *Streptococcus* spp. Regarding conventional microbiology, isolates were considered to be correctly identified if the same species was found with the PCR. Misidentification was considered when the magnetic detection and conventional microbiology identified a different species than the reference method. For example, a sample that was identified as *Streptococcus* spp. by PCR and that was identified as *S. aureus* by magnetic detection or a sample that was identified as *S. aureus* by PCR and not identified as such by magnetic detection. For both magnetic detection and conventional microbiology methods, sensitivity, specificity and positive predictive value (PPV) were calculated in comparison with PCR species identification. Sensitivity was calculated as the proportion of the true positive isolates that were correctly identified with the magnetic detection or microbiological tests, e.g., the proportion of *S. aureus* isolates based on PCR analysis that were identified as such by magnetic detection and microbiology testing. Specificity was calculated as the proportion of the true negatives that were correctly identified with the magnetic detection and the microbiological tests, e.g., the proportion of isolates other than *S. aureus* based on PCR analysis that were identified as something other than *S. aureus* by magnetic detection and by microbiological testing. Finally, PPV was calculated as the proportion of isolates identified as a specific species based on magnetic detection or on microbiological testing that truly represented that particular species, e.g., the proportion of isolates that were identified as *S. aureus* by magnetic detection or microbiological testing that had been identified as *S. aureus* based on PCR analysis.

3. Results

3.1. Evaluation of biosensor's quantification

The calibration trials outcome is shown in Figure 45. The number of peaks per signal amplitude were calculated evidencing no linear correlation with increasing bacterial concentration. The milk samples with functionalized nanoparticles with the anti-*Staphylococcus* spp. antibody, evidenced the highest peak number with *S. epidermidis* when compared with the other two bacteria-antibody pairs (Figure 45). Overall, the biosensor could detect *S. aureus* and *S. epidermidis* in milk samples from 100 CFU/ml.

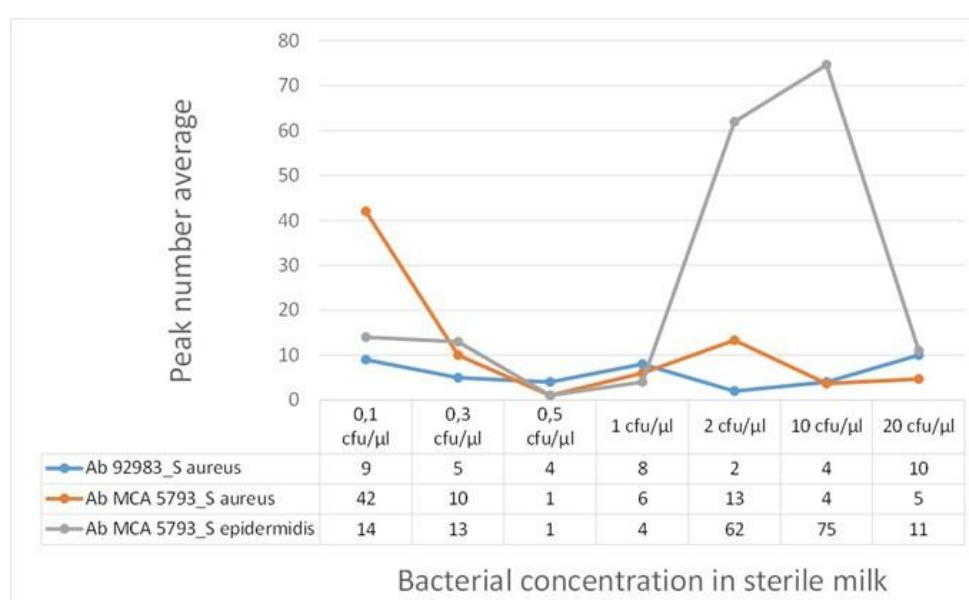


Figure 45. Calibration trials results for milk samples with seven bacterial concentrations (*S. aureus* or *S. epidermidis*) and functionalized NP's with pAb anti-*S. aureus* (Ab 92983) or mAb anti-*Staphylococcus* spp. (Ab MCA 5793). Peak number average for each bacteria-antibody pair are counted.

3.2. Validation of magnetic detection

Forty nine mastitic milk samples with known bacteriology results, obtained through conventional microbiology were analyzed by PCR. A total of 123 agent identifications were attained by PCR for all 49 milk samples analyzed with mAb anti-*Staphylococcus* spp. and pAb anti-*S. aureus*. The species detected by PCR were, in decreasing order of detection, *Staphylococcus* spp., *S. aureus*, Yeasts and *E. coli* followed by *S. uberis* and *Prototheca*. As a result of the high sensitivity of the PCR methodology, an average of 3 different pathogens were detected per

mastitic milk sample, not allowing for the true causative agent of mastitis to be determined. Therefore it was decided to use the conventional bacteriology results as the basis for the true identification, confirmed by the PCR (Table 4).

mastitic milk isolates	n	Magnetic detection						Microbiological tests		
		anti- <i>Staphylococcus aureus</i>			anti- <i>Staphylococcus</i> spp.			Correctly identified		
		n	%	MI ¹	n	%	MI	n	%	MI
<i>S. aureus</i>	9	3	50.0	3	5	83.3	1	9	100.0	0
<i>Staphylococcus</i> spp.	11	6	75.0	2	5	71.4	2	10	90.9	1
<i>S. agalactiae</i>	3	2	66.7	1	3	100.0	0	3	100.0	0
<i>S. uberis</i>	1	1	100.0	0	1	100.0	0	1	100.0	0
<i>Streptococcus</i> spp.	1	0	0.0	1	0	0.0	0	0	0.0	1
<i>Enterococcus</i> spp.	4	1	33.3	2	1	100.0	0	0	0.0	4
<i>E. coli</i>	7	2	100.0	0	4	80.0	1	7	100.0	0
Yeasts	6	4	100.0	0	3	100.0	0	4	66.7	2
<i>Prototheca</i>	7	3	100.0	0	2	40.0	3	7	100.0	0
Total	49	22	71.0	9	24	77.4	7	41	83.7	8

Correctly identified = True Positives + True Negatives

¹ MI (misidentified) = False Negatives + False Positives

Table 4 - Identification of isolates in mastitic milk samples with both magnetic detection (pAb anti-*Staphylococcus aureus*; mAb anti-*Staphylococcus* spp.) and with conventional microbiology, compared to PCR analysis as the reference method.

Magnetic detection with the anti-*Staphylococcus aureus* antibody tested 31 mastitic milk samples from the total of 46, which 6 and 9 were identified as *S. aureus* by conventional microbiology (Table 4), respectively. However, from these 31 samples tested, 7 were identified as *S. aureus* by PCR and the one not identified as such by microbiology, was it as *Prototheca*. The magnetic detection with the anti-*S. aureus* antibody identified 4 *S. aureus* isolates correctly out of 7 (57.1%) milk samples with this species according to PCR results. Eighteen mastitic milk samples did not lead to an identification by this polyclonal antibody as they did not present *S. aureus* according to the PCR, thus being true negatives (Table 5). Misidentification was observed for 9 of 31 (29%) isolates in all mastitic milk samples tested with the anti-*S. aureus* antibody (Table 4). Only 3 misidentified *S. aureus* isolates were found in milk samples with this species analyzed by PCR, evidencing a failure of recognition by this monoclonal antibody (Table 4). Adding to that, the remaining 6 mastitic milk samples were misidentified as having *S. aureus* (Table 4), while really presenting *S. uberis*, Yeasts, *S. agalactiae* and other staphylococcal species according to the PCR. Overall 57.1% sensitivity, 75% specificity and 40% PPV were found for magnetic detection with the anti-*S. aureus* ScpA antibody. The highest specificity

value represents the proportion of the true negatives (18) that were correctly identified with this monoclonal antibody (Table 5).

	Magnetic detection		Microbiological tests
	pAb anti- <i>Staphylococcus aureus</i>	mAb anti- <i>Staphylococcus</i> spp.	
True Positives	4	23	41
True Negatives	18	1	0
False Negatives	3	6	1
False Positives	6	1	7
Sensitivity	57.1%	79.3%	97.6%
Specificity	75.0%	50.0%	-
¹ PPV	40.0%	95.8%	85.4%

¹ PPV = Positive Predictive Value

Table 5 - Sensitivity, specificity and positive predictive value of the magnetic detection and the conventional microbiology, using PCR analysis as the reference method.

Using the monoclonal anti-*Staphylococcus* spp. antibody in magnetic detection, the 31 mastitic samples tested included 6 *S. aureus* and 7 *Staphylococcus* spp. identified by conventional microbiology (Table 4). However, PCR analysis identified 29 as *Staphylococcus* spp. of which 8 samples also evidenced *S. aureus*, showing incomplete identifications by microbiological analysis. The magnetic detection with the anti-*Staphylococcus* spp. antibody identified correctly 23 staphylococci present in 29 (79.3%) milk samples with mostly staphylococci other than *S. aureus*, or also with *S. aureus* according to PCR analysis, were identified correctly. Only one mastitic milk sample was not detected by this monoclonal antibody (true negative) because it did not present any *Staphylococcus* spp. according to the PCR (Table 5). Misidentification was observed for 7 isolates out of the 31 (22.6%) mastitic samples tested. Six of them were found in milk samples with staphylococcal species analyzed by PCR, evidencing a failure of recognition by this anti-*Staphylococcus* spp. antibody (Table 4). Moreover, only one false positive was found in a mastitic sample without any staphylococci evidenced by PCR. Overall a sensitivity of 79.3%, a specificity of 50% and a PPV of 95.8% were found for magnetic detection with the anti-*Staphylococcus* spp. antibody. (Table 5).

Regarding microbiological testing for all 49 samples considered, 100% of *S. aureus*, *S. agalactiae*, *S. uberis*, *E. coli* and *Prototheca* were correctly identified when comparing with PCR (Table 4). Incomplete microbiological identifications of 85.7% (42/49) and a misidentification of 14.3% (7/49) were observed. Microbiological tests evidenced a PPV value of 85.4% and a sensitivity of 97.6%

to identify mastitis pathogens in milk samples, showing that conventional microbiology identified correctly true positives (41/49) (Table 5).

4. Discussion

Sensitivities of 57.1% and 79.3% and specificity values of 75% and 50% were obtained for magnetic identification of staphylococci species in mastitic milk samples with an anti-*S. aureus* ScpA antibody and an anti-*Staphylococcus* spp. antibody, respectively. The higher PPV value (95.8%) evidenced for magnetic detection with the anti-*Staphylococcus* spp. antibody may reinforce its bonding avidity for each immunogenic cell wall protein of *S. aureus* and of *S. epidermidis* comparing to the polyclonal antibody. These specificities were confirmed by our Western Blotting assays which evidenced three to six stained immunogenic proteins in *S. aureus* cell wall proteins' pattern and one immunogenic protein in both *S. aureus* and *S. epidermidis*, recognized by the selected polyclonal (1.5 µg/ml, 3h, RT) and monoclonal (2.25 µg/ml, 3h, RT) antibodies, respectively.

The knowledge of *S. aureus* as an important cause of udder infections in dairy herds sustains the interest in treatment and prevention studies of *S. aureus* mastitis (Fabres-Klein, Aguilar, Silva MP, Silva DM & Ribon 2014). So, comparing the sensitivity (57.1%, 79.3%) and specificity (75%, 50%) values of this magnetic detection with another study based on immuno-agglutination, which compared 6 commercially available slide agglutination tests for *S. aureus* identification in milk samples (Zschöck et al., 2005), the highest sensitivity (86.7%) and specificity (90.1%) values were obtained for a test consisting of latex particles coated with human fibrinogen and immunoglobulin G. Still, strain typing methods that are DNA sequence-based have also been used to improve *S. aureus* detection. A Bittar, Ouchenane, Smati, Raoult and Rolain's (2009) study to differentiate between positive and negative *S. aureus* strains for Pantón–Valentine leucocidin, used MALDI-TOF MS (matrix-assisted laser desorption ionization time-of-flight mass spectrometry) analysis which evidenced higher sensitivity (100%) and specificity (90.6%), compared with our magnetic detection method.

On the other hand, considering that the minimum bacterial presence detected by the present immunological recognition was 100 CFU/ml, independently of which

antibody and targeted bacteria were considered, when compared to a sandwich ELISA test recently patented (Libing et al., 2012) to detect *S. aureus* in artificially contaminated milk, a lower detection limit of 10^5 CFU/ml was found. However, a competitive immunoassay performed by an amperometric magnetoimmunosensor (de Ávila, Pedrero, Campuzano, Escamilla-Gómez & Pingarrón, 2012) for the specific detection and quantification of staphylococcal protein A and *S. aureus* cells, evidenced a better detection limit of 1 CFU/ml, also in artificially contaminated milk samples.

The microbiological misidentification ratio of 14.3% observed in our study was due to 7 erroneous identifications compared with PCR analysis. The use of PCR for the identification of mastitis pathogens may have the advantage (Taponen et al., 2009) of leading to decreased false negative results, but it may also be clinically challenging. PCR's higher sensitivity leads to the identification of all milk sample pathogens and contaminants alike (Hiitiö et al., 2015), being difficult to assign mastitis causality to a particular microorganism.

Regarding the validation of the magnetic detection method, some false positive results (6 for pAb anti-*S. aureus* and 1 for mAb anti-*Staphylococcus* spp.) could be explained by NP's agglomeration by the mastitic milk matrix heterogeneity, sporadic low cleaning efficiency of the channel's inlet chamber and also due to electrical conductivity of mastitic milk samples. Bovine mastitis leads to changes in ion concentrations due to increased vascular permeability, which produces modifications in the electrical conductivity of milk (Hovinen et al., 2006). The conductance in milk causes sensor's resistivity variation, translated by higher background noise. Despite a detergent (Tween 20) being in milk samples to reduce fat globules dimensions, to distribute the bacterial cells in the milk, to improve nanoparticles mobilization and to allow a more homogeneous milk matrix, the optimization trials (not described in this manuscript) showed the need for a compromise between Tween 20 quantity and magnetic peak discrimination. Different volumes of PBST in 500 μ l of milk samples were used. The higher volumes (≥ 100 μ l) evidenced bubbles inside the microchannel which hampered milk flowing, caused nanoparticles agglomeration and did not help magnetic peaks discrimination between control samples (milk with only NP's) and samples with bacteria.

On the other hand, false negatives (3 for pAb anti-*S. aureus* and 6 for mAb anti-*Staphylococcus* spp.) may have occurred because of three circumstances. Firstly, the binding yield variations between antibodies and NP's or failure in bacterial cells magnetic labelling, or both. This fact should be recognized as possible because IgM and nanoparticle's dimensions are closer, so it will be more difficult to have the same number of attached IgM when comparing with NP's functionalization with smaller IgG. Secondly, according to Henriksen's study (2015), it is possible that the rotating nature of the magnetic dipole field of NP's magnetized by an external magnetic field, can induce signal cancelation. Therefore, the fields from two differently placed NP's can partially cancel each other. Finally, microchannel current height (50 μm) could be reduced to improve sensor's detection by forcing bacterial cells dragging over it, but mastitic milk trials showed that milk clots hampered sample flowing and height decrease led to microchannel obstruction, pointing to the need for a compromise between sensor's detection and sample fluidity.

With regards to calibration trials, bacterial cells group together randomly depending on growth conditions (Quinn et al., 1994). Each bacteria may express a different number of cell wall proteins, including the immunogenic ones (van der Woude & Bäumlner, 2004). Together, these facts limit the knowledge of how many immunogenic proteins there are per cell and consequently, how many proteins will be recognized by each specific antibody used. On the other hand, the chemical and colloidal changes of milk components in a state of inflammatory response (Walstra et al., 2006) as occurs with mastitis, prevent and reduce bacterial magnetic labelling efficacy (Duarte et al., 2015a). Consequently, it was not possible to predict peaks profile (number, shape) for each bacterial concentration.

Although the sensitivity of the immuno-magnetic detection method was important to determine the potential future use of such technology, many additional factors must be considered, including speed and ease of use, flexibility, portability and costs (Mortari & Lorenzelli, 2014). This methodology showed it was possible for a mastitic milk sample to be processed until a final result was obtained in five hours, but was not suitable for processing a large number of samples (maximum of 10-12 per day). It also showed technical simplicity when established, and ease of scoring and interpreting the results. Despite the lower

sensitivities obtained, both antibodies used were capable to detect bacterial cells in real milk samples. However, other antibodies could be used for further identification of different bovine mastitis pathogens, reinforcing this method flexibility.

This biosensor can be submitted to further improvements which may include milk pre-treatment step incorporation into the microfluidic platform and also further studies on electronics to allow multiplex analysis of several samples at a time. At this moment, this biosensor requires an external computer for system operation and displaying test results, so a fully integrated system into a single device could also be made.

CHAPTER VII

General Discussion, Conclusions and Future
Directions.

DISCUSSION

1. Doctoral study overview

The early identification of bovine mastitis pathogens is of major importance for taking adequate control measures, reducing the risk of chronic infections and targeting antimicrobial therapy to be prescribed. Also, several studies showed that the early detection of mastitis may increase the cure rate by 60 % and reduce the time required to recover normal milk production when combined with appropriate antimicrobial therapy (Milner, Page & Hillerton, 1997). The rapid identification of pathogens such as *Staphylococcus* spp. and *Streptococcus* spp. and among these, the discrimination of major contagious pathogens *Staphylococcus aureus*, *Streptococcus agalactiae* and *Streptococcus uberis* (Bradley, 2002; Zadoks, et al., 2011), will therefore contribute to decrease the economic burden of bovine mastitis. Coagulase-negative staphylococci, as *Staphylococcus epidermidis*, are considered minor mastitis pathogens, but they are the most common agents isolated from milk samples in several large scale surveys worldwide (Tenhagen et al., 2006).

One of the most widely used methods for subclinical mastitis diagnosis is the California Mastitis Test, a common indirect method for SCC measurement. However, this method only discriminates sick from healthy animals and is unable to identify the causative agent of infection. Therefore, microbiological culture is still considered the gold standard for diagnosing mastitis pathogens (Britten, 2012), allowing for a targeted control and treatment decision, in addition to presenting high sensitivity and specificity. Another advantage of microbial culture-based methods is the possibility of identifying the antibiotic susceptibility of bacteria. The limitations of microbiological culture include delays in obtaining results and suboptimal accuracy in identifying mastitis pathogens. The use of PCR-based tests may be of interest for IMI diagnosis when milk samples with high SCC are culture-negative or when culturing only detects minor pathogens (Taponen et al., 2009; Bexiga et al., 2011). PCR is a semi-quantitative technique that generates information about the number of copies of DNA fragments that have been detected in a sample, being difficult to assign mastitis causality to a particular microorganism. We also cannot assume that one bacterial species is

more important in terms of the negative effects on a mammary gland, simply because it is present in higher numbers.

This fact was observed when the biosensor's results were compared with PCR, with an average of 4 (chapter V) or 3 (chapter VI) different pathogens were detected per mastitic milk sample as a result of the high sensitivity of the PCR methodology, not allowing for the true causative agent of mastitis to be determined. Therefore it was decided to use the conventional bacteriology results as the basis for the true identification of mastitic milk samples, confirmed by the PCR.

Immunodiagnosics also create new perspectives for the diagnosis of bovine mastitis as an alternative to microbiological culture. Methods based on serology have desired characteristics for an ideal diagnostic test such as speed, sensitivity, ease of handling and low cost (Fabres-Klein et al., 2014). The market already provides several commercialized immunoassays for the diagnosis of diseases of veterinary relevance (Zschöck et al., 2005).

The developed magnetic detection method was based on immunological recognition of bacteria by specific antibodies (chapters II to VI). The detection of surface proteins enables rapid species identification as evidenced in our work by true positives and true negatives values found for each specific antibody [(13/31) 41.9% for anti-*S. agalactiae* antibody; (15/31) 48.4% for anti-GB Streptococci; (22/31) 71% for anti-*S. aureus* ScpA and (24/31) 77.4% for anti-*Staphylococcus* spp. antibody].

The successful choice of a test that evaluates milk requires methodological knowledge and diagnostic capabilities for each test currently available. The sensitivity of culture tests may be complemented by PCR analysis, which are often combined together to yield more robust results. However, to make treatment decisions, this combination does not allow for a timely answer. Proteomic research for reliable biomarkers, as enzymes and acute phase proteins (Pyörälä, 2003; Grönlund, et al., 2003; Åkerstedt et al., 2011; Mansor et al., 2013), is viable for the early detection of mastitis and drug efficacy, and to discover potentially novel targets for the development of alternative therapies (Lippolis & Reinhardt, 2010). However, these innovations are still not possible to use for routine diagnosis. Therefore, it remains important to develop a low-cost tool for the differentiation of clinically relevant mastitis pathogens that may be used on-farm.

The suitability of a detection method for routine diagnosis depends on its specificity, sensitivity, cost, processing time, and suitability for a large number of milk samples. New technical advances in mastitis diagnosis still require specialized training and experience to interpret results. The personnel responsible should be aware of the strict compliance to each step in the process for good quality control in obtaining reliable data.

Flow cytometers have been optimized for use in portable platforms, where cell separation, identification and counting can be achieved in a compact and modular format. This feature was combined with magnetic detection in this thesis work, where magnetoresistive sensors were integrated within microfluidic channels to detect magnetically labelled cells.

Over the past years, the drawbacks of conventional flow cytometers have encouraged efforts to take advantage of microfabrication technologies and advanced microfluidics to achieve smaller, simpler, more innovative and low-cost instrumentation with enhanced portability for on-site measurements. This miniaturization approach has in general made use of inexpensive polymers such as polydimethylsiloxane (PDMS) (Huh et al., 2005) and detection techniques easily integrated with electronics (Chung & Kim, 2007), such as magnetoresistive sensors (Loureiro et al., 2011). A previous reported work for magnetic particle detection (Loureiro et al., 2011; Freitas et al., 2012) used an integrated cytometer platform, consisting on magnetoresistive sensors, readout/ acquisition electronics and a microfluidic channel where the sample with magnetic particles was injected.

The aim of the present work was to develop, characterize and apply a magnetic detection device for the identification and quantification of *Staphylococcus aureus*, *Staphylococcus epidermidis*, *Streptococcus agalactiae* and *Streptococcus uberis* in a complex matrix (raw milk), based on the aforementioned platform (Loureiro et al., 2011).

Sensitivities of 73% and 41% and specificity values of 25% and 57% were obtained for magnetic identification of streptococci species with an anti-*S. agalactiae* antibody and an anti-GB Streptococci antibody, respectively. With regards to magnetic identification of staphylococci species in mastitic milk samples with an anti-*S. aureus* ScpA antibody and an anti-*Staphylococcus* spp.

antibody, sensitivities of 57.1% and 79.3% and specificity values of 75% and 50% were obtained respectively.

The knowledge of *S. aureus* as an important cause of udder infections in dairy herds sustains the largest interest in treatment and prevention studies of *S. aureus* mastitis (Fabres-Klein et al., 2014). So, comparing sensitivity and specificity values of this magnetic detection with another study that used immunological detection of mastitis pathogens through an ELISA for detecting *S. aureus* in milk, a sensitivity between 69-90% and specificity values of 61-97% (Hicks et al., 1994) were observed. That test had a detection limit of 10^4 – 10^5 CFU/ml, when the minimum bacterial presence detected by the present immunological recognition was 100 CFU/ml, independently of antibody and targeted bacteria. Adding to that, a sandwich ELISA test recently patented to detect *S. aureus* in artificially contaminated milk (Libing et al., 2012), found a similar detection limit of 10^5 CFU/ml. However, a competitive immunoassay performed by an amperometric magneto immunosensor (de Ávila et al., 2012) for the specific detection and quantification of staphylococcal protein A and *S. aureus* cells, evidenced a detection limit of 1 CFU/ml, also in artificially contaminated milk samples.

Comparing again the sensitivity (41% and 73%; 57.1% and 79.3%) and specificity values (25% and 57%; 50% and 75%) obtained for magnetic identification of streptococci and staphylococci species respectively, with another study based on immuno-agglutination, which compared 6 commercially available slide agglutination tests for *S. aureus* identification in milk samples (Zschöck et al., 2005), the highest sensitivity (86.7%) and specificity (90.1%) values were obtained for a test consisting of latex particles coated with human fibrinogen and immunoglobulin G. Still, strain typing methods that are DNA sequence-based have also been used to improve *S. aureus* detection. A Bittar and coworkers' (2009) study to differentiate between positive and negative *S. aureus* strains for Pantón–Valentine leucocidin, used MALDI-TOF MS analysis which evidenced higher sensitivity (100%) and specificity (90.6%), compared with our magnetic detection method.

Another different method for the identification of bovine mastitis pathogens resorts to microarray technology, which was capable of detecting 7 common species of mastitis-causing pathogens within 6 hours, with an observed sensitivity

of 94.1% and specificity of 100% (Lee et al., 2008). The platform used was based on PCR technology where pathogen-specific targets of DNA were amplified and transferred to react and hybridize with specific probes that were pre-spotted on the biochip. At the end of the process, colorimetric techniques were used to identify pathogen patterns present on the sample. The detection limit of this method was 10^3 – 10^5 CFU/ml. Despite the advantage of using nucleic acid amplification strategies, which increases the sensitivity, specificity and efficiency, these methods always required pre-isolation of bacterial cells from milk, not allowing for the direct analysis of mastitic milk samples and consequently, the use on-farm, unless that pre-treatment step was incorporated inside the analysis system, reducing its time and cost.

According to Lazcka and coworkers (2007), in order to become attractive, biosensors first need to show that they are capable of reaching at least the same detection levels as traditional techniques (between 10 and 100 CFU/ml). Next, they need to do so in a fraction of time without overlooking cost. Currently, the detection limits of biosensors for on-site use have been a hundred to a million cells per ml of sample (10^2 – 10^6 CFU/ml) and are able to achieve extremely high sensitivities (Yoon & Kim, 2012).

Therefore, despite the need for improvement in the bacteriological infection screening and considering sensitivity and specificity low values, the magnetic detection method the current study describes, may be a tool in the future to complement traditional methods in identification of some important mastitis pathogens. Data gathered from this thesis work, including the minimum bacterial concentration detected of 100 CFU/ml, may provide a useful tool for rapid on-farm diagnosis of mastitis pathogens, contributing to both improving animal health and welfare and rationalizing and reducing the use of antibiotics, with positive effects on the economy of dairy farming and on Public Health.

2. Strengths, Weaknesses, Opportunities and Threats

Two main strengths of this magnetic detection method were previously identified, as the successful evidence of immunological recognition of targeted bacteria by the specific antibodies used, and the nanoparticles attachment to selected antibodies on positive milk samples (sterile milk with functionalized nanoparticles and spiked with known bacterial concentration) when compared to the control samples (sterile milk with only functionalized nanoparticles).

Despite this, bacterial quantification is a limitation as there is lack of knowledge of how many immunogenic proteins are expressed per cell, and consequently, how many proteins will be recognized by each specific antibody used. The previously performed simulations (Chapter V of this Thesis) were helpful for peak's amplitude and shape interpretation, without the assurance of bacterial cells number.

Loureiro and coworker's (2011) study describes a possible way to extrapolate cells number from a known saturation moment of nanoparticles of a sample using a hemocytometer. Unfortunately for us, that research group was working with single human cells from acute myeloid leukemia cell line, and not with bacterial clusters.

The number of nanoparticles attached to bacterial cells due to the interaction between the specific antibody and the immunogenic cell wall protein, depends primarily on the number and distribution of the different antigens over the bacterial cell's surface. Even knowing the saturation moment of one nanoparticle ($2.7 \times 10^{18} \text{ Am}^2$), it was not possible, in our working case, to extrapolate the average number of nanoparticles per bacterial cluster because we could not know the total number of cells in it.

Adding to this, neighboring cells to bacterial clusters probably could not be magnetically identified. This second method's weakness is explained by the rotating nature of the magnetic dipole field of nanoparticles magnetized by an external magnetic field, which can induce signal cancelation (Henriksen et al., 2015). Therefore, the magnetic fields from two differently placed nanoparticles could partially cancel each other.

Nevertheless, we can identify five opportunities for improvement of the developed magnetic method. The first one is about the biosensor's suitability for routine diagnosis, meaning applicability to large numbers of milk samples. The

current number of analyzed samples is 10 to 12 per day. The external permanent magnet positioned below the 28 sensors (7 per microchannel), creates a magnetic field that affects its transfer curves and sensitivities, except for one sensor focused by the magnet for correct positioning. Thus, only one microchannel can be used, from four available, limiting to one the sample analysis rate. To correct this issue, some trials were performed varying magnet's type and strengths and also relative distances to sensor's PCB (Soares, 2015). However, for the magnet optimal distance found (2 cm), corresponding to unchanged transfer curves for every 28 SV's, a nanoparticle size of 130nm or more, was needed to be magnetically detected. Further optimization trials could be done to confirm bacterial identification in mastitic milk samples with these larger nanoparticles (higher volume) but inherent binding yield issues should be expected.

The biosensor's flexibility is the second opportunity for improvement which includes other specific antibodies to be used for further identification of other important bovine mastitis pathogens.

Thirdly, the binding yield variations of nanoparticles functionalization could also be enhanced. The difficulty of having the same number of attached IgM (30nm) to a nanoparticle (50nm) is predictable when compared to smaller IgG (15nm), which is translated by uncontrollable binding yield variation. This issue is justified by both antibodies stereochemistry and nanoparticle's volume, which is not possible to change. Consequently, it affects bacterial cells magnetic labelling efficiency. However, there are some methods that can be used, like thermogravimetric analysis, which applied to a functionalized nanoparticle's solution, will be able to extrapolate the weight for antibodies and nanoparticles in a sample and consequently, to quantify the binding yield. The thermogravimetric method consists of a thermal analysis which changes physical and chemical properties of materials measured, as a function of increasing temperature (with constant heating rate), or as a function of time (with constant temperature and/or constant mass loss). This method is commonly used to determine selected characteristics of materials that exhibit either mass loss or gain due to decomposition, oxidation, or loss of volatiles (such as moisture). The inconvenience of this analysis in our case, was the minimum quantity of sample required. Forty milligrams was too much when compared to 364.03 μ g in solution per trial day when we used IgG antibodies or 366.25 μ g in solution per trial day

when we used IgM antibodies, which cost to obtain such higher quantity of functionalized nanoparticles, was also expensive.

The fourth magnetic method's improvement opportunity includes the multi-channel printed circuit board electronic troubleshooting. The multi-channel PCB was the main component of the magnetic detection device. Consequently, the identification of the causative problem was critical for further correction and continuing the daily work. The major problem found was translated visually on signal output oscillations, which prevented further measurements. There were two different correction types: the simplest, which included batteries or some electronic parts replacement (as capacitors); or a more complex, which required the knowledge of the correlation between the multi-channel electronic circuit contacts and the sensor interface. The last, was usually diagnosed and solved by technical expertise on electronics from INESC-ID.

Finally, the last opportunity found was on the mastitic milk samples distribution for biosensor's analysis. The biosensor validation was performed with 91 different mastitic milk samples, corresponding to 124 independent trials with four specific antibodies (four groups of 31 milk samples analyzed by specific antibodies) (Figure 46). The last two papers, corresponding to current Thesis chapters V and VI, describe half of that work each.

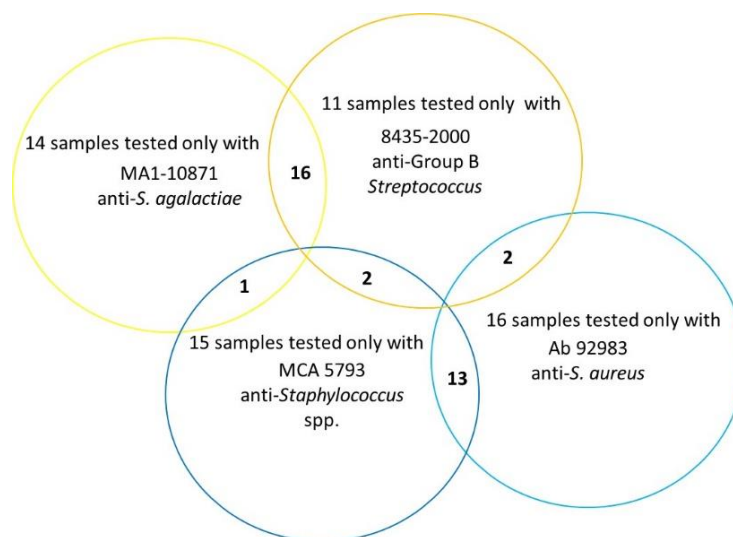


Figure 46. Number of mastitic samples analyzed per antibody. The interception numbers corresponds to the common samples analyzed by respective antibodies.

Samples distribution could have been performed in another way (Figure 47). The same mastitic milk samples could have been tested with the four primary antibodies, which would mean a monitoring of both staphylococci and

streptococci in each sample, as PCR analysis results, allowing higher numbers of samples tested with each antibody by the biosensor.

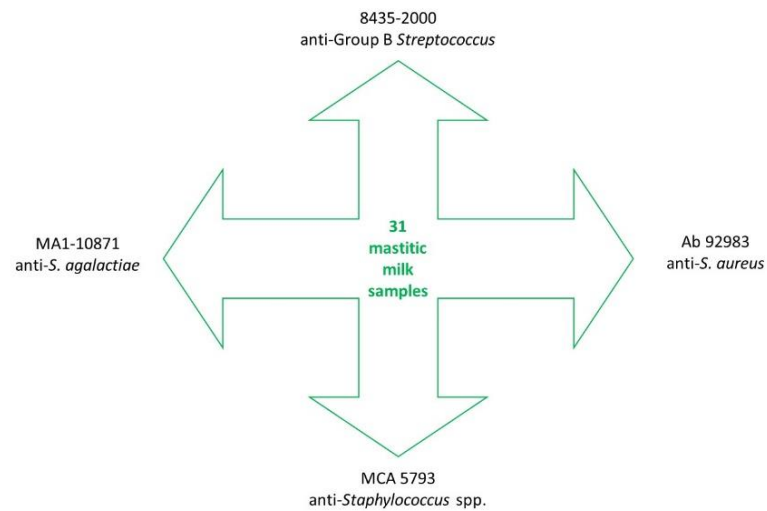


Figure 47. Sampling design proposal.

However, one of the main concerns was to evaluate biosensor's suitability to detect and identify mastitis pathogens in different milk matrix features, which was successfully evidenced with the 91 mastitic samples used.

Two threats were identified and are described below.

The first one was based on the sterile and mastitic milk matrix heterogeneity. The first main goal of this project was the achievement of a portable lab-on-chip device able to be used on-site and to analyze raw milk collected directly from a potentially infected cow. However, milk is a colloid of fat globules and water with dissolved carbohydrates and protein complexes (Walstra, 2006), where bacteria, when are present, are distributed throughout the emulsion, suspended in solution as well as entrapped and adsorbed on proteins micelles and fat globules. This knowledge, led us to several months of trials with different experimental conditions, including thawing or filtering milk samples (pore diameter $\geq 2\text{-}3\mu\text{m}$) to remove fat globules from raw milk; re-design of the microchannel's layout including pillars for milk sieving, to help fat globules to disperse (Figure 48B); detergent/ surfactant concentration (PBST) added to raw milk; temperature variation (4°C or RT) of milk samples with bacterial labeled cells, before biosensor analysis; different bacterial concentrations spiked into sterile milk to

achieve detection limit and nanoparticle's content optimization in control milk samples for no magnetic signal achievement.

The thawing and filtering steps removed fat globules but also bacterial cells from mastitic milk samples. These hypotheses to improve magnetic detection in raw milk samples were thus abandoned.

Regarding to the microchannels re-design (Figure 48A), based on Wolff and coworkers' work (2003), a hydrodynamic focusing of the milk sample on the microfluidic device was achieved through the milk stream injection into a single sheath flow focused into a section with magnetoresistive sensors. On the other hand, the alternative microfluidic design mask with pillars inside the microchannel, tested during biosensor's measurements, presented smooth flow for sterile milk but huge difficulties on mastitic milk flowing.

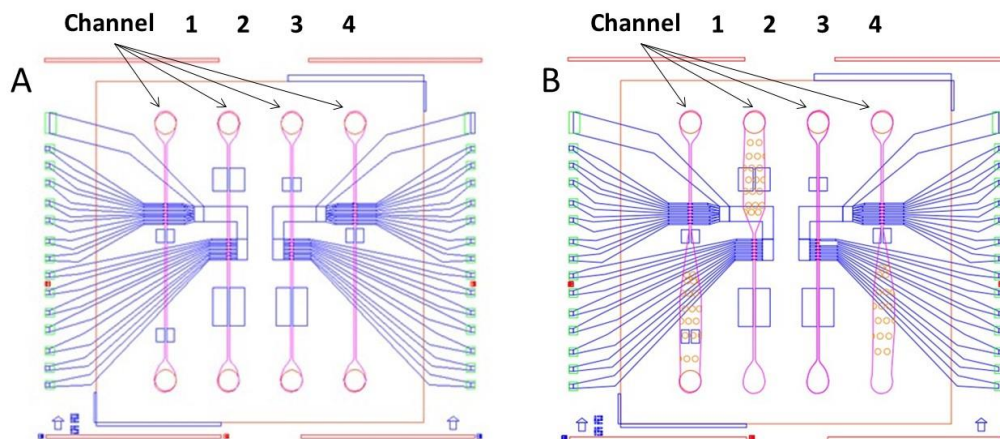


Figure 48. Microfluidic microchannel's CAD masks. A) linear microchannels used for conclusive results. B) microchannels with pillars inside, tested for raw milk sieving.

We evidenced that we could not get away from a milk sample pre-treatment step, even a short one, which should include higher temperature, surfactant addition and stronger agitation, to reduce fat globule dimensions, to distribute the bacterial cells in the milk, to improve nanoparticles mobilization and to allow for a more homogeneous milk matrix. The 60°C temperature value was tested because it is the same used by the dairy industry for the milk homogenization step, to reduce fat globules dimensions and to allow its uniform distribution in raw milk. Those conditions were expected to help better access to bacterial cells by functionalized nanoparticles and were confirmed by further results.

Finally, the last threat to the biosensor's performance was the fact that magnetoresistive sensors were affected by electrical conductivity of mastitic milk.

An effect of bovine mastitis is changes in milk's ion concentrations due to increased vascular permeability leading to modifications in its electrical conductivity (Hovinen et al., 2006). The conductance in milk causes sensor's resistivity variation translated by higher background noise instead of true magnetic signal.

Studies taking advantage of the electrical conductivity of ions in a sample (Hassan et al., 2014), or impedance signal of particles and cells using the surrounding media as a reference (Gawad, Schild & Renaud, 2001), are not suitable for mastitic milk samples because these present high sensitivity to the sample matrix and could not distinguish between conductance of milk components and bacterial presence, which greatly hinders these devices' use outside laboratory facilities. This knowledge reinforces the better suitability of the magnetic detection method studied and described in this thesis.

CONCLUSIONS

The main findings of this doctoral work were:

1. Immunoblotting results evidenced antigenic recognition by four commercially available antibodies and how many immunogenic cell wall proteins were detected per selected aetiological agent (*Staphylococcus aureus*, *Staphylococcus epidermidis*, *Streptococcus agalactiae* and *Streptococcus uberis*).
2. The large discrepancy in peak's amplitude and shape, evidenced in milk samples spiked with bacterial cells, can be explained by cells number variation in each agglomerate and by the different flowing heights above the sensor.
3. Magnetic peak's amplitude and shape interpretation, should consider the immunogenic cell wall proteins number as the probable specific antibody binding sites to cell, instead of a settled 1600 number of 50nm functionalized nanoparticles able to cover a spherical cell of 1 μm diameter.
4. Raw milk samples were submitted to a pre-treatment consisting of heating (15 min at 60°C) and homogenization (15 min in vortex) to achieve a clear magnetic signal during biosensor validation.
5. Peaks over 50 μV were evidenced in milk samples with magnetically labelled bacteria, indicating that the observed signals were undoubtedly from magnetic origin.
6. This immunological recognition was able to detect bacterial presence in milk samples spiked above 100 CFU/ml, independently of antibody and targeted bacteria.
7. Sensitivities of 73% and 41% and specificity values of 25% and 57% were obtained for magnetic identification of streptococci species with an anti-*Streptococcus agalactiae* antibody and an anti-GB Streptococci antibody, respectively.
8. The higher PPV value (54%) evidenced for magnetic detection with the anti-GB streptococci antibody may reinforce the bonding avidity between this polyclonal antibody and the only two immunogenic cell wall proteins of *S. uberis* comparing to 10 or more antigens known in *S. agalactiae*.
9. Sensitivities of 57.1% and 79.3% and specificity values of 75% and 50% were obtained for magnetic identification of staphylococci species in mastitic milk samples with an anti-*S. aureus* ScpA antibody and an anti-*Staphylococcus* spp. antibody, respectively.
10. The higher PPV value (95.8%) evidenced for magnetic detection with the anti-*Staphylococcus* spp. antibody may reinforce its bonding avidity for each immunogenic cell wall protein of *S. aureus* and of *S. epidermidis* when compared to the anti-*S. aureus* ScpA antibody.

FUTURE DIRECTIONS

Development prospects for new bovine mastitis diagnosis methodologies point to new biomarkers and technological advances for high sensitivity and specificity, fast and efficient devices that can offer a “cow-side” use.

Giouroudi and Keplinger (2013) outlined that several novel manipulation, separation and detection mechanisms based on magnetic methods are continuously emerging, proving that magnetic biosensing has the potential to become competitive and probably replace in the future the current optical and fluorescence detection technologies, while maintaining the high sensitivity and fast readout time.

Consequently, the current magnetic detection device used in this doctoral work, can also be a part of that future. Taking into account the mentioned strengths and opportunities, this biosensor can be submitted to further improvements which may include milk pre-treatment step incorporation into the microfluidic platform and also further studies on electronics to allow multiplex analysis of several samples at a time. At this moment, this biosensor requires an external computer for system operation and displaying test results, so a fully integrated system into a single device could also be made.

The bacterial quantification, however, may be done within lower/upper threshold limits. Simulations of the sensor output as a function of the nanoparticle distribution over the cells (using colonies/clusters configurations compatible with the experimentally observed in microscope) can provide indication on minimum and maximum numbers. Further work could be done towards a more accurate quantification based on simulations.

REFERENCES

- Abcam (2011). *Western Blotting – A beginner's guide*. Accessed in June 20, 2011, available at <http://www.abcam.com/tag/western%20blot%20protocols>.
- AbDSerotec (2013). *General procedure for direct ELISA*. Accessed in May 5, 2013, available at <https://www.abdserotec.com/direct-elisa-protocol-with-streptavidin-biotin-detection.html>.
- Aebbersold, R., Rist, B. & Gygi, S.P. (2006). Quantitative proteome analysis: methods and applications. *Annals of the New York Academy of Sciences*, 919, 33-47.
- Akagi, J., Takeda, K., Fujimura, Y., Matuszek, A., Khoshmanesh, K. & Wlodkowic, D. (2013). Microflow cytometry in studies of programmed tumor cell death. *Sensors and Actuators B: Chemical*, 189, 2–10.
- Åkerstedt, M., Forsbäcka, L., Larsena, T. & Svennersten-Sjaunja, K. (2011). Natural variation in biomarkers indicating mastitis in healthy cows. *Journal of Dairy Research*, 78, 88–96.
- Åkerstedt, M., Waller, K.P., Larsen, L.B., Forsbäck, L., Sternesjö, A. (2008). Relationship between haptoglobin and serum amyloid A in milk and milk quality. *International Dairy Journal*, 18(6), 669–674.
- Autebert, J., Coudert, B., Bidard, F.-C., Pierga, J.-Y., Descroix, S., Malaquin, L. & Viovy, J.-L. (2012). Microfluidic: an innovative tool for efficient cell sorting. *Methods*, 57(3), 297–307.
- Baibich, M.N., Broto, J.M., Fert, A., Nguyen Van Dau, F., Petroff, F., Etienne, P., Creuzet, G., Friederich, A. & Chazelas, J. (1988). Giant magnetoresistance of (001)Fe/(001)Cr magnetic superlattices. *Physical Review Letters*, 61(21), 2472–2475.
- Barbour, A. (2002). Antigenic variation by relapsing fever *Borrelia* species and other bacterial pathogens. pp. 972–994. In Craig, N. L., Craigie, R., Gellert, M., and Lambowitz, A. M. (ed.), *Mobile DNA II*. Washington, D.C.: ASM Press.
- Barreiro, J.R., Ferreira, C.R., Sanvido, G.B., Kostrzewa, M., Maier, T., Wegemann, B., Böttcher, V., Eberlin, M.N., & dos Santos, M.V. (2010). Short communication: identification of subclinical cow mastitis pathogens in milk by matrix-assisted laser desorption/ionization time-of-flight mass spectrometry. *Journal of Dairy Science*, 93, 5661–5667.
- Bedidi-Madani, N., Greenland, T. & Richard Y. (1998). Exoprotein and slime production by coagulase-negative staphylococci isolated from goats' milk. *Veterinary Microbiology*, 59(2-3), 139-145.
- Beier, D. & Gross, R. (2006). Regulation of bacterial virulence by two-component systems. *Current Opinion in Microbiology*, 9(2), 143–152.
- Bexiga, R., Koskinen, M.T., Holopainen J., Carneiro, C., Pereira, H., Ellis, K.A. & Vilela, C.L. (2011). Diagnosis of intramammary infection in samples

yielding negative results or minor pathogens in conventional bacterial culturing. *Journal of Dairy Research*, 78, 49–55.

- Bexiga, R., Rato, M.G., Lemsaddek, A., Semedo-Lemsaddek, T., Carneiro, C., Pereira, H., Mellor, D.J., Ellis, K.A. & Vilela, C.L. (2014). Dynamics of bovine intramammary infections due to coagulase-negative staphylococci on four farms. *Journal of Dairy Research*, 81(2), 208-214.
- Bittar, F., Ouchenane, Z., Smati, F., Raoult, D. & Rolain, J.M. (2009). MALDI-TOF MS for rapid detection of staphylococcal Pantone–Valentine leukocidin. *International Journal of Antimicrobial Agents*, 34, 467–470.
- Bizzini, A. & Greub, G. (2010). Matrix-assisted laser desorption ionization time-of-flight mass spectrometry, a revolution in clinical microbial identification. *Clinical Microbiology and Infection*, 16(11), 1614–1619.
- Boeck, G. (2001). Current status of flow cytometry in cell and molecular biology. *International Review of Cytology*, 204, 239–298.
- Boehmer, J.L. (2011). Proteomic analyses of host and pathogen responses during bovine mastitis. *Journal of Mammary Gland Biology and Neoplasia*, 16, 323–338.
- Boehmer, J.L., DeGrasse, J.A., McFarland, M.A., Tall, E.A., Shefcheck, K.J., Ward, J.L., Bannerman, D.D. (2010). The proteomic advantage: label-free quantification of proteins expressed in bovine milk during experimentally induced coliform mastitis. *Veterinary Immunology and Immunopathology*, 138(4), 252–266.
- Böhme, K., Morandi, S., Cremonesi, P., No, I.C.F., Barros-Velázquez, J., Castiglioni, B., Brasca, M., Cañas, B. & Calo-Mata, P. (2012). Characterization of *Staphylococcus aureus* strains isolated from Italian dairy products by MALDI-TOF mass fingerprinting. *Electrophoresis*, 33, 2355–2364.
- Bourry, A. & Poutrel, B. (1996). Bovine mastitis caused by *Listeria monocytogenes*: kinetics of antibody responses in serum and milk after experimental infection. *Journal of Dairy Science*, 79, 2189–2195.
- Bradley, A. (2002). Bovine mastitis: an evolving disease. *The Veterinary Journal*, 164(2), 116–128.
- Britten, A.M. (2012). The role of diagnostic microbiology in mastitis control programs. *Veterinary Clinics: Food Animal Practice*, 28(2), 187–202.
- Bronner, S., Monteil, H. & Prévost, G. (2004). Regulation of virulence determinants in *Staphylococcus aureus*: complexity and applications. *FEMS Microbiology Review*, 28(2), 183–200.
- Bustin, S.A. (Ed.) (2004). Quantification of nucleic acids by PCR. In: *A–Z of Quantitative PCR*. (pp. 5–46) (IUL Biotechnology, No. 5). La Jolla, CA: IUL Press.
- Carretto, E., Barbarini, D., Couto, I., de Vitis, D., Marone, P., Verhoef, J., de Lencastre, H., Brisse, S. (2005). Identification of coagulase-negative staphylococci other than *Staphylococcus epidermidis* by automated ribotyping. *Clinical Microbiology and Infection*, 11(3), 177–184.

- Cash, P. (2000). Proteomics in medical microbiology. *Electrophoresis*, 21(6), 1187–1201.
- Chung, T.D. & Kim, H.C. (2007). Recent advances in miniaturized microfluidic flow cytometry for clinical use. *Electrophoresis*, 28(24), 4511–4520.
- Cole, J.N., Djordjevic, S.P. & Walker, M.J. (2008). Isolation and solubilization of gram-positive bacterial cell wall-associated proteins. In A. Posch (Ed.) *Methods in Molecular Biology*, vol 425. *2D PAGE: Sample Preparation and Fractionation*, vol 2, (pp 295-311). Totowa, NJ: Humana Press.
- Costa, T., Piedade, M.S., Germano, J., Amaral, J. & Freitas, P.P. (2014) A neuronal signal detector for biologically generated magnetic fields. *IEEE Transactions on Instrumentation and Measurement*, 63(5), 1171 – 1180.
- Cremonesi, P., Pisoni, G., Severgnini, M., Consolandi, C., Moroni, P., Raschetti, M., Castiglioni, B. (2009). Pathogen detection in milk samples by ligation detection reaction-mediated universal array method. *Journal of Dairy Science*, 92(7), 3027–3039.
- de Ávila, B.E.F., Pedrero, M., Campuzano, S., Escamilla-Gómez, V. & Pingarrón, J.M. (2012). Sensitive and rapid amperometric magnetoimmunosensor for the determination of *Staphylococcus aureus*. *Analytical and Bioanalytical Chemistry*, 403(4), 917-25.
- Díaz, M., Herrero, M., García, L.A. & Quirós, C. (2010). Application of flow cytometry to industrial microbial bioprocesses. *Biochemical Engineering Journal*, 48(3), 385–407.
- Di Carlo, D. (2009). Inertial microfluidics. *Lab on a Chip*, 9(21), 3038–3046.
- Dieny, B. (1994). Giant magnetoresistance in spin-valve multi-layers. *Journal of Magnetism and Magnetic Materials*, 136(3), 335–359.
- Dohoo, I.R. & Leslie, K.E. (1991). Evaluation of changes in somatic cell counts as indicators of new intramammary infections. *Preventive Veterinary Medicine*, 10(3), 225–237.
- Douglas, V.L., Fenwick, S.G, Pfeiffer, D.U., Williamson, N.B. & Holmes, C.W. (2000). Genomic typing of *Streptococcus uberis* isolates from cases of mastitis, in New Zealand dairy cows, using pulsed-field gel electrophoresis. *Veterinary Microbiology*, 75(1), 27–41.
- Duarte, C.M., Fernandes, A.C., Cardoso, F.A., Bexiga, R., Cardoso, S. & Freitas, P.P. (2015a). Magnetic counter for Group B Streptococci detection in milk. *IEEE Transactions on Magnetics*, 51(1). doi 10.1109/TMAG.2014.2359574.
- Duarte, C.M., Freitas, P.P. & Bexiga, R. (2015b). Technological advances in Bovine Mastitis Diagnosis – an overview. *Journal of Veterinary Diagnostic Investigation*, 27(6), 665 –672.
- Dubelaar, G.B.J., Gerritzen, P.L., Beeker, A.E.R., Jonker, R.R. & Tangen, K. (1999). Design and first results of CytoBuoy: A wireless flow cytometer for in situ analysis of marine and fresh waters. *Cytometry*, 37(4), 247–254.

- Driskell, J.D. & Tripp, R.A. (2009). Emerging technologies in nanotechnology-based pathogen detection. *Clinical Microbiology Newsletter*, 31(18), 137–144.
- Edwards, B.S., Oprea, T., Prossnitz, E.R. & Sklar, L.A. (2004). Flow cytometry for high-throughput, high-content screening. *Current Opinion in Chemical Biology*, 8(4), 392–398.
- Edwards, M.C. & Gibbs, R.A. (1994). Multiplex PCR: advantages, development, and applications. *Genome Research*, 3, S65–S75.
- Esfandyarpour, R., Javanmard, M., Koochak, Z., Harris, J.S. & Davis, R.W. (2013). Nanoelectronic impedance detection of target cells. *Biotechnology and Bioengineering*, 111(6), 1161–1169.
- Fabres-Klein, M.H., Aguilar, A.P., Silva, M.P., Silva, D.M. & Ribon, A.O.B. (2014). Moving towards the immunodiagnosis of staphylococcal intramammary infections. *European Journal of Clinical Microbiology and Infectious Diseases*, 33, 2095–2104.
- Fenili, D. & Pirovano, B. (1998). The automation of sediment urinalysis using a new urine flow cytometer. *Clinical Chemistry and Laboratory Medicine*, 36(12), 909–917.
- ¹Fernandes, A.C., Duarte, C.M., Cardoso, F.A., Bexiga, R., Cardoso, S. & Freitas, P.P. (2014). Lab-on-chip cytometry based on magnetoresistive sensors for bacteria detection in milk. *Sensors*, 14, 15496–15524.
- ²Fernandes, E., Martins, V.C., Nóbrega, C., Carvalho, C.M., Cardoso, F.A., Cardoso, S., Dias, J., Deng, D., Kluskens, L.D. & Freitas, P.P. (2014). A bacteriophage detection tool for viability assessment of *Salmonella* cells. *Biosensors and Bioelectronics*, 52, 239–246.
- Frankowski, M., Theisen, J., Kummrow, A., Simon, P., Ragusch, H., Bock, N., Schmidt, M. & Neukammer, J. (2013). Microflow cytometers with integrated hydrodynamic focusing. *Sensors*, 13(4), 4674–4693.
- Freitas, P.P., Silva, F., Oliveira, N.J., Melo, L.V., Costa, L. & Almeida, N. (2000). Spin valve sensors. *Sensors and Actuators A: Physical*, 81(1-3), 2–8.
- Freitas, P.P., Ferreira, R., Cardoso, S. & Cardoso, F. (2007). Magnetoresistive sensors. *Journal of Physics: Condensed Matter*, 19(16), 1–21.
- Freitas, P.P., Cardoso, F.A., Martins, V.C., Martins, S.A.M., Loureiro, J., Amaral, J., Chaves, R.C., Cardoso, S., Fonseca, L.P., Sebastião, A.M., Pannetier-Lecoœur, M. & Fermon, C. (2012). Spintronic platforms for biomedical applications. *Lab on a Chip*, 12(3), 546–557.
- Fu, A.Y., Spence, C., Scherer, A., Arnold, F.H. & Quake, S.R. (1999). A microfabricated fluorescence-activated cell sorter. *Nature Biotechnology*, 17, 1109–1111.
- Fu, A.Y., Chou, H.-P., Spence, C., Arnold, F.H. & Quake, S.R. (2002). An integrated microfabricated cell sorter. *Analytical Chemistry*, 74, 2451–2457.

- Fu, L.-M., Yang, R.-J., Lin, C.-H., Pan, Y.-J. & Lee, G.-B. (2004). Electrokinetically driven micro flow cytometers with integrated fiber optics for on-line cell/particle detection. *Analytica Chimica Acta*, 507(1), 163–169.
- Gabriel, H. & Kindermann, W. (1995). Flow cytometry. Principles and applications in exercise immunology. *Sports Medicine*, 20(5), 302–320.
- Garcia-Cordero, J.L., Barrett, L.M., O'Kennedy, R. & Ricco, A.J. (2010). Microfluidic sedimentation cytometer for milk quality and bovine mastitis monitoring. *Biomedical Microdevices*, 12(6), 1051–1059.
- Garratty, G. & Arndt, P.A. (1999). Applications of flow cytofluorometry to red blood cell immunology. *Cytometry*, 38(6), 259–267.
- Gawad, S., Schild, L. & Renaud, Ph. (2001). Micromachined impedance spectroscopy flow cytometer for cell analysis and particle sizing. *Lab on a Chip*, 1, 76-82.
- Gehanno, V., Freitas, P.P., Veloso, A., Ferrira, J., Almeida, B., Soasa, J.B., Kling, A., Soares, J.C. & da Silva, M.F. (1999). Ion beam deposition of Mn-Ir spin valves. *IEEE Transactions on Magnetics*, 35(5), 4361–4367.
- Gfeller, K.Y., Nugaeva, N. & Hegner, M. (2005). Micromechanical oscillators as rapid biosensor for the detection of active growth of *Escherichia coli*. *Biosensors and Bioelectronics*, 21(3), 528–533.
- Gillespie, B.E. & Oliver, S.P. (2005). Simultaneous detection of mastitis pathogens, *Staphylococcus aureus*, *Streptococcus uberis*, and *Streptococcus agalactiae* by multiplex real-time polymerase chain reaction. *Journal of Dairy Science*, 88(10), 3510–3518.
- Giouroudi, I. & Keplinger, F. (2013). Microfluidic biosensing systems using magnetic nanoparticles. *International Journal of Molecular Sciences*, 14, 18535-18556.
- Golberg, A., Linshiz, G., Kravets, I., Stawski, N., Hillson, N.J., Yarmush, M.L., Marks, R.S. & Konry, T. (2014). Cloud-enabled microscopy and droplet microfluidic platform for specific detection of *Escherichia coli* in water. *PLoS One*, 9(1), e86341.
- Gonçalves, D., Prazeres, D.M.F., Chu, V. & Conde, J.P. (2008). Detection of DNA and proteins using amorphous silicon ion-sensitive thin-film field effect transistors. *Biosensors and Bioelectronics*, 24(4), 545–551.
- Gonzalo C, Linage, B., Carriedo, J. A., de la Fuente, F., & San Primitivo, F. (2006). Evaluation of the overall accuracy of the DeLaval cell counter for somatic cell counts in ovine milk. *Journal of Dairy Science*, 89(12), 4613–4619.
- Gosling, J.P. (1990). A decade of development in immunoassay methodology. *Clinical Chemistry*, 36(8), 1408–1427.
- Gossett, D.R., Weaver, W.M., Mach, A.J., Hur, S.C., Tse, H.T.K., Lee, W., Amini, H. & Carlo, D.D. (2010). Label-free cell separation and sorting in microfluidic systems. *Analytical and Bioanalytical Chemistry*, 397(8), 3249–3267.

- Gröhn, Y.T., Eicker, S.W., Ducrocq, V. & Hertl, J.A. (1998). Effect of diseases on the culling of Holstein dairy cows in New York state. *Journal of Dairy Science*, 81(4), 966-978.
- Groisman, A. & Simonnet, C. (2006). High-throughput and high-resolution flow cytometry in molded microfluidic devices. *Analytical Chemistry*, 78(16), 5653–5663.
- Grönlund, U., Hultén, C., Eckersall, P.D., Hogarth, C. & Waller, K.P. (2003). Haptoglobin and serum amyloid A in milk and serum during acute and chronic experimentally induced *Staphylococcus aureus* mastitis. *Journal of Dairy Research*, 70(4), 379–386.
- Groschup, M.H., Hahn, G. & Timoney, J.F. (1991). Antigenic and genetic homogeneity of *Streptococcus uberis* strains from the bovine udder. *Epidemiology and Infection*, 107(2), 297-310.
- Guidry, A.J., Berning, L.M. & Hambleton, C.N. (1993). Opsonization of *Staphylococcus aureus* by bovine immunoglobulin isotypes. *Journal of Dairy Science*, 76(5), 1285–1289.
- Gunnarsson A., Jönsson, P., Marie, R., Tegenfeldt, J. & Höök, F. (2008). Single-molecule detection and mismatch discrimination of unlabeled DNA targets. *Nano Letters*, 8(1), 183–188.
- Hammes, F., Berney, M., Wang, Y., Vital, M., Koster, O. & Egli, T. (2008). Flow-cytometric total bacterial cell counts as a descriptive microbiological parameter for drinking water treatment processes. *Water Research*, 42(1-2), 269–277.
- Harding, C.L., Lloyd, D.R., McFarlane, C.M. & Al-Rubeai, M. (2000). Using the microcyte flow cytometer to monitor cell number, viability, and apoptosis in mammalian cell culture. *Biotechnology Progress*, 16(5), 800–802.
- Hassan, U., Watkins, N.N., Edwards, C. & Bashir, R. (2014). Flow metering characterization within an electrical cell counting microfluidic device. *Lab on a Chip*, 14(8), 1469–1476.
- Heikens, E., Fleer, A., Paauw, A., Florijn, A. & Fluit, A.C. (2005). Comparison of genotypic and phenotypic methods for species-level identification of clinical isolates of coagulase-negative staphylococci. *Journal of Clinical Microbiology*, 43(5), 2286–2290.
- Heir, E., Sundheim, G. & Holck, A.L. (1999). Identification and characterization of quaternary ammonium compound resistant staphylococci from the food industry. *International Journal of Food Microbiology*, 48(3), 211–219.
- Heller, M., Berthold E., Pfützner H., Leirer R. & Sachse K. (1993). Antigen capture ELISA using a monoclonal antibody for the detection of *Mycoplasma bovis* in milk. *Veterinary Microbiology*, 37(1–2), 127-133.
- Helou, M., Reisbeck, M., Tedde, S.F., Richter, L., Bär, L., Bosch, J.J., Stauber, R.H., Quandt, E. & Hayden, O. (2013). Time-of-flight magnetic flow cytometry in whole blood with integrated sample preparation. *Lab on a Chip*, 13(6), 1035–1038.

- Henriksen, A.D., Wang, S.X. & Hansen, M.F. (2015). On the importance of sensor height variation for detection of magnetic labels by magnetoresistive sensors. *Scientific Reports*, 5, 12282.
- Hicks, C.R., Eberhart, R.J. & Sischo, W.M. (1994). Comparison of microbiologic culture, an enzyme-linked immunosorbent assay, and determination of somatic cell count for diagnosing *Staphylococcus aureus* mastitis in dairy cows. *Journal of the American Veterinary Medical Association*, 204(2), 255–260.
- Hiitiö, H., Riva, R., Autio, T., Pohjanvirta, T., Holopainen, J. & Pyörälä, S. (2015). Performance of a real-time PCR assay in routine bovine mastitis diagnostics compared with in-depth conventional culture. *Journal of Dairy Research*, 82(2), 200-208.
- Hill, A.W., Heneghan, D.J. & Williams, M.R. (1993). The opsonic activity of bovine milk whey for the phagocytosis and killing by neutrophils of encapsulated and non-encapsulated *Escherichia coli*. *Veterinary Microbiology*, 8(3), 293–300.
- Hiss, S., Mielenz, M., Bruckmaier, R.M. & Sauerwein, H. (2004). Haptoglobin concentrations in blood and milk after endotoxin challenge and quantification of mammary Hp mRNA expression. *Journal of Dairy Science*, 87(11), 3778–3784.
- Hiss, S., Mueller U., Neu-Zahren, A. & Sauerwein, H. (2007). Haptoglobin and lactate dehydrogenase measurements in milk for the identification of subclinically diseased udder quarters. *Veterinarni Medicina*, 52(6), 245–252.
- Holdaway, R.J., Holmes, C.W. & Steffert, I.J. (1996). A comparison of indirect methods for diagnosis of subclinical intramammary infection in lactating dairy cows. Part 2: the discriminative ability of eight parameters in foremilk from individual quarters and cows. *Australian Journal of Dairy Technology*, 51(2), 72–78.
- Hortet, P. & Seegers, H. (1998). Calculated milk production losses associated with elevated somatic cell counts: review and critical discussion. *Veterinary Research*, 29(6), 497-510.
- Hovi, M. & Roderick, S. (1999). Mastitis in organic dairy herds - results of a two year survey. *Proceedings of a soil association conference – Mastitis, the organic perspective. Stoneleigh, 3 September*. Reading, UK.
- Hovinen, M., Aisla, A.M. & Pyörälä S. (2006). Accuracy and reliability of mastitis detection with electrical conductivity and milk colour measurement in automatic milking. *Acta Agriculturae Scandinavica, Section A — Animal Science*, 56(3-4), 121–127.
- Hudson, L & Hay, F.C. (1989). *Practical Immunology*. (3rd ed.). Boston: Blackwell Scientific Publications.
- Huh, D., Gu, W., Kamotani, Y., Grotberg, J.B. & Takayama, S. (2005). Microfluidics for flow cytometric analysis of cells and particles. *Physiological Measurement*, 26(3), R73–R98.

- Hyytiä-Trees, E.K., Cooper, K., Ribot, E.M. & Gerner-Smidt, P. (2007). Recent developments and future prospects in subtyping of foodborne bacterial pathogens. *Future Microbiology*, 2(2), 175–185.
- Ieven, M., Verhoeven, J., Pattyn, S.R. & Goossens, H. (1995). Rapid and economical method for species identification of clinically significant coagulase-negative staphylococci. *Journal of Clinical Microbiology*, 33(5), 1060–1063.
- Issaq, H.J. & Blonder, J. (2009). Electrophoresis and liquid chromatography/tandem mass spectrometry in disease biomarker discovery. *Journal of Chromatography B*, 877(13), 1222–1228.
- Janeway, C.A., Travers, P., Walport, M. & Shlomchik, M.J. (2001). *Immunobiology. The immune system in health and disease*. (5th ed.). New York: Garland Science.
- Kemna, E.W., Segerink, L.I., Wolbers, F., Vermes, I. & van den Berg, A. (2013). Label-free, high-throughput, electrical detection of cells in droplets. *Analyst*, 138(16), 4585–4592.
- Kettlitz, S.W., Valouch, S., Sittel, W. & Lemmer, U. (2012). Flexible planar microfluidic chip employing a light emitting diode and a PIN-photodiode for portable flow cytometers. *Lab on a Chip*, 12(1), 197–203.
- Kim, J.S., Anderson, G.P., Erickson, J.S., Golden, J.P., Nasir, M. & Ligler, F.S. (2009). Multiplexed detection of bacteria and toxins using a microflow cytometer. *Analytical Chemistry*, 81(13), 5426–5432.
- Kitchen, B.J., Middleton, G. & Salmon, M. (1978). Bovine milk N-acetyl- β -D-glucosaminidase and its significance in the detection of abnormal udder secretions. *Journal of Dairy Research*, 45(1), 15–20.
- Kitchen, B.J. (1981). Review of the progress of dairy science: bovine mastitis: milk compositional changes and related diagnostic tests. *Journal of Dairy Research*, 48(1), 167–188.
- Klopfleisch, R. & Gruber, A.D. (2012). Transcriptome and proteome research in veterinary science: what is possible and what questions can be asked? *Scientific World Journal*, 2012, 254962.
- Korhonen, H. & Kaartinen, L. (1995). Changes in the composition of milk induced by mastitis. In: Sandholm M., Honkanen-Buzalski T., Kaartinen L., Pyörälä S. (Eds.). *The Bovine Udder and Mastitis*. (pp. 76–82). Gummerus, Jyväskylä, Finland.
- Koskinen, M.T., Holopainen, J., Pyörälä, S., Bredbacka, P., Pitkälä, A., Barkema, H.W., Bexiga, R., Roberson, J., Sølverød, L., Piccinini, R., Kelton, D., Lehmusto, H., Niskala, S. & Salmikivi, L. (2009). Analytical specificity and sensitivity of a real-time polymerase chain reaction assay for identification of bovine mastitis pathogens. *Journal of Dairy Science*, 92(3), 952–959.
- KPL (2013). Kirkegaard & Perry Laboratories, Inc. *Technical guide for ELISA*. Acedido em Mai. 5, 2013, disponível em <https://www.kpl.com/technical/index.cfm?pID=215>.

- Kruger, J., Singh, K., O'Neill, A., Jackson, C., Morrison, A. & O'Brien, P. (2002). Development of a microfluidic device for fluorescence activated cell sorting. *Journal of Micromechanics and Microengineering*, 12(4), 486–494.
- Laemmli, U.K. (1970). Cleavage of structural proteins during the assembly of the head of bacteriophage T4. *Nature*, 227(5259), 680 – 685.
- Lago, A., Godden, S.M., Bey, R., Ruegg, P.L. & Leslie, K. (2011). The selective treatment of clinical mastitis based on on-farm culture results: I. Effects on antibiotic use, milk withholding time, and short-term clinical and bacteriological outcomes. *Journal of Dairy Science*, 94(9), 4441–4456.
- Larsen, T. (2005). Determination of lactate dehydrogenase (LDH) activity in milk by a fluorometric assay. *Journal of Dairy Research*, 72(2), 209–216.
- Lazcka, O., Del Campo, F.J. & Muñoz, F.X. (2007). Pathogen detection: a perspective of traditional methods and biosensors. *Biosensors and Bioelectronics*, 22(7), 1205–1217.
- Lee, K.H., Lee, J.W., Wang, S.W., Liu, L.Y., Lee, M.F., Chuang, S.T., Shy, Y.M., Chang, C.L., Wu, M.C. & Chi, C.H. (2008). Development of a novel biochip for rapid multiplex detection of seven mastitis-causing pathogens in bovine milk samples. *Journal of Veterinary Diagnostic Investigation*, 20, 463–471.
- Lequin, R.M. (2005). Enzyme immunoassay (EIA)/enzyme-linked immunosorbent assay (ELISA). *Clinical Chemistry*, 51(12), 2415–2418.
- Libing, W., Chuanlai X., Qianqian Y., Xiaofang D., Shanshan S. & Xun Z. (2012). Kit for rapid detection of *Staphylococcus aureus* in sample and detection method thereof. Pat. No. CN102323416 (A).
- Lippolis, J.D. & Reinhardt, T.A. (2010). Utility, limitations, and promise of proteomics in animal science. *Veterinary Immunology and Immunopathology*, 138(4), 241–251.
- Ljungberg, U.K., Jansson, B. Niss, U., Nilsson, R., Sandberg, B.E.B., & Nilsson, B. (1993). The interaction between different domains of staphylococcal protein A and human polyclonal IgG, IgA, IgM and F(ab')₂: separation of affinity from specificity. *Molecular Immunology* 30(14), 1279-1285.
- Loughman, A., Sweeney, T., Keane, F.M., Pietrocola, G., Speziale, P. and Foster, T.J. (2008). Sequence diversity in the A domain of *Staphylococcus aureus* fibronectin-binding protein A. *BMC Microbiology*, 8, 74.
- Loureiro, J., Andrade, P.Z., Cardoso, S., da Silva, C.L., Cabral, J.M. & Freitas, P.P. (2011). Magneto-resistive chip cytometer. *Lab on a Chip*, 11(13), 2255–2261.
- Mach, H., Bhambhani, A., Meyer, B.K., Burek, S., Davis, H., Blue, J.T. & Evans, R.K. (2011). The use of flow cytometry for the detection of subvisible particles in therapeutic protein formulations. *Journal of Pharmaceutical Sciences*, 100(5), 1671–1678.

- Madigan, M.T., Martinko, J.M., Bender, K.S., Buckley D.H. & Stahl, D.A. (2011). *Brock biology of microorganisms*. (13th ed.). San Francisco, CA: Benjamin Cummings.
- Malou, N. & Raoult, D. (2011). Immuno-PCR: a promising ultrasensitive diagnostic method to detect antigens and antibodies. *Trends in Microbiology*, 19(6), 295–302.
- Mansor, R., Mullen, W., Albalat, A., Zerefos, P., Mischak, H., Barrett, D.C., Biggs, A., Eckersall, P.D. (2013). A peptidomic approach to biomarker discovery for bovine mastitis. *Journal of Proteomics*, 85, 89–98.
- Martins, V.C., Germano, J., Cardoso, F.A., Loureiro, J., Cardoso, S., Sousa L., Piedade, M., Fonseca, L.P. & Freitas, P.P. (2010). Challenges and trends in the development of a magnetoresistive biochip portable platform. *Journal of Magnetism and Magnetic Materials*, 322(9-12), 1655–1663.
- Matsushita, T., Dinsmore, R.P., Eberhart, R.J., Jones, G.M., McDonald, J.S., Sears, P.M., Adams, D.S. (1990). Performance studies of an enzyme-linked immunosorbent assay for detecting *Staphylococcus aureus* antibody in bovine milk. *Journal of Veterinary Diagnostic Investigation*, 2(3), 163–166.
- McCarron, J.L., Keefe, G.P., McKenna, S.L., Dohoo, I.R. & Poole, D.E. (2009). Laboratory evaluation of 3M Petrifilms and University of Minnesota Biplates as potential on-farm tests for clinical mastitis. *Journal of Dairy Science*, 92(10), 2297–2305.
- Mellmann, A., Bimet, F., Bizet, C., Borovskaya, A.D., Drake, R.R., Eigner, U., Fahr, A.M., He, Y., Ilina, E.N., Kostrzewa, M., Maier, T., Mancinelli, L., Moussaoui, W., Prévost, G., Putignani, L., Seachord, C.L., Tang, Y.W., Harmsen, D. (2009). High interlaboratory reproducibility of matrix-assisted laser desorption ionization-time of flight mass by spectrometry-based species identification of nonfermenting bacteria. *Journal of Clinical Microbiology*, 47(11), 3732–3734.
- Milner, P., Page, K.L. & Hillerton, J.E. (1997). The effects of early antibiotic treatment following diagnosis of mastitis detected by a change in the electrical conductivity of milk. *Journal of Dairy Science*, 80, 859–863.
- Mortari, A. & Lorenzelli, L. (2014). Recent sensing technologies for pathogen detection in milk: A review. *Biosensors and Bioelectronics*, 60(15), 8-21.
- Mueller, U.G. & Wolfenbarger, L.L. (1999). AFLP genotyping and fingerprinting. *Trends in Ecology and Evolution*, 14(10), 389–394.
- Mujika, M., Arana, S., Castaño, E., Tijero, M., Vilares, R., Ruano-López, J.M., Cruz, A., Sainz, L. & Berganza, J. (2009). Magnetoresistive immunosensor for the detection of *Escherichia coli* O157:H7 including a microfluidic network. *Biosensors and Bioelectronics*, 24(5), 1253–1258.
- Munoz, M.A., Welcome, F.L., Schukken, Y.H. & Zadoks, R.N. (2007). Molecular epidemiology of two *Klebsiella pneumoniae* mastitis outbreaks on a dairy farm in New York State. *Journal of Clinical Microbiology*, 45(12), 3964–3971.

- National Mastitis Council, (NMC). (1999). Sampling collection and handling. *Laboratory handbook on bovine mastitis*. National Mastitis Council Inc.: Verona, WI, USA.
- Ohbayashi, T., Irie, A., Murakami, Y., Nowak, M., Potempa, J., Nishimura, Y., Shinohara, M. & Imamura, T. (2011). Degradation of fibrinogen and collagen by staphopains, cysteine proteases released from *Staphylococcus aureus*. *Microbiology*, 157, 786–792.
- Ozkumur, E., Shah, A.M., Ciciliano, J.C., Emmink, B.L., Miyamoto, D.T., Brachtel, E., Yu, M., Chen, P., Morgan, B., Trautwein, J., Kimura, A., Sengupta, S., Stott, S.L., Karabacak, N.M., Barber, T.A., Walsh, J.R., Smith, K., Spuhler, P.S., Sullivan, J.P., Lee, R.J., Ting, D.T., Luo, X., Shaw, A.T., Bardia, A., Sequist, L.V., Louis, D.N., Maheswaran, S., Kapur, R., Haber D.A. & Toner M. (2013). Inertial focusing for tumor antigen-dependent and -independent sorting of rare circulating tumor cells. *Science Translational Medicine*, 5, 179ra47, doi:10.1126/scitranslmed.3005616.
- Papautsky, I. & Zhou, J. (2013). Fundamentals of inertial focusing in microchannels. *Lab on a Chip*, 13(6), 1121–1132.
- Pilla, R., Schwarz, D., König, S. & Piccinini, R. (2012). Microscopic differential cell counting to identify inflammatory reactions in dairy cow quarter milk samples. *Journal of Dairy Science*, 95(8), 4410–4420.
- Pilla, R., Malvisi, M., Snel, G.G.M., Schwarz, D., König, S., Czerny, C.P. & Piccinini, R. (2013). Differential cell count as an alternative method to diagnose dairy cow mastitis. *Journal of Dairy Science*, 96(3), 1653–1660.
- Pinho, L., Thompson, G., Rosenbusch, R. & Carvalheira, J. (2012). Genotyping of *Mycoplasma bovis* isolates using multiple-locus variable-number tandem-repeat analysis. *Journal of Microbiological Methods*, 88(3), 377–385.
- Pinijsuwan, S., Rijiravanich, P., Somasundrum, M. & Surareungchai, W. (2008). Sub-femtomolar electrochemical detection of DNA hybridization based on latex/gold nanoparticle assisted signal amplification. *Analytical Chemistry*, 80(17), 6779–6784.
- Piyasena, M.E., Suthanthiraraj, P.P.A., Applegate, R.W., Jr., Goumas, A.M., Woods, T.A., López, G.P. & Graves, S.W. (2012). Multinode acoustic focusing for parallel flow cytometry. *Analytical Chemistry*, 84(4), 1831–1839.
- Piyasena, M.E. & Graves, S.W. (2014). The intersection of flow cytometry with microfluidics and microfabrication. *Lab on a Chip*, 14(6), 1044–1059.
- Pyörälä, S. (2003). Indicators of inflammation in the diagnosis of mastitis. *Veterinary Research*, 34, 565–578.
- Qiu, J., Zhou, Y., Chen, H. & Lin, J.-M. (2009). Immunomagnetic separation and rapid detection of bacteria using bioluminescence and microfluidics. *Talanta*, 79(3), 787–795.

- Quinn, P.J., Carter, M.E., Markey, B. & Carter, G.R. (1994). Veterinary Clinical Microbiology. Mosby (Eds.). Elsevier, London, pp. 127-136.
- Raemy, A., Meylan, M., Casati, S., Gaia, V., Berchtold, B., Boss, R., Wyder, A., & Graber, H.U. (2013). Phenotypic and genotypic identification of streptococci and related bacteria isolated from bovine intramammary infections. *Acta Veterinaria Scandinavica*, 55(1), 53.
- Rainard, P. & Riollet, C. (2006). Innate immunity of the bovine mammary gland. *Veterinary Research*. 37(3), 369–400.
- Rieseberg, M., Kasper, C., Reardon, K.F. & Scheper, T. (2001). Flow cytometry in biotechnology. *Applied Microbiology and Biotechnology*, 56(3), 350–360.
- Riffon, R., Sayasith, K., Khalil, H., Dubreuil, P., Drolet, M., Lagacé, J. (2001). Development of a rapid and sensitive test for identification of major pathogens in bovine mastitis by PCR. *Journal of Clinical Microbiology*, 39, 2584–2589.
- Rivas, A.L., Quimby, F.W., Blue, J. & Coksaygan, O. (2001). Longitudinal evaluation of bovine mammary gland health status by somatic cell counting, flow cytometry, and cytology. *Journal of Veterinary Diagnostic Investigation*, 13(5), 399–407.
- Saei, H.D., Ahmadi, M., Mardani, K. & Batavani, R.A. (2010). Genotyping of *Staphylococcus aureus* isolated from bovine mastitis based on PCR-RFLP analysis of the *aroA* gene. *Comparative Clinical Pathology*, 19(2), 163–168.
- Sargeant, J.M., Leslie, K.E., Shirley, J.E., Pulkrabek, B.J. & Lim, G.H. (2001). Sensitivity and specificity of somatic cell count and California Mastitis Test for identifying intramammary infection in early lactation. *Journal of Dairy Science*, 84(9), 2018–2024.
- Schepers, A.J., Lam, T.J., Schukken, Y.H., Wilmink, J.B. & Hanekamp, W.J. (1997). Estimation of variance components for somatic cell counts to determine thresholds for uninfected quarters. *Journal of Dairy Science*, 80(8), 1833–1840.
- Schmid, S., Tinguely, M., Cione, P., Moch, H. & Bode, B. (2011). Flow cytometry as an accurate tool to complement fine needle aspiration cytology in the diagnosis of low grade malignant lymphomas. *Cytopathology*, 22(6), 397–406.
- Schwarz, D., Diesterbeck, U.S., Failing, K., König, S., Brügemann, K., Zschöck, M., Wolter, W. & Czerny, C.P. (2010). Somatic cell counts and bacteriological status in quarter foremilk samples of cows in Hesse, Germany—a longitudinal study. *Journal of Dairy Science*, 93(12), 5716–5728.
- Smith, P.K., Krohn, R.I., Hermanson, G.T., Mallia, A.K., Gartner, F.H., Provenzano, M.D., Fujimoto, E.K., Goeke, N.M., Olson, B.J. & Klenk, D.C. (1985). Measurement of protein using bicinchoninic acid. *Analytical Biochemistry*, 150(1), 76–85.

- Smolenski, G., Haines, S., Kwan, F.Y., Bond, J., Farr, V., Davis, S.R., Stelwagen, K. & Wheeler, T.T. (2007). Characterization of host defence proteins in milk using a proteomic approach. *Journal of Proteome Research*, 6(1), 207–215.
- Soares, A.R.S. (2015). *Portable lab-on-chip platform for bovine mastitis diagnosis in raw milk*. Master degree Dissertation in Biomedical and Biophysics Engineering. Lisbon: Faculdade de Ciências – Universidade de Lisboa.
- Sordillo, L.M. & Streicher, K.L. (2002). Mammary gland immunity and mastitis susceptibility. *Journal of Mammary Gland Biology and Neoplasia*, 7(2), 135–146.
- Spencer, D., Elliott, G. & Morgan, H. (2013). Simultaneous fluorescence and impedance micro cytometer—A modular approach. *Proceedings of the 17th International Conference on Miniaturized Systems for Chemistry and Life Sciences (MicroTAS2013)*, 27–31 October. Freiburg, Germany.
- Stein, D.S., Korvick, J.A. & Vermund, S.H. (1992). CD4+ Lymphocyte cell enumeration for prediction of clinical course of human immunodeficiency virus disease: A review. *The Journal of Infectious Diseases*, 165(2), 352–363.
- Stepanović, S., Dakić, I., Martel, A., Vanechoutte, M., Morrison, D., Shittu, A., Ježek, P., Decostere, A., Devriese, L.A., Haesebrouck, F. (2005). A comparative evaluation phenotypic and molecular methods in the identification of members of the *Staphylococcus sciuri* group. *Systematic and Applied Microbiology*, 28(4), 353–357.
- Supré, K., De Vliegher, S., Sampimon, O.C., Zadoks, R.N., Vanechoutte, M., Baele, M., De Graef, E., Piepers, S. & Haesebrouck, F. (2009). Technical note: use of transfer RNA-intergenic spacer PCR combined with capillary electrophoresis to identify coagulase-negative *Staphylococcus* species originating from bovine milk and teat apices. *Journal of Dairy Science*, 92(7), 3204–3210.
- Szczubiał, M., Dąbrowski, R., Kankofer, M., Bochniarz, M. & Albera, E. (2008). Concentration of serum amyloid A and activity of ceruloplasmin in milk from cows with clinical and subclinical mastitis. *Bulletin of Veterinary Institute of Pulawy*, 52, 391–395.
- Tan, S.J., Kee, M.Z.L., Mathuru, A.S., Burkholder, W.F. & Jesuthasan, S.J. (2013). A microfluidic device to sort cells based on dynamic response to a stimulus. *PLoS One*, 8(11), e78261, doi:10.1371/journal.pone.0078261.
- Taponen, S., Koort, J., Björkroth, J., Saloniemi, H. & Pyörälä, S. (2007). Bovine intramammary infections caused by coagulase-negative staphylococci may persist throughout lactation according to amplified fragment length polymorphism based analysis. *Journal of Dairy Science*, 90(7), 3301–3307.
- Taponen, S., Salmikivi, L., Simojoki, H., Koskinen, M.T. & Pyörälä, S. (2009). Real-time polymerase chain reaction-based identification of bacteria in

- milk samples from bovine clinical mastitis with no growth in conventional culturing. *Journal of Dairy Science*, 92(6), 2610–2617.
- Tenhagen, B.A., Koster, G., Wallmann, J. & Heuwieser, W. (2006). Prevalence of mastitis pathogens and their resistance against antimicrobial agents in dairy cows in Brandenburg, Germany. *Journal of Dairy Science*, 89(7), 2542-2551.
- Tizard, I.R. (2009). *Imunologia veterinária*. (8th ed.). Rio de Janeiro: Elsevier Editora Limitada.
- Towbin, H., Staehelin, T. & Gordon, J. (1979). Electrophoretic transfer of proteins from polyacrylamide gels to nitrocellulose sheets: Procedure and some applications. *Proceedings of the National Academy of Sciences of the United States of America*, 76(9), 4350-4354.
- van Belkum A, et al. Tassios PT, Dijkshoorn L, Haeggman S, Cookson B, Fry NK, Fussing V, Green J, Feil E, Gerner-Smidt P, Brisse S, Struelens M & European Society of Clinical Microbiology and Infectious Diseases (ESCMID) Study Group on Epidemiological Markers (ESGEM) (2007). Guidelines for the validation and application of typing methods for use in bacterial epidemiology. *Clinical Microbiology and Infection*, 13(Suppl 3), 1–46.
- van der Woude, M.W. & Bäumlér, A.J. (2004). Phase and antigenic variation in bacteria. *Clinical Microbiology Reviews*, 17(3), 581–611.
- Viguiér, C., Arora, S., Gilmartin, N., Welbeck K. & O’Kennedy, R. (2009). Mastitis detection: current trends and future perspectives. *Trends in Biotechnology*, 27(8), 486–493.
- Vissio, C., Dieser, S.A., Agnelli, H.L., Odierno, L.M. & Larriestra, A.J. (2014). Accuracy of the composite somatic cell count to detect intra-mammary infection in dairy cows using latent class analysis. *Preventive Veterinary Medicine*, 113(4), 547–555.
- Voldman, J., Gray, M.L., Toner, M. & Schmidt, M.A. (2002). A microfabrication-based dynamic array cytometer. *Analytical Chemistry*, 74(16), 3984–3990.
- Walstra, P., Wouters, J. & Geurts, T. (2006). *Dairy science and technology*. (2nd Ed.). New York: Taylor & Francis Group.
- Wang, G., Mao, W., Byler, R., Pate, K., Henegar, C., Alexeev, A. & Sulchek, T. (2013). Stiffness dependent separation of cells in a microfluidic device. *PLoS One*, 8(10), e75901, doi:10.1371/journal.pone.0075901.
- Wang, S.X. & Li, G. (2008). Advances in giant magnetoresistance biosensors with magnetic nanoparticle tags: review and outlook. *IEEE Transactions on Magnetics*, 44(7), 1687–1702.
- Wedemeyer, N. & Pötter, T. (2001). Flow cytometry: An ‘old’ tool for novel applications in medical genetics. *Clinical Genetics*, 60(1), 1–8.
- Welbeck, K., Leonard, P., Gilmartin, N., Byrne, B., Viguiér, C., Arora, S. & O’Kennedy, R. (2011). Generation of an anti-NAGase single chain

- antibody and its application in a biosensor-based assay for the detection of NAGase in milk. *Journal of Immunological Methods*, 364(1-2), 14–20.
- Wolff, A., Perch-Nielsen, I.R., Larsen, U.D., Friis, P., Goranovic, G., Poulsen, C.R., Kutter, J.P. & Telleman, P. (2003). Integrating advanced functionality in a microfabricated high-throughput fluorescent-activated cell sorter. *Lab on a Chip*, 3(1), 22–27.
- Willey, J.M., Sherwood, L. & Woolverton, C.J. (2008). *Prescott, Harley and Klein's Microbiology*. (7th ed.). New York: McGraw Hill Higher Education.
- Yang, S.-Y., Hsiung, S.-K., Hung, Y.-C., Chang, C.-M., Liao, T. & Lee, G.-B. (2006). A cell counting/ sorting system incorporated with a microfabricated flow cytometer chip. *Measurement Science and Technology*, 17(7), 2001–2009.
- Yang, A.H.J. & Soh, H.T. (2012). Acoustophoretic sorting of viable mammalian cells in a microfluidic device. *Analytical Chemistry*, 84(24), 10756–10762.
- Yazdankhah, S.P., Hellemann, A.L., Rønningen, K. & Olsen, E. (1998). Rapid and sensitive detection of *Staphylococcus* species in milk by ELISA based on monodisperse magnetic particles. *Veterinary Microbiology*, 62(1), 17–26.
- Yeo, L. & Friend, J. (2010). Fabrication of microfluidic devices using polydimethylsiloxane. *Biomicrofluidics*, 4(2), 026502.
- Yoon, J.-Y. & Kim, B. (2012). Lab-on-a-chip pathogen sensors for food safety. *Sensors*, 12, 10713-10741.
- Yu, H.-W., Kim, I.S., Niessner, R. & Knopp, D. (2012). Multiplex competitive microbead-based flow cytometric immunoassay using quantum dot fluorescent labels. *Analytica Chimica Acta*, 750, 191–198.
- Zadoks, R.N. & Watts, J.L. (2009). Species identification of coagulase-negative staphylococci: genotyping is superior to phenotyping. *Veterinary Microbiology*, 134(1-2), 20–28.
- Zadoks, R.N., Middleton, J.R., McDougall, S., Katholm, J. & Schukken, Y.H. (2011). Molecular epidemiology of mastitis pathogens of dairy cattle and comparative relevance to humans. *Journal of Mammary Gland Biology and Neoplasia*, 16(4), 357–372.
- Zschöck, M., Nessler, A. & Sudarwanto, I. (2005). Evaluation of six commercial identification kits for the identification of *Staphylococcus aureus* isolated from bovine mastitis. *Journal of Applied Microbiology*, 98(2), 450–455.